Enhanced Primary Treatment of Bypass Wastewater Using Potassium Ferrate(VI) and Iron Electrocoagulation

by

Haitham Yousri Elsayed Elnakar

A thesis submitted in partial fulfillment of the requirements for the degree of

Doctor of Philosophy
in
Environmental Engineering

Department of Civil and Environmental Engineering
University of Alberta

ABSTRACT

In-plant wastewater treatment strategies to deal with bypass wastewater in excess of plant capacity are critical in securing sustainable wastewater management. The overall goal of this research was to test potassium ferrate(VI), iron electrocoagulation, and their combination for the enhancement of primary wastewater treatment as a sustainable process retrofit capable of attenuating the magnitude of untreated bypass wastewater discharge into water bodies.

The first part of the study investigated the dual capacity of potassium ferrate(VI) as disinfectant / oxidant and coagulant to provide adequate treatment to bypass wastewaters. The effect of rapid mixing speed was investigated for the first time along with potassium ferrate(VI) dosage considering *Escherichia coli* (*E. Coli*), Fecal Coliform (FC), Total Suspended Solids (TSS), and Orthophosphates (PO_4^{3-}) as the process responses. All responses other than PO_4^{3-} showed good agreement between the observed and modeled values. *E. Coli* and FC removals were found to increase with the increase of both the mixing intensity and potassium ferrate(VI) dosages. TSS removal exhibited optimal responses. The effluent quality achieved by potassium ferrate(VI), as an independent treatment, can be sufficient for certain types of unrestricted and restricted irrigation reuse purposes suggested by World Health Organisation (WHO) guidelines. Furthermore, this study investigated, for the first time, the role of rapid mixing on the rate of potassium ferrate(VI) decay and disinfection in bypass wastewaters from extreme wet weather flow events. The double

exponential model was able to represent the potassium ferrate(VI) decay in all conditions with a high coefficient of determination and low mean square error. There was no significant increase in the potassium ferrate(VI) dissociation and disinfection rates with the increase of the rapid mixing speeds from 500 to 1000 rpm which revealed that the reactions were kinetically controlled. The coagulation capability of potassium ferrate(VI) enhanced the sedimentation ability and contributed almost the same as the chemical disinfection capability to the overall *E. Coli* removal.

The second part of the research investigated the effectiveness of enhancing primary treatment of domestic sewage by iron electrocoagulation for the removal of soluble chemical oxygen demand (sCOD) at neutral pH conditions. The experimental results showed that sCOD removal efficiencies increased with increasing electrolysis time, current density, and temperature. The temperature effect was notably demonstrated in this study, for the first time, for the treatment of domestic wastewater using iron electrocoagulation. Using a 15 mA/cm² current density, an average 52% sCOD removal efficiency was achieved after 15 minutes at 23°C while approximately 40 minutes were needed to attain comparable removal efficiency at 8°C. Experimental results and theory showed that adsorption equilibrium was not reached in an electrocoagulation cell; consequently, applying adsorption isotherms to describe the process is not appropriate. An alternative approach using variable-order-kinetic (VOK) models derived from Langmuir and Langmuir-Freundlich adsorption expressions was employed in this study. These models require de facto estimation of ferric hydroxide

(adsorbent) mass that accounts for the conversion of ferrous ion (Fe^{2+}) to particulate end products. The Langmuir-based VOK model was found to be the better model to describe sCOD removal at 8°C and 23°C under all the operating conditions tested. The mechanism of sCOD removal is proposed to be chemisorption.

The third and final part of the study introduced a novel enhancement technique of primary wastewater treatment by hybrid potassium ferrate(VI) – iron electrocoagulation system. Oxidation contribution and pH increase resulted from potassium ferrate(VI) incorporation were found to be the most significant factors that significantly enhanced the iron electrocoagulation process in tackling sCOD. Oxidation can help increase the sCOD removal by about 10% while pH increase promoted favourable conditions to quickly oxidize Fe^{2+} to form $Fe(OH)_3$ precipitates. By using response surface methodology – Box Behnken design, current density and potassium ferrate(VI) and their interaction were significant in achieving higher sCOD removal and faster Fe^{2+} oxidation. It was not possible to correlate zeta potential measurements to sCOD reduction although an isoelectric point was achieved for both iron the electrocoagulation and hybrid potassium ferrate(VI) and iron electrocoagulation systems which indicated that the sCOD removal mechanisms were not entirely related to charge neutralization.

PREFACE

This thesis is an original work by Haitham Elnakar, who designed and conducted the experiments, collected and analyzed the data, as well as prepared the manuscripts. All parts of this thesis were reviewed under the supervision of Dr. Ian D. Buchanan. Some colleagues also contributed to sample collection or chemical preparation. Some of the analyses were done in other departments of the University of Alberta, or research institutes in Edmonton, as specified below.

Chapter 2 of this thesis has been submitted to Environmental Technology as "Elnakar, H. and Buchanan, I.: Treatment of bypass wastewater using potassium ferrate(VI): Assessing the role of mixing". Mr. Muhammad Faizan Khan contributed to wastewater sampling and some of my bench-scale experiments, Ms. Shimiao Dong also contributed to some of my bench-scale experiments, and Mr. Chengjin Wang contributed to the potassium ferrate(VI) preparation. Zeta potential were analyzed in Dr. Hongbo Zeng's research laboratory in the Department of Chemical and Materials Engineering at the University of Alberta. X-ray powder diffraction (XRD) analysis was done in Alberta Innovates Technology Futures.

Chapter 3 of this thesis has been submitted to Journal of Environmental Management as "Elnakar, H. and Buchanan, I.: The role of mixing in potassium ferrate(VI) consumption kinetics and disinfection of bypass wastewater". Mr. Muhammad Khan contributed to wastewater sampling, Ms. Shimiao Dong also contributed to some of

my bench-scale experiments, and Mr. Chengjin Wang contributed to the potassium ferrate(VI) preparation.

Chapter 5 of this thesis will be submitted as “Elnakar, H. and Buchanan, I.: Novel integrated potassium ferrate(VI) and iron electrocoagulation for the treatment of bypass wastewater”. Zeta potential were analyzed in Dr. Hongbo Zeng’s research laboratory in the Department of Chemical and Materials Engineering at the University of Alberta.

"Has there come upon the human being a span of time when he was nothing yet to be mentioned?" Surah al-Insan (76:1)

To my beloved mother and to the soul of my father

To my wife Manar, to my son Shadi, and to my daughter Mariam

This thesis work was defended on August 31, 2018, last day as a Vanier Canada scholar!

ACKNOWLEDGEMENTS

I would like to sincerely express my appreciation to my supervisor, Dr. Ian D. Buchanan for his support, guidance and encouragement without which this thesis is not possible. During our supervisor-student relationship, he adopted a non-confrontational approach and encouraged me to think critically of my proposed research ideas and hypotheses. In addition, I highly value the experience I gained assisting Dr. Buchanan in teaching, during which I benefited from his depth and breadth of knowledge and his truly compassionate and professional manner in dealing with students. My appreciation also goes to my PhD supervisory committee members: Dr. Selma E. Guigard and Dr. Bipro R. Dhar for their great support and to my thesis defence committee: Dr. Hongde Zhou from University of Guelph, Dr. Tong Yu, Dr. William Wenming Zhang, Dr. Lijun Deng from University of Alberta for their valuable comments and feedback on my thesis work.

I acknowledge the generous financial support for my doctoral studies received by the following scholarships, prizes and funds (in the order they were received): University of Alberta Doctoral Recruitment Scholarship (September 2013-August 2014), Alberta Innovates- Technology Futures Scholarship (May 2014-August 2017), Vanier Canada Graduate Scholarship (May 2015-August 2018), President's Doctoral Prize of Distinction (May 2015-August 2018), and Shell Canada Enhanced Learning Fund (January 2018). Such substantial support was fundamental in allowing me, as an international student, to comfortably focus on the academic aspects of my studies. The

research related financial support provided by the Natural Sciences and Engineering Research Council of Canada (NSERC) is also acknowledged.

The continuous and unlimited support of my former M.Sc. supervisor, Dr. Emad Imam, in providing me with valuable advice and recommendation letters is highly appreciated and will always be remembered. I am also grateful to all my past and present colleagues and friends who helped me adapt to my life in Edmonton in addition to those who tried hard to influence the progress of my studies. I also thank the current and former technicians in Department of Civil and Environmental Engineering for their logistical and laboratory related support: Mrs. Chen Liang and Mr. Yupeng (David) Zhao, Ms. Maria Demeter, and Ms. Nian Sun.

TABLE OF CONTENTS

LIST OF TABLES

LIST OF FIGURES

LIST OF ABBREVIATIONS AND NOMENCLATURE

ABTS	2,2'-azino-bis(3-ethylbenzothiazoline-6-sulphonic acid)
AIC_c	Akaike Information Criterion
ANOVA	Analysis of variance
BBD	Box-Behnken Design
DC	Direct Current
DO	Dissolved Oxygen
E. Coli	*Escherichia coli*
EDCs	Endocrine Disrupting Compounds
FC	Fecal Coliform
MPN	Most Probable Number
PO_4^{3-}	Orthophosphates
PPCPs	Pharmaceuticals and Personal Care Products
PPP	Purchasing Power Parity
RAO	Remedial Action Objectives
RSM	Response Surface Method
sCOD	Soluble Chemical Oxygen Demand
SWM	Stormwater Management
tCOD	Total Chemical Oxygen Demand
TSS	Total Suspended Solids
VOK	Variable-Order-Kinetic

VSS	Volatile Suspended Solids
WWTP	Wastewater Treatment Plant
XRD	X-Ray Diffraction

CHAPTER 1. INTRODUCTION AND RESEARCH OBJECTIVES

1.1 Introduction

Promoting sustainable urban development requires securing adequate infrastructure capable of adapting to the challenges of climate change, growing population, and demographic trends (IPCC, 2007; OECD, 2011). High chances of extreme weather conditions and increased urban population densities exert stresses on current wastewater infrastructure and require changes in design approaches and adaptation processes. It has been estimated that US$ 41 trillion will be needed worldwide to rehabilitate aging infrastructure and to build new urban infrastructure for the period 2005–2030 (UNEP, 2013). More than 55% of that amount (US$ 22.6 trillion) should be allocated for water-related infrastructure with wastewater infrastructure having the most considerable portion (UNEP, 2013).

In terms of wastewater treatment infrastructure, the global trends suggest that the average high-, middle-, lower middle, and lower-per capita gross domestic product (purchasing power parity or PPP) countries treat about 70%, 38%, 28% and 8% of the generated municipal and industrial wastewater (UNESCO, 2017). While the motivation to treat wastewater differs between PPP group thresholds, developing countries are particularly lagging in addressing the wastewater treatment challenges due to absent or undersized infrastructure, technical and institutional capacity, and funding (UN, 2015; UNESCO, 2017). Nevertheless, increasing wastewater treatment coverage in any country does not necessarily connect with improved wastewater

management practices as it is estimated that 74% of urban and 66% of rural wastewater services are not effective in preventing human contact with untreated or partially treated wastewater (UNESCO, 2017).

The bypass of untreated or undertreated wastewater to the receiving environment can be characterized as planned or unplanned. The planned untreated bypass wastewaters are usually necessary to accomplish maintenance work on collection or treatment systems. An example of this is the 4.9 billion liters bypass of untreated wastewater into the St. Lawrence River over 89 hours in 2015 so that the City of Montreal could undertake major maintenance and construction work on the city's main sewer system (Environment and Climate Change Canada, 2017). The City of Montreal planned to bypass untreated wastewater at hydraulically and environmentally favorable conditions so that the discharge would have the least impact on both people and aquatic life (Environment and Climate Change Canada, 2017).

The unplanned bypass wastewaters can be defined as the wastewater flows in excess of the capacity of an existing collection system or treatment plant that have not been accounted for during the planning and design phases. Elevated ambient air temperatures, fluctuating and extreme precipitation patterns and increased effective population density of the area served by combined or separate sewer systems are all sources that can be overlooked during the planning and design stages and can result in bypass wastewater discharges. Bypass wastewaters can lead to unplanned reuse, in that water withdrawn by downstream users will contain a significant fraction of untreated

or undertreated wastewater (National Research Council, 2012; Rice et al., 2016; Wiener et al., 2016). Nevertheless, such bypass wastewaters are supposed to be released in compliance with local regulations that usually include providing some sort of treatment. The release of untreated wastewater can pose risks to fish and other aquatic life, as noted under Section 36(3) of the Canadian Federal Fisheries Act, (i.e., the "no deleterious substances" clause) (Government of Canada, 1985). Every community is encouraged to investigate locally feasible remedial alternatives to address contaminants of particular concern, resulting in the development of remedial action objectives (RAO). The RAO for any community generating wastewater should be to prevent direct contact with pollutants that may cause an intolerable risk.

In some communities especially in the lower PPP countries, the pre-defined RAO are sometimes unachievable as such countries adopt RAO established in higher-income countries that have accumulated experience and substantial technical and financial capacity to implement stringent standards. Such practice forces lower-income countries to overspend on a limited number of treatment plants in specific communities, leaving the wastewater generated from other communities untreated. A better approach should not only account for the standards of the point source treated wastewater, but it should take into consideration the receiving environment characteristics, intended water uses, and reuse alternatives. Proper planning will further help to tackle the challenges of climate change and population growth and

allow shifting from conventional technologies to newer clean technologies that are capable of meeting more realistic RAO.

1.2 Background

1.2.1 Sources of bypass wastewaters from an urban catchment

Climatic and population data are primary inputs in designing wastewater infrastructure; consequently, any significant change in climate or population density can have a dramatic effect on sewerage system components design and/ or operation. Wastewater conveyance and treatment system components are sized based on peak and minimum flow rates averaged over certain durations (i.e., hour, day, 15-day, and month) (Metcalf & Eddy, 2004). The peak hour flow rate is commonly used in sizing the sewer systems, grit chambers, sedimentation tanks, filters, and disinfection units (Alberta Government, 2013; Imam and Elnakar, 2014; Metcalf & Eddy, 2004). This peak hour flow rate is the maximum flow rate averaged over an hour and is based on specific probability of non-exceedance (Alberta Government, 2013; Imam and Elnakar, 2014). The selection of the appropriate probability of non-exceedance is based on different factors including economics, engineering judgment, and sewer flow type (i.e., combined or separate) (Imam and Elnakar, 2014). As the design peak hour flow is not the absolute maximum flow rate, different sewerage system components are expected to receive flows higher than their design capacity under certain conditions based on the sewerage system type.

A sanitary sewerage system is designed to accommodate dry weather flow wastewater generated by residential, industrial, commercial, and institutional sectors and a wet weather flow allowance to account for infiltration and inflow. This system is separate from the system that collects surface run-off (snowmelt and stormwater). Such separation prevents overloading the sanitary sewer systems and treatment stations during rainy periods by excluding the vast majority of surface drainage which is collected in a separate stormwater management system and discharged to nearby water bodies or reused after rudimentary treatment.

Nevertheless, a completely separated sanitary sewer system can be overloaded due to new sewer hook-ups to support increasing population density, increased underground water infiltration allowed by aging infrastructure, increased surface water inflow due to road sags developing at manhole locations and illegal drain connections. Such overloading can sometimes not be accommodated by the design capacity of the wastewater treatment plant (WWTP) leading to a potential loss of treatment efficiency and a portion of the flow being bypassed around the plant and released untreated. In order to meet wastewater treatment objectives, auxiliary economically viable treatment units should be developed to perform efficiently and to reduce that volume of untreated wastewater discharged to the water bodies.

Storm sewer systems collect surface runoff from urban and industrial catchments into underground pipes and usually discharge it untreated it to a nearby water body such as a lake, stream or river with the goal of flood prevention. Such untreated stormwater

discharges are currently considered one of the sources of pollutants into receiving water bodies (Zgheib et al., 2012). During a rainstorm, the storm sewer system transports contaminants from the catchment areas and discharges them to water bodies at several locations causing potential impacts on the receiving water ecosystems. Stormwater management (SWM) has traditionally focused on flood prevention. However, SWM goals have been expanded recently to also include mitigating the impacts of stormwater on the receiving environment.

Several older communities are served by combined sewer systems which convey both sanitary sewage and stormwater runoff in the same sewer pipes to treatment plants. During heavy wet weather events due to rainfalls or snowmelt, the flow may exceed the hydraulic design capacity of the collection system or WWTP. This results in sewer overflows or treatment plant bypasses, both of which release untreated combined sewerage to surface waters (U.S. EPA, 1999a).

Efforts to manage the risks of combined sewer overflows have evolved over the last several decades (U.S. EPA, 2008, 1999b, 1999a). One of the straightforward ways to overcome the existing combined sewer system problem is to move towards a separate sewer system (U.S. EPA, 1999a). However, this solution is often not economically feasible and may also impact the safety of buildings in older portions of cities serviced by combined sewer systems. As a result, treating the excess flows is the most viable solution to overcome this problem. Such treatment can be decentralized by placing it

at the end of the overflow sewer section or centralized by conveying all the overflow to the treatment plant.

Wetlands are commonly constructed to improve stormwater quality before its release to downstream surface waters. However, hydraulic and contaminant loadings must be controlled in order to preserve their integrity. Systems to divert extreme flows around wetlands are typically incorporated into their design. The majority of contaminant loading is conveyed within runoff from the more frequently occurring and less intense events. Physical and chemical treatment may be applied as needed upstream of wetlands to the "first flush" of contaminants contained within these flows.

Figure 1.1 shows a conceptual diagram of the types of sewerage systems that may exist in a typical urban catchment with bypass wastewaters reaching water bodies. The wastewater discharges conveyed through separate or combined sewer system should receive a certain level of treatment based on the RAO set by the community served. Any wastewater discharge that undergoes treatment but does not conform to the treatment plant RAO can be considered a bypass wastewater. If there is no treatment plant in place, dry and wet weather flow wastewater discharges are directly sent untreated to the receiving environment. If the receiving environment is a low flow river or irrigation canal, the prolonged periods of high concentrations of contaminants and drastic discharge quantities can be considered a bypass wastewater. On the other hand, if there is an undersized treatment plant in place, bypass wastewaters will be the result of the flows in excess of the treatment plant capacity. In the Canadian context, the

yearly discharges of untreated or undertreated wastewater is reported to be 150 billion liters, all dumped into Canadian waterways which poses an environmental, human health and economic problem (Government of Canada, 2017).

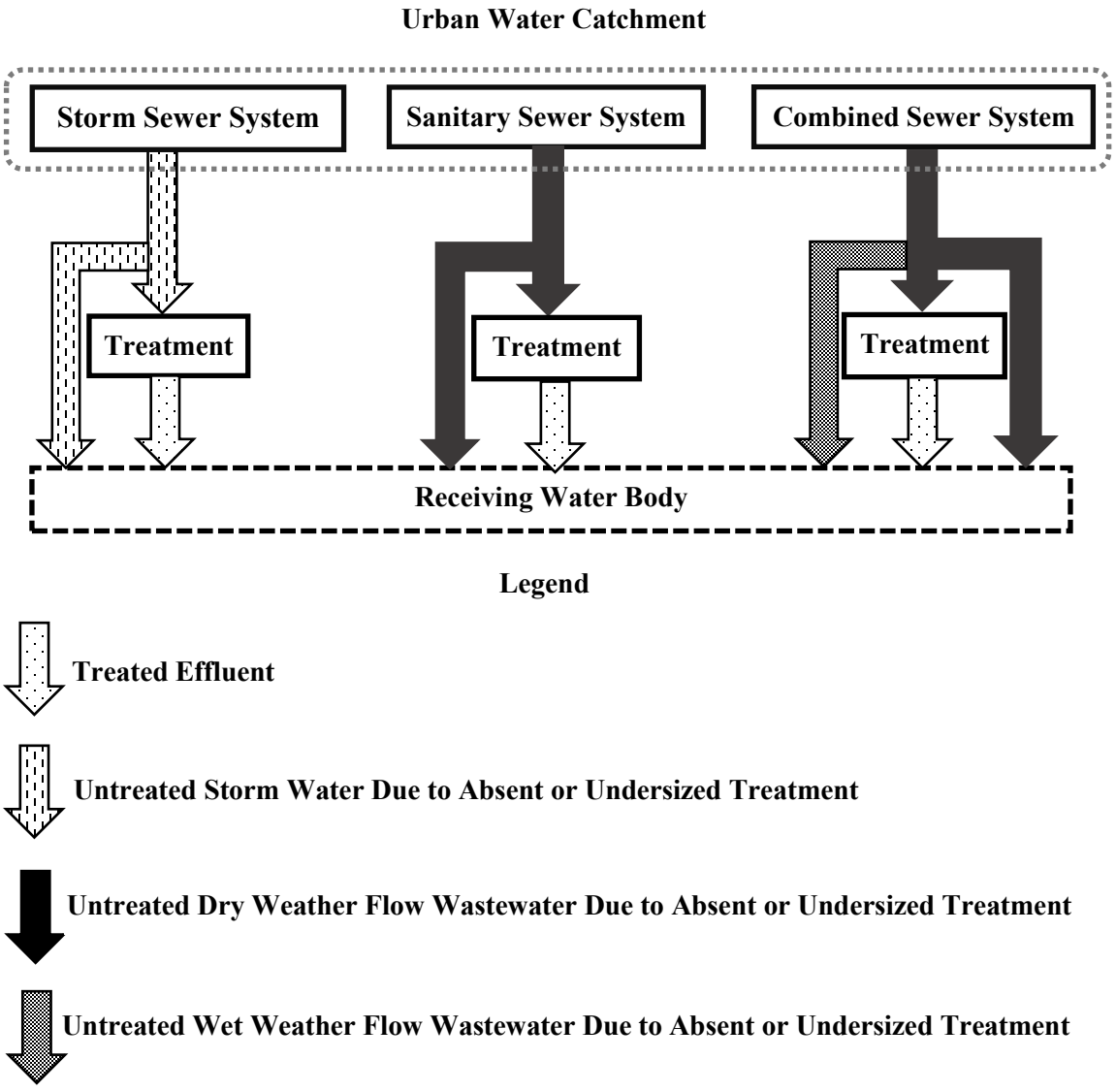

Figure 1.1 Conceptual diagram of the types of sewerage systems that may exist in an urban catchment with bypass wastewaters reaching water bodies.

1.2.2 Treatment methods to address untreated bypass wastewaters

Treatment methods such as wetlands, high rate ballasted clarification, HydroSeparator®, and physically or chemically enhanced primary treatment have been developed to provide at least partial treatment and reduce the magnitudes of wastewater overflows bypassed untreated to the environment (Chhetri et al., 2016; Masi et al., 2017; U.S. EPA, 2013). The major drawback of wetlands is the low treatability of soluble organic compounds; thus, a pre-treatment to wetlands may be necessary (Masi et al., 2017). The high rate ballasted clarification combines coagulation, flocculation, and settling processes in compact plants that have not been tested thoroughly under a wide range of wastewater influent conditions and also have long start-up times (Jolis and Ahmad, 2004; Plum et al., 1998; U.S. EPA, 2013). A HydroSeparator® combines a series of inclined-plate settlers (lamella clarifier), and is followed by a mesh filter (Chhetri et al., 2016). While the main goal of using a HydroSeparator® is to remove suspended solids from wastewater overflows, the technology can be chemically enhanced by adding coagulants and by providing downstream disinfectants (Chhetri et al., 2016) which may add to the complexity of the technology.

Physically and/or chemically enhanced primary treatment is either placed as one of the first processes within a typical wastewater treatment train (Metcalf & Eddy, 2004), used as a stand-alone auxiliary treatment to the wastewater flows in excess of the WWTP capacity (City of Edmonton, 2000) or used as the sole process treating

wastewater generated from small rural communities to even large cities (Gehr et al., 2003; Harleman and Murcott, 1999; Wang et al., 2009). Conventional primary treatment can be enhanced using either or both of physical means such as lamella plate settlers or/and chemical means such as chemical coagulation using iron or aluminum salts. Such enhancement allows new-build primary treatment to be designed according to much higher overflow rates which means cheaper construction, or existing primary treatment tanks to be retrofitted to handle higher flows with no additional tankage. In addition, higher removal efficiencies can be achieved (Harleman and Murcott, 1999; Metcalf & Eddy, 2004).

1.2.3 Iron-based technologies as an alternative to treat bypass wastewaters

Several alternative enhancement techniques to primary wastewater treatment utilize the adsorptive and reductive properties of iron and its mineral and oxide products to remove a wide range of microorganisms, inorganic and organic contaminants. After oxygen, silicon, and aluminum, iron is considered the fourth most abundant element in the Earth's crust. Elemental iron, Fe(0), can be found under certain environmental and geological conditions, but is produced primarily in blast furnaces in the iron-making process. Various purities of elemental iron can be used as electrode materials in electrochemical-based treatment technologies (Mollah et al., 2001, 2004). Due to its high reactivity, iron may exist in different valence states such as the relatively water-soluble Fe^{2+} (ferrous iron) and the highly water-insoluble Fe^{3+} (ferric iron). Ferric iron has been widely utilized as a chemical coagulant in water and wastewater treatment

(Crittenden et al., 2012; Metcalf & Eddy, 2004). Higher valence state iron, such as the Fe(VI) derivative or Ferrate, can also be prepared and has been tested in different water and wastewater treatment applications (Jiang, 2007; Sharma, 2002). Two iron-based treatment technologies were examined in this Ph.D. research for the purpose of enhancing primary wastewater treatment. These were potassium ferrate(VI) and iron electrocoagulation.

1.2.3.1 Potassium ferrate(VI)

Iron in its +6-oxidation state is known as Ferrate, Fe(VI), which is considered one of the promising multi-purpose chemical enhancement alternatives to primary wastewater treatment (Murmann and Robinson, 1974; Sharma, 2002). The dissociation of potassium ferrate (K_2FeO_4), which is a common Fe(VI) salt, is represented by Reaction 1.1 (Patterson et al., 2001). Reaction 1.1 shows that potassium ferrate(VI)'s oxidation in water produces oxygen (O_2) and ferric hydroxide ($Fe(OH_3)$) (Sharma, 2002; Sharma et al., 2005). The redox potential of Fe(VI) ions under acidic pH conditions is very high compared to all other oxidants or disinfectants at E_0 = +2.20V (Alsheyab et al., 2009), and it reduces rapidly to Fe^{3+} and oxygen (Sharma, 2002; Sharma et al., 2005).

$$4K_2FeO_4 + 10H_2O \rightarrow 4Fe(OH)_3 + 8KOH + 3O_2 \quad (1.1)$$

At basic pH, Fe(VI) becomes a mild oxidant with E_0 = +0.6 to +0.7 V (Alsheyab et al., 2009; Ghernaout and Naceur, 2011) with the oxygen ligands exchange very slowly

with water at pH 10 (Sharma, 2002; Sharma et al., 2005). Such unique chemistry of potassium ferrate(VI) suggest its versatility to act as oxidant, disinfectant and coagulant (Jiang, 2007; Jiang and Lloyd, 2002; Sharma, 2002; Tien et al., 2008). None of the oxidants or disinfectants tested in wastewater treatment such as peracetic acid, performic acid, or ozone can act as both as oxidant/disinfectant and coagulant (Chhetri et al., 2014; Gehr et al., 2003).

Potassium ferrate(VI) has been tested with different types of water, targeting various contaminants including phosphates, pharmaceuticals, and microorganisms (Lee et al., 2009; Yang et al., 2012). The oxidation effect of potassium ferrate(VI) can change the organic composition of the water and reduce the water toxicity (Alsheyab et al., 2009; Ghernaout and Naceur, 2011). In a recent literature review, it was suggested that potassium ferrate(VI) generators could be combined with an electroflotation system (Talaiekhozani et al., 2017). Other than this suggestion, there is little literature about engineering potassium ferrate(VI)-based treatment system.

Oxidation capability

Potassium ferrate(VI) was examined in oxidizing micropollutants as part of advanced wastewater treatment of secondary treated effluent (Lee et al., 2009). More than 85% efficiency has been observed in removing micropollutants containing electron-rich moieties (ERM) such as phenols, anilines, amines, and olefins. Such efficiency has been achieved with potassium ferrate(VI) doses higher than 5 mg/L at pH 7 and 8. Potassium ferrate(VI) has been found to achieve micropollutants removal efficiencies

comparable to ozone with potassium ferrate(VI) having an added benefit of removing phosphates (Lee et al., 2009). Similar results were found when applying potassium ferrate(VI) to remove 68 selected endocrine disrupting compounds (EDCs) and pharmaceuticals and personal care products (PPCPs) (Yang et al., 2012). In a study that focused on the treatment of combined sewer overflow using potassium ferrate(VI), a dose of about 0.24 mg/L was found to be optimal (Gandhi et al., 2014). At this dose, the soluble organics were removed in addition to considerable reduction (about 70%) in total and volatile solids (Gandhi et al., 2014). Other researchers found that potassium ferrate(VI) performed better than ferric sulfate in removing color and dissolved organic carbon-containing humic and fulvic acids (Jiang et al., 2001; Tien et al., 2008).

Disinfection capability

The disinfection potential of potassium ferrate(VI) has been investigated using several strains of microorganisms in pure water, buffered water, river water, water stored in ships' ballast tanks, and secondary wastewater effluents (Cho et al., 2006a; Gilbert et al., 1976; Hu et al., 2012; Jessen et al., 2008; Jiang et al., 2007, 2006; Kazama, 1995; Kwon et al., 2014; Murmann and Robinson, 1974; Schink and Waite, 1980; Waite, 1979). Furthermore, potassium ferrate(VI) was demonstrated to not lead to any reversible inactivation or regrowth of the tested microorganisms (Bandala et al., 2009; Hu et al., 2012; Jiang et al., 2007; Kazama, 1995; Schink and Waite, 1980). For a given temperature and water matrix, four main parameters usually affect the disinfection process. These are potassium ferrate(VI) dosage, contact time, pH, and mixing

conditions. While the ranges of potassium ferrate(VI) dosages and contact times reported in the literature vary widely, the required dosages are usually less than those required by other chemicals used for the same treatment goal (Jiang et al., 2006) Another factor of importance is the mixing conditions which have been demonstrated to have a significant impact on disinfection (Field, 1973; Metcalf & Eddy, 2004; U.S. EPA, 1999b). However, the literature contains no report of the extent to which mixing speed impacts potassium ferrate(VI) disinfection capabilities.

Coagulation capability

There are mixed reports on potassium ferrate(VI) coagulation capability relative to removing organic matter and particles. It is found that potassium ferrate(VI) oxidation had a significant effect on enhancing the coagulation of surface waters, especially when the waters had high organic content (Ma and Liu, 2002). Another study showed that there was much better floc formation in terms of floc index with potassium ferrate(VI) than with ferric chloride at a neutral pH (Graham et al., 2010). On the other hand, precipitate resulting from potassium ferrate(VI) as compared with ferric chloride showed significantly more nano-size particles with negative charges which contribute to the colloidal suspension stability (Goodwill et al., 2015). Such conclusion raised a concern regarding the application of potassium ferrate(VI) for coagulation purposes.

1.2.3.2 Iron electrocoagulation

Iron electrocoagulation has been known for treating industrial wastewater and groundwater. However, little attention has been given to its use for municipal

wastewater treatment. The advantages of iron electrocoagulation over conventional chemical coagulation include: (1) abundance and low price of iron (about 0.5-0.8 $/kg); (2) lower sludge quantities composed of large flocs with less bound water that are easier to settle and dewater; (3) no chemical additive is used and no by-products are formed that needs further neutralization or treatment since the 'electron' is the focal element in the treatment; (4) easy control of the treatment with less maintenance as it uses simple and easily automated equipment; (5) the ability to be utilized with existing treatment processes such as sedimentation tanks; (6) generally non-toxic and is mainly regulated for aesthetic and organoleptic reasons; and (7) the ability to provide high effluent throughput rates (Hakizimana et al., 2017; Mollah et al., 2001).

Overall, by using an iron anode, $Fe(OH)_n$, with n = 2 or 3, is formed. Two major iron electrocoagulation mechanisms have been proposed; one for the production of $Fe(OH)_2$ (Reactions 1.2 to 1.5), and the other for the production of $Fe(OH)_3$ (Reactions 1.6-1.9) (Feng et al., 2012; Mollah et al., 2001). As depicted in Reaction 1.2, the oxidation at the anode mainly leads to the release of ferrous ion (Fe^{2+}) as the dissolution rate of ferric ion (Fe^{3+}) can be assumed negligible (Ben Sasson et al., 2009). In mechanism 1, Fe^{2+} cations oxidize very slowly leading to ferrous hydroxides as shown in Reactions 1.2 to 1.5. In mechanism 2, Fe^{2+} is immediately transformed into ferrous hydroxide then is quickly oxidized by dissolved oxygen to ferric hydroxide as shown in Reactions 1.6 to 1.9. Detailed iron electrochemical studies are not within the scope of this Ph.D. thesis.

Mechanism 1

Anode: $Fe(s) \rightarrow Fe^{2+}_{(aq)} + 2e^-$ (1.2)

$Fe^{2+}_{(aq)} + 2OH^-_{(aq)} \rightarrow Fe(OH)_{2(s)}$ (1.3)

Cathode: $2H_2O_{(l)} + 2e^- \rightarrow H_{2\,(g)}\uparrow + 2OH^-_{(aq)}$ (1.4)

Overall: $Fe(s) + 2H_2O_{(l)} \rightarrow Fe(OH)_{2(s)} + H_{2\,(g)}\uparrow$ (1.5)

Mechanism 2

Anode: $4Fe(s) \rightarrow 4Fe^{2+}_{(aq)} + 8e^-$ (1.6)

$4Fe^{2+}_{(aq)} + 10H_2O_{(l)} + O_{2(g)} \rightarrow 4Fe(OH)_{3(s)} + 8H^+_{(aq)}$ (1.7)

Cathode: $8H^+_{(aq)} + 8e^- \rightarrow 4H_{2\,(g)}\uparrow$ (1.8)

Overall: $4Fe(s) + 10H_2O_{(l)} + O_{2(g)} \rightarrow 4Fe(OH)_{3(s)} + 4H_{2\,(g)}\uparrow$ (1.9)

Organic pollutants in different wastewater matrices are sometimes removed by means of iron electrocoagulation (Chou et al., 2010; Dubrawski and Mohseni, 2013b, 2013a; Eyvaz et al., 2014; Jaafarzadeh et al., 2016; Kabdaşli et al., 2009; Kalyani et al., 2009; Kuokkanen et al., 2015; Ma and Zhang, 2016; Mansouri et al., 2011; Moreno-Casillas et al., 2007; Orescanin et al., 2013, 2011; Singh et al., 2016; Tsai et al., 1997). There are two major processes involved in the electrocoagulation cell that contribute to organic pollutants' removal. Firstly, metal precipitates are generated through the electrochemical process, and these metal precipitates can remove the contaminants through physio-chemical processes that may include: 1) inclusion, where the contaminants find holes in the metals species to occupy; 2) occlusion, where the flocs completely surround the contaminant, trapping it in their structure, so it cannot return

to the solution; or 3) adsorption, where contaminants adhere to the surface flocs (Mollah et al., 2001).

Adsorption isotherms

Adsorption isotherms such as Langmuir, Freundlich, Dubinin–Radushkevich, Temkin, and others have been examined in the process of elucidating contaminants' removal mechanisms and for modeling iron electrocoagulation process (Balasubramanian et al., 2009; Kalyani et al., 2009; Nariyan et al., 2017; Şengil and özacar, 2006; Yoosefian et al., 2017). In the literature, it is assumed that the theoretically calculated iron will completely and solely be transformed to $Fe(OH)_3$ precipitate which acts as the adsorbent. This assumption neglects the effects of changes in operating parameters such as pH, dissolved oxygen, actual iron released, redox potential and treatment time that can have a significant impact on the reactions and the end products (Lakshmanan et al., 2009). In addition, there is a conflict regarding the specification of the iron electrocoagulation end products in real wastewater samples that are in most reports based on speculation rather than on a clear experiential and/or theoretical approach (Ben Sasson et al., 2009; Dubrawski et al., 2015; Kalyani et al., 2009; Lakshmanan et al., 2009; Mollah et al., 2001, 2004; Şengil and özacar, 2006). The theoretical end products of iron electrocoagulation treatment in acidic and near neutral treatment conditions should be either $Fe(OH)_2$, $Fe(OH)_3$ or a mixture of both in equilibrium with their soluble ions. This results in high proportions of total Fe remaining as soluble ferrous (Fe^{2+}) under acidic to neutral pH conditions (Lakshmanan et al., 2009).

Adsorption and zeta potential

The electrostatic charges of colloidal particles are usually quantified by measuring the suspension zeta potential. Zeta potential is defined as the electric potential difference between the shear plane of a colloidal particle and the bulk of the solution. Consequently, zeta potential can be considered as an indirect measure of the electrical charge of colloidal particles. Since the actual potential between the surface of the particle and the solution cannot be measured experimentally, zeta potential is usually quantitatively measured by determining electrophoretic mobility (velocity) of a particle moving under an electric potential of known intensity. Colloidal particles in wastewater maintain a stable dispersion by carrying a surface charge that is usually negative (Metcalf & Eddy, 2004). It is hypothesized that the iron electrocoagulation process can break down the equilibrium of the electrostatic charge fields that stabilize colloids through inducing chemical reactions to form precipitates (Mollah et al., 2001). There are very limited reports on the relationship between the coagulant dosage generated during iron electrocoagulation process and the altered zeta potential of municipal wastewater samples at various treatment time periods and current densities.

1.3 Problem statement and knowledge gap

Addressing the problem of bypass wastewaters requires two complementary actions: mitigation and adaptation. Minimizing the amount of the generated wastewater and stormwater collected in the sewerage system should be one of the primary goals of any mitigation plan. At the same time, improving the adaptive capacity of the

municipalities and WWTPs to handle bypass wastewaters should be achieved. To date, few studies have provided innovative treatment technologies to handle bypass wastewaters as one of the adaptation strategies. Among the limited solutions provided to treat bypass wastewaters has been the enhancement of primary wastewater treatment. However, a small number of enhancement options has been listed in the literature as discussed above. Chemically enhanced primary treatment using metal salts has mainly been investigated and applied to enhance the solids removal from wastewater flows (City of Edmonton, 2000; Morrissey and Harleman, 1992). However, there is a need to enhance the oxidation and disinfection capability to tackle a broader range of pollutants. This study proposes the enhancement of primary wastewater treatment using potassium ferrate(VI) and/or iron electrocoagulation. One or more gaps in knowledge exist relative to each of these applications. This Ph.D. research is intended to address these deficiencies.

1.3.1 Potassium ferrate(VI) knowledge gap

Ferrate(VI) was initially characterized by its purple color about 300 years ago, and by late 19th century, its chemical benefits had started to be realized (Jiang and Lloyd, 2002). Since then, various techniques have been made to prepare ferrate(VI) salts and several studies were aimed at testing its dual capabilities of oxidation and coagulation on a wide array of applications. Although ferrate(VI) development and applications started a long time ago, its full-scale application has not yet been achieved, and there are still several gaps in knowledge regarding its applications in domestic wastewater

treatment. The knowledge gaps identified in the literature and addressed by this research can be summarized as follows:

(1) The needs related to retrofitting existing coagulation–flocculation–sedimentation systems to accommodate ferrate(VI) based treatment;

(2) Information regarding minimum appropriate potassium ferrate(VI) mixing intensities and dosages when applied for oxidation or disinfection of high oxidant demand like wastewater;

(3) Research on potassium ferrate(VI) efficacy for the disinfection of high oxidant demand wastewater;

(4) Research regarding the contribution of coagulation capability of ferrate(VI) to the overall microorganisms' attenuation; and

(5) Options to utilize or deal with nano-size ferrate(VI) precipitation species.

1.3.2 Iron electrocoagulation knowledge gap

Similar to potassium ferrate(VI), iron electrocoagulation as a wastewater treatment technology was proposed near the end of the 19^{th} century. Unlike potassium ferrate(VI), full-scale application of iron electrocoagulation was instituted in the early stages of its introduction as a wastewater treatment technology. In 1889, iron electrodes were used to treat canal water in Salford, England to which seawater was added as a chlorine source to provide disinfection (Vik et al., 1984). Although the technology has been found to be viable and effective in the treatment of a variety of

water and wastewater related pollutants, attention has been given primarily to the treatment of industrial effluents. Based on the information provided above, the following gaps in knowledge have been identified in the science and application of iron electrocoagulation in general and with specific attention given to the treatment of raw municipal wastewater:

(1) Limitations regarding the application of adsorption isotherms to elucidate the removal mechanisms of organic pollutants;

(2) Limited information regarding zeta potential change during iron electrocoagulation process treating municipal wastewater. Specifically, the relationship between the coagulant dosage generated during iron electrocoagulation process and the increased zeta potential of wastewater samples remains to be elucidated; and

(3) Providing innovative options to tackle the problem of soluble Fe^{2+} remaining in the effluent after iron electrocoagulation treatment without increasing the overall treatment time.

1.4 Research objectives

The primary research goal is to test potassium ferrate(VI) and iron electrocoagulation for the enhancement of primary wastewater treatment as a standalone or auxiliary treatment capable of attenuating the magnitude of untreated bypass wastewater discharge into water bodies. The research scope will focus on addressing the gaps identified in the problem statement and research objectives section.

The objectives of the study on enhanced primary treatment using potassium ferrate(VI) are as follows:

(1) to test the efficiency of potassium ferrate(VI) to enhance the oxidation or disinfection and coagulation capabilities of the primary treatment of bypass wastewater resulted from wet weather flow events (i.e., removal of *Escherichia coli* (*E. Coli*), Fecal Coliform (FC), Total Suspended Solids (TSS), and Orthophosphates (PO_4^{3-})); and

(2) to study the effect of rapid mixing speeds used in existing WWTP's coagulation facilities on the removal of each of the five responses monitored (i.e., *E. Coli*, FC, TSS, and PO_4^{3-}).

The objectives of the study on *E.Coli* disinfection using potassium ferrate(VI) are as follows:

(1) to model potassium ferrate(VI) consumption at different rapid mixing speeds in high oxidant demand bypass wastewater;

(2) to test inactivation models to generate a representative model of *E. Coli* disinfection at different mixing speeds; and

(3) to estimate the contribution of the coagulation capability of potassium ferrate(VI) in further enhancing the overall *E. Coli* removal.

The objectives of the study on enhanced primary treatment using iron electrocoagulation are as follows:

(1) to test the efficiency of iron electrocoagulation in removing soluble chemical oxygen demand (sCOD) from bypass wastewater at neutral pH, two different temperatures (8°C and 23°C), and different current densities;

(2) to examine adsorption isotherm models for sCOD removal based on more realistic estimation of the adsorbent mass; and

(3) to examine assumptions and recommend appropriate experimental protocols for using adsorption models to elucidate removal mechanisms of sCOD in iron electrocoagulation-based treatment.

The objectives of the study on enhancing primary wastewater treatment by hybrid potassium ferrate(VI) – iron electrocoagulation system are as follows:

(1) to study the feasibility of utilizing the oxidation capability of potassium ferrate(VI) to remove sCOD and of its resultant nanoparticles to improve the coagulation capabilities of iron electrocoagulation; and

(2) to evaluate the applicability of using potassium ferrate(VI) as one of the options to reduce the Fe^{2+} existing in the effluents at high concentrations in acidic and near neutral treatment conditions.

(3) to investigate the role of charge neutralization as measured by zeta potential at optimum treatment conditions.

1.5 Thesis organization

This thesis consists of six chapters focusing on enhancing the treatment of untreated bypass wastewaters using potassium ferrate(VI), iron electrocoagulation or a hybrid system utilizing both. The general overview of the sources of bypass wastewater, potassium ferrate(VI) and iron electrocoagulation are presented in Chapter 1.

Investigation of the dual capabilities of potassium ferrate(VI) and the effect of high mixing speeds in removing *E. Coli*, FC, TSS, and PO_4^{3-} from bypass wastewater resulted from wet weather flow wastewater event is presented in Chapter 2. A response surface methodology – central composite design statistical method was used to explain the relationships between the two explanatory variables (i.e., potassium ferrate(VI) dosage and mixing speed) and each of the five responses monitored (i.e., *E. Coli*, FC, TSS, and PO_4^{3-}).

In Chapter 3, the effect of different high mixing conditions on potassium ferrate(VI) dissociation and *E. Coli* removal is investigated in four bypass wastewaters resulted from different wet weather flow events without pH adjustment. Potassium ferrate(VI) consumption is modeled to estimate the kinetic constants at different mixing speeds. In addition, inactivation models are tested to generate a representative model of *E. Coli* disinfection to elucidate the relative importance of concentration and contact time.

In Chapter 4, iron electrocoagulation-based treatment is assessed as another option for the enhancement of primary wastewater treatment. The major goal of this research was

to examine and critically review the usage of adsorption isotherm models for chemical oxygen demand (COD) removal based on a more realistic estimation of the adsorbent that considered the soluble ferrous ion (Fe^{2+}) in the effluent. Discussion on the assumptions and suggested experimental protocols were addressed.

In Chapter 5, a hybrid system composed of potassium ferrate(VI) and iron electrocoagulation system is investigated. Such hybrid system will utilize the oxidation capabilities of potassium ferrate(VI) to remove COD and oxidize Fe^{2+} then utilize the potassium ferrate(VI) resultant particles to enhance the iron electrocoagulation coagulation capabilities in removing the coagulated particulate matter. In addition, an investigation of using adsorption isotherms to describe the relationship between the coagulant dosage generated during iron electrocoagulation process and the increased zeta potential of wastewater samples at various treatment conditions is included.

In Chapter 6, overall conclusions of the performed research and recommendations for future work are presented.

CHAPTER 2. TREATMENT OF BYPASS WASTEWATER USING POTASSIUM FERRATE(VI): ASSESSING THE ROLE OF MIXING[1]

2.1 Introduction

Unplanned wastewater can be defined as the wastewater flows in excess to the capacity of an existing collection system or treatment plant that have not been accounted for during the planning and design phases. During the planning and design stages, factors such as elevated ambient air temperatures, fluctuating and extreme precipitation patterns, increased effective population density of the area served by combined or separate sewer systems can be overlooked, resulting in inflows that exceed plant capacity. Unless plant upgrades are instituted to accommodate these inflow spikes, a portion of these unplanned wastewater flows must be diverted from the treatment plant and discharged into the environment untreated in order to protect treatment processes. This bypass wastewater can lead to unplanned reuse, in that water withdrawn by downstream users will contain a significant fraction of untreated or undertreated wastewater (National Research Council, 2012; Rice et al., 2016; Wiener et al., 2016). Therefore, auxiliary treatment processes should be implemented at wastewater treatment plant (WWTP) to control or provide adequate treatment to the inflows in

[1] A version of this chapter has been submitted to Environmental Technology as "Elnakar, H. and Buchanan, I.: Treatment of bypass wastewater using potassium ferrate(VI): Assessing the role of mixing".

excess of the existing treatment plant capacity and reduce or eliminate bypass flows (Struck et al., 2009). Such processes are either standalone or part of an overall treatment train.

Potassium ferrate(VI) is a promising reagent in wastewater treatment because it can be an effective oxidant, coagulant and disinfectant (Lee et al., 2009; Sharma et al., 2005; Yang et al., 2012). The redox potential of ferrate (Fe(VI)) ions under acidic pH conditions is among the highest of all oxidants/disinfectants at E_0 = +2.20V; at basic pH, it becomes a mild oxidant with E_0 = 0.6-0.7 V (Alsheyab et al., 2009; Ghernaout and Naceur, 2011). During the oxidation process, Fe(VI) is reduced to ferric (Fe^{3+}), which is one of most commonly used coagulants. The coagulation process can help remove organic matter and particles.

It was found that peroxidation has a significant effect on enhancing the coagulation step (Xie et al., 2016). Potassium ferrate(VI) as one of the oxidants used in the peroxidation step has been shown to have a significant effect on enhancing the coagulation of surface waters, especially when the waters had high organic content (Ma and Liu, 2002). Another study showed that there was much better floc formation in terms of flocculation index with potassium ferrate(VI) than with ferric chloride at a neutral pH (Graham et al., 2010). Other researchers found that potassium ferrate(VI) performed better than ferric sulfate in removing color and dissolved organic carbon (Jiang et al., 2001; Tien et al., 2008). Potassium ferrate(VI) has been demonstrated to be a powerful disinfectant for an extensive range of microorganisms (Bandala et al.,

2009; Hu et al., 2012; Jiang et al., 2007; Kazama, 1995; Schink and Waite, 1980). The coagulation step may also further enhance the removal of microorganisms.

The selection of the optimum operating conditions that are most feasible and satisfy the treatment goal is of paramount importance. The ranges of potassium ferrate(VI) dosages reported in the literature are very wide due to the diversity of water matrices studied. Pre-acidification or alkalization followed by pH adjustment may be effective for the removal of certain the target contaminants (Graham et al., 2010; Jiang et al., 2007; Sharma, 2002) as it controls the generation of $HFeO_4^-$, a protonated form of Fe(VI), which impacts the reaction rates (Sharma, 2002). However, such change to the pH of the wastewater adds extra cost to the treatment.

If potassium ferrate(VI) is utilized to replace coagulants in existing coagulation / flocculation / sedimentation facilities (City of Edmonton, 2000), another factor of importance will be the selection of mixing speed in the flash mixing process step. It was demonstrated that the mixing speeds have a significant impact on both coagulation (Cornwell and Bishop, 1983; Metcalf & Eddy, 2004; Vadasarukkai and Gagnon, 2015) and disinfection (Field, 1973; Metcalf & Eddy, 2004; U.S. EPA, 1999b). For the coagulation process, mixing has long been assessed to optimize colloid destabilization (Cornwell and Bishop, 1983; Metcalf & Eddy, 2004; Vadasarukkai and Gagnon, 2015). When potassium ferrate(VI) is added during the rapid mixing coagulation step, it is hypothesized that potassium ferrate(VI) species will contact microorganisms quickly and uniformly. As a result, mixing is not only helping in the destabilization

process according to the double layer theory, it also has a potential impact on the rate of chemical reaction (Cornwell and Bishop, 1983). While potassium ferrate(VI) has been introduced previously under 150 - 400 rpm rapid mixing conditions to raw and secondary treated wastewaters using a jar-test apparatus (Jiang et al., 2006; Kwon et al., 2014), the impact of mixing speed on the overall contaminants' removal using potassium ferrate(VI) based treatment has not been thoroughly investigated.

The mainstream studies surveyed in the literature focus on either oxidation/disinfection or coagulation using potassium ferrate(VI). In addition, the removal of contaminants from an engineered treatment process that includes rapid mixing, slow mixing, and no-mixing to simulate coagulation, flocculation, and sedimentation has not been thoroughly investigated. Given the complexity of the system that involves physical and chemical processes, the removal of the target contaminants depends on the individual and combined effects of the main process parameters. In previous investigations of potassium ferrate(VI) treatment in water and wastewater treatment, the process was tested by varying one main process parameter at a time. This experimental design cannot investigate the interactions involved in the treatment process and also requires a large number of experimental runs to cover the experimental domain (Montgomery, 2001).

The goal of this study was to investigate the dual capabilities of potassium ferrate(VI) and the effect of mixing speed in removing *Escherichia coli* (*E. Coli*), Fecal Coliform (FC), Total Suspended Solids (TSS), and Orthophosphates (PO_4^{3-}) from bypass

wastewater resulting from heavy wet weather events. A response surface methodology - central composite design statistical method was used to quantify the relationships between the two explanatory variables (i.e. potassium ferrate(VI) dosage and mixing speed) and each of the four responses monitored (i.e. *E. Coli*, FC, TSS, and PO_4^{3-}).

2.2 Materials and methods

2.2.1 Source water

Wastewater samples were collected from a wastewater treatment plant in central Alberta, Canada that occasionally receives flows in excess to its capacity during wet weather flow events, resulting in some bypass flow. The samples were collected during wet weather from a channel leading from the grit removal process to the primary sedimentation tanks. Therefore, these samples are deemed to be representative of wet weather bypass flow at the plant. Samples were stored at 4ºC in a cold room. The characteristics of the collected samples are summarized in Table 2.1.

2.2.2 Coagulation-Flocculation-Sedimentation experimental setup

Potassium ferrate(VI) treatment was conducted at room temperature (25±1 ºC) in 2-L square beakers using a digital mixer (IKA, USA) for the rapid mixing (coagulation) stage. The speed of the digital mixer was adjusted according to the experimental design speed and was operated for 1 min for each run. The same beaker containing the coagulated wastewater was then immediately subjected to slow mixing conditions to simulate flocculation using a variable speed jar test apparatus (Phipps & Bird, USA)

operated at 30 rpm for 20 minutes in each run. The same size of flat paddle impeller (25 mm x 75 mm) was used for coagulation and flocculation mixing stages. The four responses modeled in this study were measured after receiving 81 minutes' treatment that included 1 minute of rapid-mixing, 20 minutes of slow-mixing and 60 minutes of no-mixing.

Table 2.1 Characterization of bypass wastewater used for experiments

Parameter	Units	High	Low	Median
pH	-	6.7	6.4	6.7
Zeta Potential	mV	-25.0	-21.0	-23.0
Total Chemical Oxygen Demand	mg/L	353.9	212.3	280.0
Soluble Chemical Oxygen Demand	mg/L	272.0	162.8	215.0
Total Suspended Solids	mg/L	96.0	71.8	83.0
Volatile Suspended Solids	mg/L	53.6	35.4	44.0
Total Phosphorus	mg/L	7.6	7.1	7.4
Reactive Phosphorus	mg/L	7.2	6.5	6.8
Escherichia coli	MPN/100mL	5.2E+06	2.9E+06	4.0E+06
Total Coliform	MPN/100mL	3.7E+07	1.5E+07	2.6E+07
Fecal Coliform	MPN/100mL	2.0E+07	1.2E+07	1.6E+07

2.2.3 Determination of operating parameters

Preliminary experiments were conducted without pH adjustment using potassium ferrate(VI) as the only chemical to be added. This condition was selected to assess the performance of potassium ferrate(VI) when used as the sole treatment reagent. As

shown in Figure 2.1, a series of tests was performed in which 0.01, 0.05, 0.1, 0.15 or 0.2 mM potassium ferrate(VI) was added under magnetic stirring and pH was measured after 80 minutes. Determination of the maximum allowable dosage was selected such that the final pH would not exceed 9.5 as required by Alberta effluent discharge standards (Alberta Government, 2013).

2.2.4 Analytical methods

The bypass wastewater samples' characteristics were measured before each experiment. pH was measured using an Accumet electrode and Accumet Excel (Fisher Scientific, Ottawa, ON, Canada). TSS and volatile suspended solids (VSS) were analyzed using standard methods 2540-D and 2540-E; respectively (APHA AWWA WEF, 1998). The following parameters were analyzed using HACH methods with specific method numbers in parentheses (HACH, USA): total and soluble chemical oxygen demand (8000), and total phosphorus (10127), reactive phosphorus (8048). Total Coliform, FC, and *E. Coli* (in most probable number per 100 ml) were determined from a 100 ml diluted sample using Colilert®-18 media and the IDEXX Quanti-Tray®/2000 kit (IDEXX, USA). Zeta potential was measured using a Malvern Zetasizer instrument (Malvern Instruments, Worcestershire, UK). The X-ray diffraction (XRD) analysis for semi-quantification of mineral species in a wastewater sample was performed with a Siemens D5000 X-ray diffractometer (Munich, Germany). Samples collected from each experimental run after applying the treatment

were specifically analyzed for the following parameters: pH, TSS, PO_4^{3-}, *E. Coli* and FC.

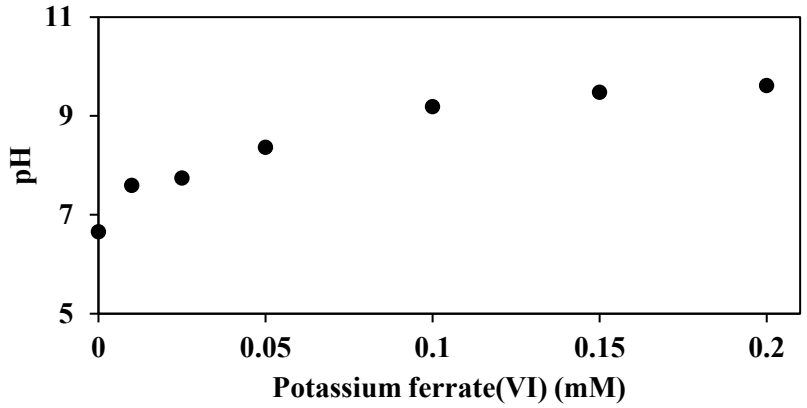

Figure 2.1 pH measured after 80 minutes of magnetic stirring in bypass wastewater having initial potassium ferrate(VI) concentrations of 0.01, 0.05, 0.1, 0.15 or 0.2 mM.

2.2.5 Chemicals and reagents

The preparation and purification of potassium ferrate(VI) were achieved by the wet method (Thompson et al., 1951). The purity of potassium ferrate(VI) product was measured at the day of each set of experiments by both the ABTS method at 415 nm and the spectrophotometric method at 510 nm and was found to be higher than 90%. Stock solutions of potassium ferrate(VI) were freshly prepared just before conducting the experiments by dissolving the potassium ferrate(VI) in its solid form in ultrapure water. Reagent-grade 2,20-azino-bis (3- ethylbenzothiazoline-6-sulfonate) (ABTS), sodium thiosulfate, boric acid, and other reagents were purchased from Sigma-Aldrich. All aqueous solutions were prepared with ultrapure water produced by a Milli-Q system (MilliporeSigma, USA).

2.2.6 Response surface method experimental design and data analysis

A response surface method was applied using central composite design-uniform precision. To maintain rotability, the star points are at a distance α from the center which is calculated based on the number of factors (k) in the factorial portion of the central composite design according to Equation 2.1.

$$\alpha = (2^k)^{1/4} \tag{2.1}$$

Therefore, for a 2-factor design, $\alpha = \sqrt{2}$. Table 2.2 summarizes the experimental conditions. The response variables were fitted by a second-order model in the form of a quadratic polynomial equation represented by Equation 2.2.

$$\eta = \beta_0 + \sum_{i=1}^{k} \beta_i x_i + \sum_{i=1}^{k} \beta_{ii} x_i^2 + \sum_{i,j=1} \sum_{i<j} \beta_{ij} x_i x_j \tag{2.2}$$

where β_0 is a constant, β_i are the k first-order coefficients, $\beta_{ii}$are the k quadratic coefficients, and β_{ij} are the $k(k-1)/2$ cross-product or interaction coefficients for the model written in terms of the factors, x_i and x_j.

The parameters and responses used in the experiments were evaluated using SAS (SAS, USA). Analysis of variance (ANOVA) was employed to perform diagnostic tests on the adequacy of the developed model. The statistical significance of proposed model and parameters tested in the model was examined using F-value and P-value at

95% confidence level. Fitness of the multi-regression model was expressed by the adjusted coefficient of determination (Adj R^2).

Table 2.2 Levels of the factors tested in the central composite design

Independent Factors	Units	Symbol	Coded and absolute levels ($\alpha = \pm \sqrt{2}$ in coded units)		
			-1	0	1
Mixing Speed	rpm	X_1	500	750	1000
Potassium ferrate(VI) Dosage	mM	X_2	0.050	0.075	0.100

2.3 Results and discussion

The wastewater quality shown in Table 2.1 reveal the characteristics of the wet weather flow conditions for the catchment served by the WWTP at the sampling time. The range of measured TSS indicates the low strength of the wet weather bypass wastewater (Henze and Comeau, 2008; Metcalf & Eddy, 2004). The VSS/TSS ratio has an average of 0.56 which is also in the low range (Henze and Comeau, 2008; Metcalf & Eddy, 2004) and reveals the existence of significant wash-out solids in the wastewater. The mineral distribution shown in Figure 2.2 indicates that the bypass wastewater's inorganic solids are dominated by quartz. The surface of the bypass wastewater particles is negatively charged, with a median zeta potential of -23 mV (Table 2.1). The log removal of the *E. Coli* and FC along with the TSS, and PO_4^{3-} removal percentages in all the 13 runs are given in Table 2.3. Regression coefficients, standard deviations, t-values and probability values are summarized in Table 2.4. Table 2.5 represents the ANOVA analysis for all responses. Zeta potential

measurements before and after treatment are shown in Table 2.6 for all runs. The following sections will discuss the results of each response.

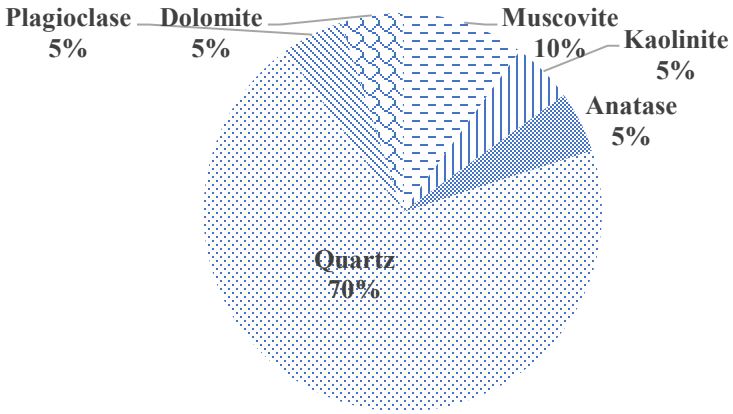

Figure 2.2 Distribution of the main minerals in the bypass wastewater

Table 2.3 Observed (Obs.) and modeled (Mod.) responses

Run	X_1	X_2	*E. Coli* (Log)		FC (Log)		TSS (%)		PO_4^{3-} (%)	
			Obs.	Mod.	Obs.	Mod.	Obs.	Mod.	Obs.	Mod.
1	396	0.075	3.00	2.95	3.06	2.98	52.56	52.40	88.74	88.36
2	750	0.075	3.20	3.18	3.21	3.19	55.70	55.48	97.19	95.22
3	750	0.040	2.93	2.90	2.90	2.88	49.37	49.50	95.06	95.22
4	750	0.075	3.41	3.18	3.36	3.19	55.56	55.48	98.62	95.22
5	500	0.050	2.87	2.95	2.91	2.82	50.63	50.36	92.27	91.79
6	1104	0.075	3.35	3.41	3.32	3.40	53.16	52.40	89.17	88.36
7	750	0.075	3.23	3.18	3.15	3.19	56.25	55.48	88.70	95.22
8	500	0.100	3.02	3.09	3.06	3.26	52.56	54.38	92.32	91.79
9	1000	0.050	3.01	3.01	3.07	3.12	50.00	50.36	91.31	91.79
10	750	0.075	3.13	3.18	3.07	3.19	54.17	55.48	92.96	95.22
11	1000	0.100	3.66	3.67	3.72	3.56	54.43	54.38	89.52	91.79
12	750	0.075	3.11	3.18	3.05	3.19	55.70	55.48	100.00	95.22
13	750	0.110	3.48	3.46	3.56	3.50	56.25	55.18	95.06	95.22

Table 2.4 Estimated regression coefficients and predictive models for different responses using coded levels (-1,1)

Response	Statistics	β_0	β_1	β_2	β_{11}	β_{22}	β_{12}
E. Coli	Value	3.18	0.16	0.20	-0.03	-0.02	0.13
	Standard error	0.04	0.05	0.05	0.08	0.08	0.10
	T-value	71.45	4.45	5.50	-0.86	-0.47	2.47
	P-value	0.000	0.003	0.001	0.419	0.654	0.043
	Model	$E.Coli = 3.18 + 0.16 * X_1 + 0.20 * X_2 + 0.13 * X_1 * X_2$					
FC	Value	3.19	0.15	0.22	0.01	0.03	0.13
	Standard error	0.05	0.06	0.06	0.09	0.09	0.11
	T-value	62.2	3.68	5.37	0.14	0.60	2.19
	P-value	0.000	0.008	0.001	0.894	0.567	0.065
	Model	$FC = 3.19 + 0.15 * X_1 + 0.22 * X_2$					
TSS	Value	55.48	0.26	2.01	-1.54	-1.57	0.62
	Standard error	0.34	0.45	0.45	0.68	0.68	0.89
	T-value	138.87	0.83	6.37	-4.55	-4.62	1.40
	P-value	0.000	0.4355	0.000	0.003	0.002	0.204
	Model	$TSS = 55.48 + 2.01 * X_2 - 1.54 * X_1^2 - 1.57 * X_2^2$					
PO_4^{3-}	Value	95.22	-0.39	-0.22	-3.43	-0.38	-0.46
	Standard error	1.60	1.78	1.78	2.71	2.71	3.57
	T-value	59.84	-0.31	-0.17	-2.54	-0.28	-0.26
	P-value	0.000	0.764	0.868	0.039	0.787	0.804
	Model	$PO_4^{3-} = 95.22 - 3.43 * X_1^2$					

Table 2.5 ANOVA analysis for all responses

Response		Degree of freedom	Sum of squares	Mean square	F-statistic	P-value
E. Coli *Adj R^2 = 81.25%*	Model	5	0.59	0.12	11.55	0.003
	Error	7	0.07	0.01		
	Total	12	0.66			
FC *Adj R^2= 78.02%*	Model	5	0.62	0.12	9.56	0.005
	Error	7	0.09	0.01		
	Total	12	0.71			
TSS *Adj R^2= 86.28%*	Model	5	64.08	12.82	16.06	0.001
	Error	7	5.59	0.80		
	Total	12	69.67			
PO_4^{3-} *Adj R^2= 11.98%*	Model	5	84.49	16.89	1.33	0.353
	Error	7	89.14	12.73		
	Total	12	173.63			

2.3.1 Statistical significance of the results

2.3.1.1 *E. Coli* response factor

As shown in Table 2.4, the linear coefficients (β_1 and β_2) and the interaction coefficient (β_{12}) demonstrate significant influences. The coefficient values show that the effects of mixing intensity (X_1), reactant concentration (X_2), and their interaction on *E. Coli* log removal are positive. As per the ANOVA test in Table 2.5, the value of F-statistic calculated for the log *E. Coli* removal (the response) is found to be 11.55 which is (3 times) greater than the tabulated value of $F_{0.05,5,7}$ (3.97). The high value of the coefficient of determination (Adj R^2= 81.25%) shows good agreement between measured and modeled values of this response. In addition, the amount of p-value probability is 0.003 (<0.05) as shown in Table 2.5 which reflects no evidence of lack of fit for the model. Contours in Figure 2.3-a indicate that there is no point of maximum or minimum response and is considered as a saddle point. The log *E. Coli* removal is found to increase with the increase of both the mixing intensity and potassium ferrate(VI) dosages.

2.3.1.2 FC response factor

Table 2.4 shows that only the linear coefficients (β_1 and β_2) demonstrate positive discernable influences on the FC log removal. As shown in Table 2.5, the value of F-statistic calculated for the log FC removal is found to be 9.56 which is around 2.4 times greater than the tabular $F_{0.05,5,7}$ value of 3.97. The agreement between measured and

modeled values of these responses according to the coefficient of determination (Adj R^2) is 78.02%. Similar to *E. Coli* response, the amount of p-value probability shown in Table 2.5 is 0.005 (<0.05) which again reflects no evidence of lack of fit for the model. Similar to the *E. Coli* response, log removal contours in Figure 2.3-b indicate that there is no point of maximum or minimum response and is considered as a saddle point. The log FC removal is also found to increase with the increase of both the mixing intensity and potassium ferrate(VI) dosages.

2.3.1.3 TSS response factor

It can be noticed in Table 2.4 that the linear coefficient (β_2) and the quadratic coefficients (β_{11} and β_{22}) demonstrate significant influences. The signs of these coefficients indicate that the effect on TSS removal efficiency of the initial potassium ferrate(VI) concentration (X_2) is positive while the effect of the quadratic coefficients (β_{11} and β_{22}) is negative. As shown in Table 2.5, the value of F-statistic calculated for the TSS percent removal is found to be 16.06 which is 4 times greater than the tabular $F_{0.05,5,7}$ value of 3.97. The high value of the coefficient of determination (Adj R^2= 86.28) shows good agreement between measured and modeled values of these responses. p-value shown in Table 2.5 is 0.001 (<0.05) which implies the goodness of fit for the model. Contours in Figure 2.3-c indicate that a point of maximum response of about 56.2±0.4% exists in the experimental region. The optimal levels are found at 806 rpm and 0.09 mM according to the conical analysis.

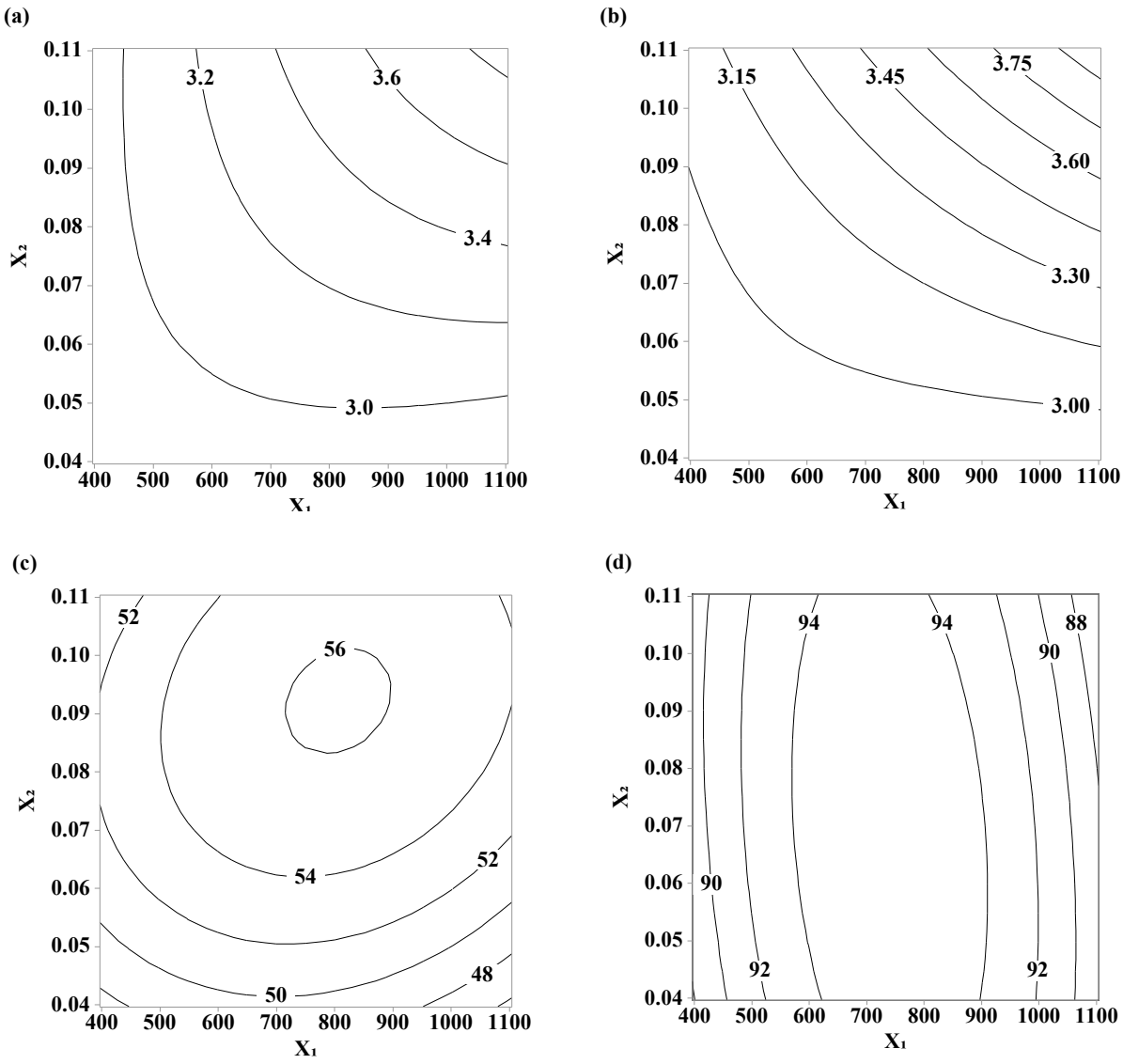

Figure 2.3 Two-dimensional contour plots for the effect of X_1 (Mixing Speed in rpm) and X_2 (potassium ferrate(VI) dosage in mM) on the log removal of (a) *E. Coli*; and (b) FC; and on percent removal of (c) TSS; and (d) PO_4^{3-}

2.3.1.4 PO_4^{3-} response factor

As noticed in Table 2.4, only the quadratic coefficient, β_{11}, demonstrates a significant influence. This indicates that orthophosphate removal was essentially independent of

ferrate(VI) concentration, as indicated in Figure 2.3-d. The negative coefficient value for the quadratic mixing variable (X_1^2) indicates that orthophosphate removals decreased as the mixing speed was either increased or decreased relative to the center point value. As shown in Table 2.5, the value of F-statistic calculated for the PO_4^{3-} removal efficiency is very low and is about 1.33 less than the tabular $F_{0.05,5,7}$ value of 3.97. A low value of the coefficient of determination (Adj R^2 = 11.98%) shows poor agreement between measured and modeled values of this response and is considered the lowest in this study. Nevertheless, the values of PO_4^{3-} removal efficiency are overall very high with the lowest observed removal efficiency being about 88.7%.

2.3.2 Reflections on the role of mixing in this study

The speciation and decomposition of ferrate(VI) have been studied previously using phosphate/ acetate buffer, and the pK_a values are shown in Reactions (2.1) to (2.3) (Rush et al., 1996). The pH in bypass wastewater increased from pH 6.7 to between pH 7.6 and 9.2 (depending on the doses) after the application of potassium ferrate(VI) (Figure 2.1). This increase was mainly due to the generation of hydroxide ions during the reaction and the self-decomposition of ferrate(VI). During the period between the addition of potassium ferrate(VI) to the mixing reactor and its full dissociation to coagulation species, disinfection as well as coagulation might occur simultaneously. Between pH 6.7 and pH 7.3, protonated ferrate(VI) ions ($HFeO_4^-$) are the predominant species, then as pH increases from pH 7.3 to pH 9.2, the percentage of unprotonated ferrate(VI) (FeO_4^{2-}) increases from 50% to 98%.

$$H_3FeO_4^+ \rightarrow H^+ + H_2FeO_4 \qquad pK_1 = 1.6 \pm 0.2 \qquad (2.1)$$

$$H_2FeO_4 \rightarrow H^+ + HFeO_4^- \qquad pK_2 = 3.5 \qquad (2.2)$$

$$HFeO_4^- \rightarrow H^+ + FeO_4^{2-} \qquad pK_3 = 7.3 \pm 0.1 \qquad (2.3)$$

By definition and practice, intense mixing interlards and diffuses the reaction components such that effective molecular transport can be achieved (Olson and Stout, 1967). Consequently, intense mixing ensures that the resultant potassium ferrate(VI) species come in contact homogeneously with the maximum possible number of wastewater particles (NSF and US EPA, 2002; Shah et al., 2012). As per the equations depicted in Table 2.4, the log removals of *E. Coli* and FC increased with the increase of both mixing speed and potassium ferrate(VI) dosage over the tested experimental region. While higher microorganism removals with an increase of potassium ferrate(VI) dosage could be explained by the release of more active oxidant/disinfectant and coagulant species, the increase in microorganism inactivation with increasing mixing intensity can be attributed to improved rapid dispersion of oxidant and more effective coagulation process which increased physical microorganism removal by sedimentation. Beyond pH 7.3, the reactivity of ferrate(VI) in bypass wastewater decreases since the contribution of ($HFeO_4^-$) ions which have a higher redox potential (1.4 V) than unprotonated ferrate(VI) (FeO_4^{2-}) (0.7 V) becomes lower. Additionally, $HFeO_4^-$ has been reported to be 3 times more effective than FeO_4^{2-} for *E. Coli* inactivation (Cho et al., 2006b). This suggests that rapid dispersion of the

chemical during the initial stages when the lower pH values prevail could increase microorganism inactivation. The role of coagulation/ flocculation and the subsequent sedimentation stages becomes more important beyond pH 7.3 which sheds the light on the need for providing optimum mixing conditions to increase the efficiency of the coagulation process. The differentiation between the contributions of potassium ferrate(VI)'s inactivation capability and by its coagulation capability to the overall microorganism removal will be reported in Chapter 3.

The TSS model equation shown in Table 2.4 shows that mixing speed is represented only by one quadratic term that has a negative coefficient. This means that high and low mixing speeds result in less removal than the midrange mixing speed as depicted in the optimal like contour lines shown in Figure 2.3-c. From one side, low mixing speeds might not have been able to adequately disperse the chemical or promote the particle collisions necessary to achieve good coagulation using potassium ferrate(VI). From the other side, high mixing speeds might have been so intense as to result in sheared flocs. This suggests that floc formation was important in TSS removal. The zeta potential results presented in Table 2.6 show that charge neutralization was not the main mechanism of TSS removal, because the negatively charged particles were neutralized by at most 50% (Amirtharajah and Mills, 1982). In this study, it has been demonstrated that increasing mixing intensity from the low to center level was beneficial but increasing it above the center level was detrimental. This suggests that sweep floc formation was a dominant particle removal mechanism.

Table 2.6 Zeta potential results

Run	Zeta Potential (mV)	
	Initial	Final
1	-24.6	-12.6
2	-24.4	-11.5
3	-27.0	-14.5
4	-27.4	-16.6
5	-23.9	-17.7
6	-26.1	-16.2
7	-24.9	-15.6
8	-24.7	-16.2
9	-27.3	-18.9
10	-27.7	-15.2
11	-24.2	-16.2
12	-26.4	-16.6
13	-25.2	-16.0

2.3.3 Qualitative significance of the results

Under the conditions tested in this study, potassium ferrate(VI) treatment at 0.04 to 0.10 mM was able to achieve *E. Coli* log removals in the range of 2.93 to 3.66 and FC log removals in the range of 2.90 to 3.72 from bypass wastewater having TSS in the range of 78 to 96 mg/L. This is comparable to the values reported in other studies that tested potassium ferrate(VI) on real wastewater samples. For example, Bandala et al. (2009) reported more than 4 log inactivation of total and fecal coliforms in secondary effluent having an average 120 mg TSS /L after treatment with potassium ferrate(VI) concentrations of 0.04 to 0.12 mM for a 5 minute contact time. Continuous mixing

was provided by a magnetic stirrer during these tests and no settling period was provided (Bandala et al., 2009). More than 4-log removal was reported for both total and fecal coliform when 0.27 mM potassium ferrate(VI) was applied to raw wastewater with TSS in the range of 97 to 303 mg/L (Jiang et al., 2006). These experiments were conducted using standard jar test apparatus and the following conditions: 1 minute of rapid mixing at 400 rpm followed by 20 minutes of slow mixing at 35 rpm and finally a 60 minute settling period (Jiang et al., 2006). Samples were withdrawn for analysis at the end of the settling period. Kwon et al. (2014) also used jar test apparatus and achieved *E. Coli* log removals ranging from 2.3 to 2.7 when potassium ferrate(VI) concentrations ranging from 0.02 to 0.09 mM were applied to a clarified secondary effluent. The jar test conditions were: 1 minute of rapid mixing at 150 rpm followed by slow mixing at 30 rpm for 20 minutes and a 30 minute settling period. Contact times ranging from 1 minute to 20 minutes were allowed for each ferrate(VI) concentration (Kwon et al., 2014). While these studies showed ferrate(VI) to be an effective disinfectant, the role of rapid mixing and the simulation of rapid mixing speeds comparable to those utilized in full-scale rapid mixing tanks have not been highlighted previously.

While there is no point of maximum or minimum response for either *E. Coli* or FC removal, TSS removal exhibited an optimal mixing speed of 806 rpm and potassium ferrate(VI) dose of 0.09 mM. TSS removals decreased at higher or lower mixing speeds and potassium ferrate(VI) doses. Potassium ferrate(VI) achieved around 55%

removal of TSS under the optimum conditions. Such low removal efficiency could be explained by the results of other studies. When compared to particles resulting from dosing with ferric chloride Fe(III), the precipitates resulting from potassium ferrate(VI) dosing have shown considerably more nano-size particles with negative charges which contribute to the colloidal suspension stability (Goodwill et al., 2015). Furthermore, it has been reported that potassium ferrate(VI) demonstrated poor settleability when tested on secondary treated effluents (Zheng and Deng, 2016). This outcome was attributed to the slow formation of ferric ions Fe^{3+} that led to inefficient coagulation and flocculation performance (Zheng and Deng, 2016).

While the model found for PO_4^{3-} removal efficiency showed poor agreement between measured and modeled values, there is a remarkable PO_4^{3-} removal efficiency at all conditions. Such poor agreement may be attributed to the noise found in the results at the center point of 750 rpm and 0.075 mM which exhibit a 4.8% coefficient of variation. Recently, it has been reported that most of the phosphate is adsorbed on potassium ferrate(VI) reaction products in the initial 20 minutes at pH less than 8 (Kralchevska et al., 2016). This is due to the sorption of the negatively charged aqueous phosphate species ($H_2PO_4^-$ and HPO_4^{2-}) on the positively charged solid surfaces of ferric oxides/oxyhydroxides nano-particles represented by ɣ-F_2O_4 (maghemite) that has point-of-zero charge (pH_{pzc}) in the range of pH 6.6 to 7.8 and ɣ-FeOOH (lepidocrocite) with pH_{pzc} in the range from 7.2 to 8.4. After being adsorbed onto potassium ferrate(VI) resulting iron(III) oxide/oxyhydroxide nanoparticles, the

phosphate concentrations have been found to slightly fluctuate with time due to sorption/desorption processes (Kralchevska et al., 2016). Such results may account for the noise found in PO_4^{3-} effluent concentrations at the center point where the removal efficiencies ranged from 88.7% to 100%.

2.3.4 Environmental implications

Effluent limits for safe discharge to surface water vary depending on the assimilative capacity of the receiving water. Nevertheless, typical values may be given as 20 mg/L, 200 MPN/100 mL, and 1 mg/L, for TSS, FC and PO_4^{3-}, respectively. For an influent having a TSS concentration equal to the mean TSS of the wastewater used in this study, potassium ferrate(VI) could produce an effluent TSS concentration of about 36 mg/L under optimum conditions. This is higher than the typical TSS limit for discharge to surface water. Under these "optimum conditions", a 3.35 log removal of FC is predicted by the model equation listed in Table 2.4. If the median initial FC counts from this study are considered, this log removal would be equivalent to an effluent 7131 MPN/ 100 mL which is higher than the FC effluent limit typically set. Regarding PO_4^{3-}, all treatment runs achieved final PO_4^{3-} concentrations less than the effluent limit typically set for discharge to surface water in Alberta. Lower potassium ferrate(VI) doses and mixing speeds than reported in the present work may be sufficient to achieve acceptable PO_4^{3-} concentrations if targeted alone (Lee et al., 2009).

A major source of bypass flow is wet weather flow from combined or partially separated sewer systems. In the Canadian context, specific treatment requirements for

these flows have only been instituted in the province of Ontario (CCME, 2014; Ontario Government, 2016). These requirements are less stringent than those set for dry weather conditions in that the flows above dry weather levels must receive treatment equivalent to primary treatment. Specifically, this entails removal of at least 30% of the carbonaceous biochemical oxygen demand and 50% of the TSS. Additionally, the monthly geometric mean of *E. Coli* should not exceed 1000 MPN/100 ml. Based on results of the present study, these limits could be satisfied by applying a potassium ferrate(VI) dosage of 0.10 mM with a rapid mixing speed of 1000 rpm. Such results suggest that potassium ferrate(VI) system could act as a stand-alone treatment for wet weather flows from combined sewers and meet the Ontario requirements.

If compared with the World Health Organization's guidelines, the effluent quality achieved by potassium ferrate(VI), as an independent treatment, could be sufficient for certain types of unrestricted and restricted irrigation reuse purposes (WHO, 2006). For example, the results achieved in this study can satisfy the requirements of options B and C of unrestricted irrigation that respectively require 3 and 2 log removals of *E. Coli*, and the requirements of options F, G, and H of restricted irrigation that require 3, 2 and 0.5 log removals of *E. Coli*; respectively (WHO, 2006). Such reuse strategies should be considered in any effort to establish specific standards for bypass wastewater treatment as it may be economically infeasible to accommodate peak flows within conventional wastewater treatment trains. More specifically, in countries where the effluents of wastewater treatment facilities are being discharged to irrigation canals,

potassium ferrate(VI) can provide efficient stand-alone treatment for indirect irrigation reuse purposes.

2.4 Conclusions

The use of potassium ferrate(VI) for wet weather bypass wastewater treatment was studied using central composite design and response surface methodology. There was good agreement between the actual data and the modeled quadratic models for *E. Coli*, FC, and TSS; consequently, empirical equations developed in this study were able to qualify the relative importance of the operational parameters to the removal efficiencies of the contaminants being modeled. Controlling both mixing speed and potassium ferrate(VI) dosages was found to be of paramount importance to maximize the potassium ferrate(VI) treatment efficiency. The model depicting the PO_4^{3-} removal efficiencies was inadequate to describe the data; however, potassium ferrate(VI) could very effectively remove PO_4^{3-} with at least 88.7% removal and meet the 1 mg/L limit for safe discharge to surface water guidelines in all cases tested. Increasing mixing intensity from the low to center level was beneficial for TSS removal but increasing it above the center level was detrimental. This suggests that sweep floc formation was a dominant TSS removal mechanism. Under the conditions tested in this study, optimum operating parameters for potassium ferrate(VI) treatment to maximize TSS removal were found to be achieved by setting the mixing speed at 806 rpm and applying a dosage of 0.09 mM. However, higher values of both operating parameters can meet

other specific requirements for the safe discharge to surface water and wastewater reuse guidelines for either discharge or reuse.

CHAPTER 3. THE ROLE OF MIXING IN POTASSIUM FERRATE(VI) CONSUMPTION KINETICS AND DISINFECTION OF BYPASS WASTEWATER[2]

3.1 Introduction

Wastewater treatment plants (WWTPs) must bypass excess wastewater flows when factors such as extreme precipitation patterns or increased effective population density have not been accounted for during the planning and design stages. The magnitudes of these peak flows frequently require diversion of at least some raw combined wastewater to receiving waters in order to protect treatment plant biological processes from microbial washout. The volume of these bypass releases is likely to increase elevating the mass of contaminants diverted to water bodies (Fono and Sedlak, 2005; Marsalek and Rochfort, 2004) and the concomitant deleterious effect on surface water quality (Passerat et al., 2011). As a component of the overall management of these combined flows, in-plant treatment strategies should be developed to adequately handle such surges (U.S. EPA, 2013). A variety of treatment methods have been proposed. These include primary sedimentation enhanced by chemical coagulants or settling tubes or lamella (Gehr et al., 2003; Jolis and Ahmad, 2004; U.S. EPA, 2013, 1999b). Less stringent wastewater discharge limits are usually adopted for the treated

[2] A version of this chapter has been submitted to Journal of Environmental Management as "Elnakar, H. and Buchanan, I.: The role of mixing in potassium ferrate(VI) consumption kinetics and disinfection of bypass wastewater".

effluent from such auxiliary/primary treatment facilities such as those adopted in Ontario, Canada that recommend at least 50% TSS removal with monthly geometric means of *E. Coli* not exceeding 1000 counts/ 100 mL (Ontario Government, 2016). Among other criteria, the most appropriate disinfection reagent would be that which could achieve the required microorganism abatement prior to discharge without forming toxic by-products that would threaten the receiving environment (U.S. EPA, 2013, 1999b).

Potassium ferrate(VI) is a rare example of iron in its +6 oxidation state and is considered one of the promising green and multi-purpose chemical enhancement alternatives to the primary sedimentation process (Murmann and Robinson, 1974; Sharma, 2002). Potassium ferrate(VI) can perform as an oxidizing disinfectant and as a coagulant (Jiang, 2007; Jiang et al., 2006; Jiang and Lloyd, 2002; Sharma, 2002; Tien et al., 2008) as it is able to simultaneously produce oxygen (O_2) and ferric hydroxide ($Fe(OH_3)$) as per Reaction 1 (Patterson et al., 2001). Peracetic acid, performic acid, or ozone used for the disinfection of bypass-like wastewater, such as combined sewer overflow, do not have both disinfection and coagulation capabilities (Chhetri et al., 2014; Gehr et al., 2003).

$$4K_2FeO_4 + 10H_2O \rightarrow 4Fe(OH)_3 + 8KOH + 3O_2 \quad (3.1)$$

The disinfection potential of potassium ferrate(VI) has been investigated using several strains of microorganisms in pure water, buffered water, river water, ballast water and

secondary wastewater effluents (Cho et al., 2006a; Gilbert et al., 1976; Hu et al., 2012; Jessen et al., 2008; Jiang et al., 2006; Kazama, 1995; Kwon et al., 2014; Murmann and Robinson, 1974; Schink and Waite, 1980; Waite, 1979). Furthermore, potassium ferrate(VI) was demonstrated to not lead to any sort of reversible inactivation or regrowth of the tested microorganisms (Basu et al., 1987; Hu et al., 2012; Jessen et al., 2008; Stevenson and Davies, 1995). Table 3.1 summarizes the range of pH values, dosages, contact times, and disinfection models tested on fecal indicator microorganisms. As it can be seen from Table 3.1, there is very little information in the literature about wastewater disinfection using potassium ferrate(VI) especially using real wastewater samples. In addition, the disinfection capabilities of potassium ferrate(VI) in a wet weather bypass wastewater matrix have not been reported before in the literature.

For a given temperature and water matrix, four main parameters usually affect the potassium ferrate(VI) disinfection process. These are potassium ferrate(VI) dosage, contact time, pH, and mixing conditions. While the ranges of potassium ferrate(VI) dosages and contact times reported in the literature vary widely, the required dosages are usually less than those required by other chemicals used for the same treatment goal (Jiang et al., 2006). In addition, controlling potassium ferrate(VI) treatment by pre-acidification or alkalization may be effective as shown in Table 1, but if pH adjustment is required, treatment costs will increase. Another factor of importance is the mixing conditions which have been demonstrated to have a significant impact on

disinfection (Field, 1973; Metcalf & Eddy, 2004; U.S. EPA, 1999b). However, the literature contains no report of the extent to which mixing speed impacts potassium ferrate(VI) disinfection capabilities.

In this study, the effect of different mixing conditions on potassium ferrate(VI) dissociation and *Escherichia coli* (*E. Coli*) removal is investigated in four bypass wastewaters without pH adjustment. Potassium ferrate(VI) consumption is modeled to estimate the kinetic constants at different mixing speeds with the goal of selecting appropriate lower mixing speeds for exiting mixing facilities based on the concept of kinetically controlled reaction (i.e. the mixing speed above which mixing speeds do not affect reaction rates). In addition, inactivation models are tested to generate a representative model of *E. Coli* disinfection by potassium ferrate(VI).

3.2 Materials and methods

3.2.1 Source water

The wastewater samples used in this study were obtained during four sampling campaigns, designated S06, S15, O26, and N27, which were carried out during wet weather flow events at a wastewater treatment plant in central Alberta, Canada. Samples were stored at 4^{o}C in a cold room. These samples are representative of wet weather wastewater that would bypass the biological treatment process to prevent microbial washout. The samples were collected from a channel leading from the grit removal process to the primary sedimentation tanks. The characteristics of the four bypass wastewater samples are summarized in Table 3.2.

Table 3.1 Summary of potassium ferrate(VI) disinfection information available in the literature: fecal indicator microorganisms, pH values, dosages, contact times, and disinfection models

Water matrix	Indicator Organism	Potassium ferrate(VI) Dosage (mM)	Contact Time (minutes)	Initial pH	Log Removal	Disinfection Model	Reference
Phosphate buffer	*E. Coli* pure cultures	0.05	14	8.0	3.0	Chick- Watson	(Gilbert et al., 1976)
		0.05	8	8.2	3.0		
		0.05	7	8.5	3.0		
	E. Coli strain ATCC 8739	0.03	4	5.6	4.5	Modified Delayed Chick–Watson model	(Cho et al., 2006a)
		0.03	10	8.2	4.5		
		0.03	5	7.2	3.2		
		0.11	1	7.2	3.2		
Tap water	*E. Coli* pure cultures	0.07	25	5.5	8.0	Chick- Watson	(Jiang et al., 2007)
		0.11	30	7.5	8.0		

Water matrix	Indicator Organism	Potassium ferrate(VI) Dosage (mM)	Contact Time (minutes)	Initial pH	Log Removal	Disinfection Model	Reference
Lab-made river water	*E. Coli* pure cultures	0.11	30	8.0	8.5	-	(Jiang et al., 2006)
Lab-made ballast water	*E. Coli* strain ATCC 11303	0.04	5	8.0	6.8	Hom	(Jessen et al., 2008)
	Enterococci strain ATCC 19434	0.04	5	8.0	5.5		
River water spiked with *E. Coli*	River water *E. Coli* in addition to spiked *E. Coli* strain ATCC 8739	0.01	30	7.1	3.7	Modified Delayed Chick–Watson model	(Cho et al., 2006a)
		0.09	1	7.1	3.2		
Secondary effluent	*E. Coli*	0.02 - 0.09	20	7.0 - 8.0	2.3 - 2.7	Chick- Watson	(Kwon et al., 2014)
	Total Coliforms	0.08	30	7.0 - 8.0	4	-	(Waite, 1979)
	Fecal Coliforms	0.08	30	7.0 - 8.0	4		
Raw influent	Total Coliforms	0.27	81	7	>4	-	(Jiang et al., 2006)
	Fecal Coliforms	0.27	81	7	>4		

Table 3.2 Key characteristics of bypass wastewater samples out of wet weather events used in the present study.

Parameter	Units	S06		S15		O26		N27	
		Median	Standard Deviation	Median	Standard Deviation	Median	Standard Deviation	Median	Standard Deviation
pH	-	6.7	0.2	7.5	0.0	6.8	0.1	6.9	0.1
Zeta Potential	mV	23.0	2.0	28.5	1.5	16.5	4.5	23.0	2.0
Total Chemical Oxygen Demand	mg tCOD/L	280.0	70.8	512.5	61.6	932.0	56.1	766.5	87.6
Soluble Chemical Oxygen Demand	mg sCOD/L	215.0	54.6	394.5	47.6	669.0	55.1	655.0	43.1
Total Suspended Solids	mg TSS/L	83.0	12.1	241.5	8.6	315.0	33.0	270.0	52.1
Volatile Suspended Solids	mg VSS/L	44.0	9.1	134.0	3.0	191.0	27.0	188.0	42.1
Total Phosphorus	mg P/L	7.4	0.3	7.5	0.8	18.3	1.1	15.2	0.4
Reactive Phosphorus	mg P/L	6.8	0.4	6.9	0.7	16.4	1.0	13.7	0.3
Escherichia coli	MPN/100mL	4.0E+06	1.2E+06	7.9E+05	4.0E+05	1.6E+06	6.7E+05	9.1E+06	3.0E+05
Total Coliforms	MPN/100mL	2.6E+07	1.1E+07	5.2E+06	3.0E+06	1.2E+07	6.0E+06	8.3E+07	2.5E+06
Fecal Coliforms	MPN/100mL	1.6E+07	4.0E+06	2.2E+06	9.5E+05	6.7E+06	5.4E+06	4.0E+07	2.7E+07

Note: Median and standard deviation values of each parameter for each sampling campaign are based on at least four subsamples measured in duplicate.

3.2.2 Experimental procedures

Experiments were conducted at room temperature (25 ± 1 ºC) in 2-L square beakers containing 1-L of bypass wastewater sample. Preliminary experiments were conducted without pH adjustment using potassium ferrate(VI) as the only chemical to be added to bypass wastewater samples. This condition was selected to assess the effect of potassium ferrate(VI) on wastewater pH when it is used as the sole treatment reagent. As shown in Figure 3.1, potassium ferrate(VI) was added to the samples under magnetic stirrer mixing to yield initial concentrations of 0.01, 0.05, 0.1, 0.15 or 0.2 mM. pH was measured after 80 minutes. This was done to determine the highest potassium ferrate(VI) dosage that could be applied without causing the final pH to exceed the maximum of pH 9.5 for discharge to surface waters in Alberta (Alberta Government, 2013).

The bypass wastewater samples' characteristics were measured before each experiment. pH was measured using an Accumet electrode and Accumet Excel (Fisher Scientific, Ottawa, ON, Canada). Total suspended solids (TSS) and volatile suspended solids (VSS) were analyzed using standard methods 2540-D and 2540-E; respectively (APHA AWWA WEF, 1998). The following parameters were analyzed using HACH methods with specific method numbers in parentheses (HACH, USA): total and soluble chemical oxygen demand (tCOD and sCOD) (8000), and total phosphorus (10127), reactive phosphorus (8048). Total Coliform, FC, and *E. Coli* (in most

probable number per 100 ml) were determined from a 100 ml diluted sample using Colilert®-18 media and the IDEXX Quanti-Tray®/2000 kit (IDEXX, USA).

A mixer (IKA, USA) was operated during the rapid mixing stage for 1 minute at a mixing speed of either 500, 750, or 1000 rpm. The 2-L square beakers containing the samples were then immediately placed in the variable speed gator jar test apparatus (Phipps & Bird, USA) and stirred at 30 rpm for 20 minutes in all runs. The same flat paddle impeller (25 mm x 75 mm) was used at all mixing stages. The experiments that entailed rapid then slow mixing speeds will be denoted as varied speed mixing in this study. Beyond the first 21 minutes of varied speed mixing, samples were allowed to settle for 60 minutes with no-mixing applied. For magnetic stirrer mixing experiments, nominal operating speed was set at an average of 1000 rpm and maintained continuously for 81 minutes.

Samples were withdrawn at predetermined times (see Table A1 in Appendix A). During the *E. Coli* inactivation study, samples were immediately quenched with excess sodium thiosulfate ($Na_2S_2O_3$). Each quenched sample was diluted serially. Individual data points represent results from three different dilutions with each dilution being measured in duplicate. For potassium ferrate consumption tests, residual potassium ferrate(VI) was quenched with excess 2,2'-azino-bis(3-ethylbenzothiazoline-6-sulphonic acid) or ABTS as soon as a sample was withdrawn from the test beaker (Lee et al., 2005). This assay was utilized because ABTS can immediately quench the residual potassium ferrate(VI) in a sample and allows a time lag between quenching

and absorbance measurement (Cataldo et al., 2017). The sample absorbance at 415 nm was measured within 30 minutes of ABTS addition using a spectrophotometer (Varian Inc., Santa Clara, CA, USA).

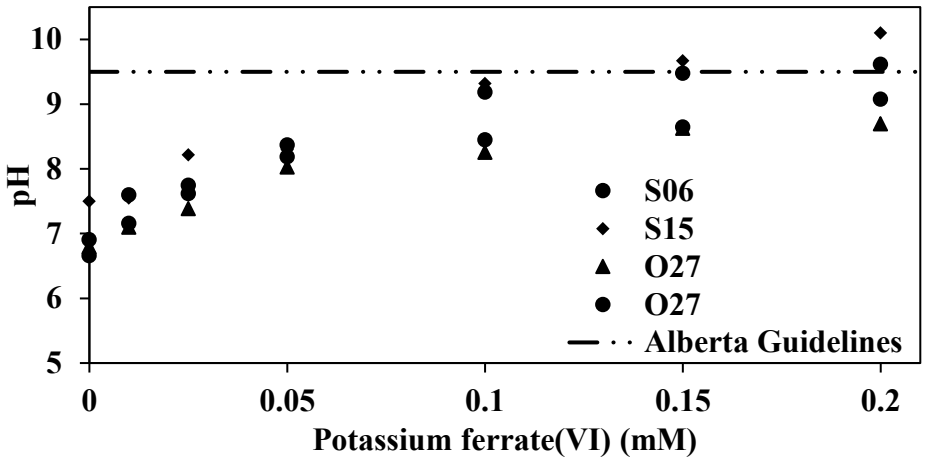

Figure 3.1 pH measured after 80 minutes of magnetic stirring in bypass wastewater samples having initial potassium ferrate(VI) concentrations of 0.01, 0.05, 0.1, 0.15 or 0.2 mM.

3.2.3 Chemicals and reagents

The wet method was used for the preparation and purification of potassium ferrate(VI) (Thompson et al., 1951). The purity of potassium ferrate(VI) product was measured at the day of each set of experiments by both the ABTS method at 415 nm and the spectrophotometric method at 510 nm and was found to be higher than 90%. Stock solutions of potassium ferrate(VI) were freshly prepared just before conducting the experiments by dissolving the potassium ferrate(VI) in its solid form in ultrapure water. Reagent-grade ABTS, $Na_2S_2O_3$, boric acid (H_3BO_3), and other reagents were purchased from Sigma-Aldrich. All aqueous solutions were prepared at the time of

each sampling event with ultrapure water produced by a Milli-Q system (Millipore, Sigma, USA).

3.2.4 Mathematical models

3.2.4.1 Potassium ferrate(VI) consumption modeling

First-order, second-order, and double exponential models were fit to the potassium ferrate(VI) residual data in order to elucidate the kinetics of potassium ferrate(VI) consumption. The first-order and second-order models are expressed in Equations 3.1 and 3.2, respectively.

$$[\text{Potassium ferrate(VI)}]_T = [\text{Potassium ferrate(VI)}]_o . \exp^{-k_1 . T} \quad (3.1)$$

$$[\text{Potassium ferrate(VI)}]_T = \frac{[\text{Potassium ferrate(VI)}]_o}{1 + k_2 . [\text{Potassium ferrate(VI)}]_o . T} \quad (3.2)$$

where: $[\text{Potassium ferrate(VI)}]_T$ is the potassium ferrate(VI) concentration at time T, $[\text{Potassium ferrate(VI)}]_0$ is the potassium ferrate(VI) initial concentration in mM, k_1 is the first-order rate constant in min^{-1}, k_2 is the second-order rate constant in $mM^{-1}min^{-1}$, and T is the time (min).

Another model of interest is the double exponential model represented by Equation 3.3 in which there are an initial rapid reaction phase and a subsequent slower reaction phase; each of which is modeled as a first-order reaction. The first phase can describe the rapid dissociation of potassium ferrate(VI) due to the disinfectant / oxidant demand exerted by the organic substances in wastewater, and the second phase can represent

potassium ferrate(VI) consumption beyond the oxidant demand effect. The double exponential model has been used previously to describe chlorine demand (Haas and Karra, 1984a, 1984b).

$$[\text{Potassium ferrate(VI)}]_T = [\text{Potassium ferrate(VI)}]_o.\left[x.\exp^{-k_{DE1}.T} + (1-x).\exp^{-k_{DE2}.T}\right] \quad (3.3)$$

where x is the fraction of potassium ferrate(VI) consumed in the first phase of the double exponential model; k_{DE1} and k_{DE2} are the rate constants in min^{-1} for the first and second phases of the double exponential model; respectively.

3.2.4.2 *E. Coli* disinfection modeling

Potassium ferrate(VI) disinfection data were modeled using Chick–Watson and Hom models. The integrated form of the Chick–Watson model is described by Equation 3.4 (Haas and Karra, 1984b).

$$\text{Log}\left(\frac{N_T}{N_o}\right) = -k_{CW}\left[\overline{\text{Potassium ferrate(VI)}}\right]^{a_{CW}}T \quad (3.4)$$

where N_0 and N_T are the *E. Coli* enumerated in MPN / 100mL at times zero and T, respectively; k_{CW} is the Chick–Watson disinfection reaction rate constant; $\left[\overline{\text{Potassium ferrate(VI)}}\right] = \int_0^T \text{Potassium ferrate(VI)}.dt/T$ is the average potassium ferrate(VI) concentration over treatment time T in mM; T is the reaction time in minutes, and a_{CW} is an empirical parameter representing the relative importance of average potassium ferrate(VI) concentration.

The Hom model is a variation of the Chick-Watson model in that an empirical exponent (b_H) is applied to the time (T) (Haas and Karra, 1984b). The integrated form of the Hom model is represented by Equation 3.5.

$$\mathrm{Log}\left(\frac{N_T}{N_o}\right) = -k_H\left[\overline{\text{Potassium ferrate(VI)}}\right]^{a_H} T^{b_H} \quad (3.5)$$

3.3 Results and Discussion

3.3.1 Bypass wastewater characteristics

As shown in Table 3.2, the characteristics of bypass wastewater samples varied from one wet weather event to another. Moreover, the constituents' median sCOD values (215-669 mg/L) suggest that it would have high oxidant demand. In addition, the VSS/TSS ratio had an average of 0.56 which is low for a municipal sanitary influent (Henze and Comeau, 2008; Metcalf & Eddy, 2004) and indicates the presence of significant amounts of inorganic solids from storm water in the bypass wastewater. The number of *E. Coli* indicator organisms measured in bypass wastewater changed from one event to the other from as low as 7.9×10^5 / 100 mL for the S06 sampling event to as high as 9.1×10^6 / 100 mL for N27. While each sample was obtained as a grab sample, together they revealed the stochastic characteristics of the bypass wastewater.

3.3.2 Potassium ferrate(VI) concentration profiles

The model fitting parameters of the first-order, second-order and double exponential models of the potassium ferrate(VI) consumption with time are summarized in Table

A2 in Appendix A. The coefficients of determination (R^2) are higher than 95% for all models and all conditions. The second-order model represented by Equation 3.2 has been reported elsewhere to be a better fit model than the first order model for potassium ferrate(VI) decay (Barlsçl and Dimoglo, 2016; Cho et al., 2006a; Jiang et al., 2015; Lee et al., 2014, 2009, 2004; Rush et al., 1996; Shin and Lee, 2016; Tiwari et al., 2007) Comparison of the results from the first order model to those of the second order model indicates that the second-order model is indeed a better fit for magnetic stirring mixing conditions, which is the mixing method used in the papers that concluded the superiority of second-order model. However, considering all models and mixing conditions, the double exponential model represented by Equation 3.3 is found to better represent the potassium ferrate(VI) consumption in terms of having the highest coefficient of determination (R^2) values and lowest root mean square error (RMSE). The lowest R^2 value is 97.20% and the maximum RMSE is 0.0058; both for S15 sampling event and at 750 rpm rapid mixing speed.

Using the double exponential model, it was found that under rapid mixing conditions 85% to 96% of the dosed potassium ferrate(VI) was consumed in the first phase of the double exponential model which represents the immediate demand exerted by the wastewater constituents on potassium ferrate(VI), while 82% to 86% was consumed during this phase under magnetic stirrer mixing conditions.

Figure 3.2 is a plot of residual potassium ferrate(VI) against reaction time in the S06 sample at 750 rpm mixing speed. Potassium ferrate(VI) concentration declines rapidly

from its initial 0.1 mM concentration. The first-order model is able to capture the initial phase of potassium ferrate(VI) consumption representing the wastewater oxidant demand, whereas the second-order model captures the potassium ferrate(VI) consumption beyond the initial oxidant demand. However, the double exponential model captures both profiles. This shows the applicability of the double exponential model over the entire reaction period and its superiority to the first-order and second-order models.

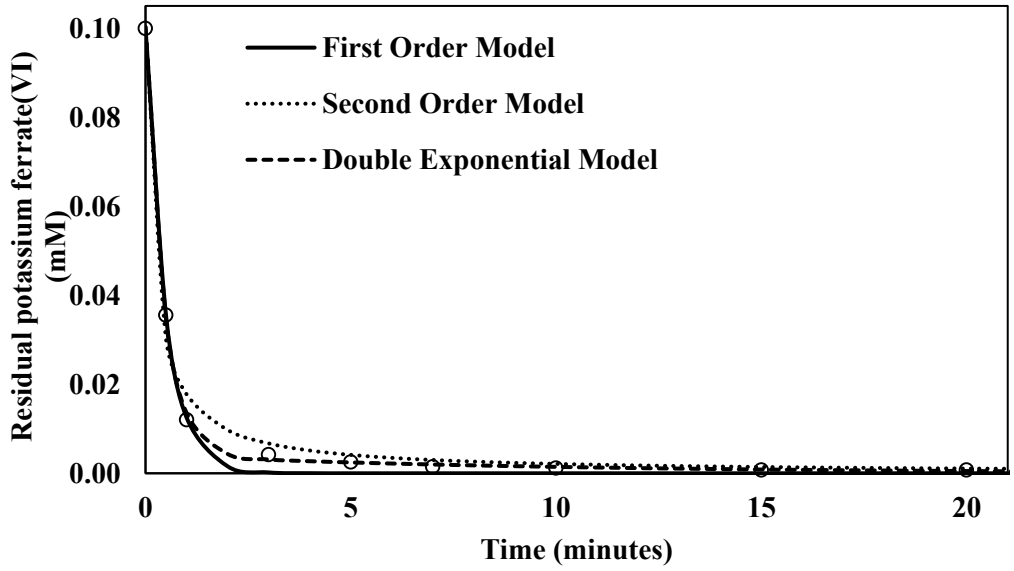

Figure 3.2 Observed residual potassium ferrate(VI) using an initial 0.1 mM dosage at 750 rpm mixing speed for S06 sample

Few studies or professional reports discuss the role of mixing in disinfection studies (Field, 1973; Metcalf & Eddy, 2004; NSF and US EPA, 2002; U.S. EPA, 1999b). In an attempt to understand the role of mixing on the initial potassium ferrate(VI) demand, Reynolds's numbers (R_e) were estimated. In a study that investigated the

vortex flow generated by a magnetic stirrer, the maximum R_e was found to be around 5 x 10^3 (Halász et al., 2007). The mixing regime using magnetic stirrer mixing was then considered transitional with one order of magnitude less than the lowest R_e number estimated in this study for a mixing speed of 500 rpm which was found to be around 4.7 x 10^4 representing turbulent conditions (Cornwell and Bishop, 1983). Turbulent conditions at 500 rpm mixing speeds and beyond were observed to increase the percentage of potassium ferrate(VI) immediately consumed by wastewater oxidant demand when compared to transitional conditions produced by magnetic stirrer mixing (Figure 3.3).

The measured potassium ferrate(VI) concentrations and the fitted double exponential consumption profiles following the application of 0.1 mM of potassium ferrate(VI) to each of the four samples are shown in Figure 3.3. Potassium ferrate(VI) decay rates were found to be relatively consistent under all sampling events and mixing conditions. The range of pH values covered by the four sampling events was apparently not great enough for the phenomenon of potassium ferrate(VI) reactivity increasing with decreasing pH to be observed as it had been in other studies (Cho et al., 2006a; Manoli et al., 2017). The values of k_{DE1} for potassium ferrate(VI) consumption in rapid mixing conditions of 500 rpm and beyond were higher than those for magnetic stirrer mixing for the same initial dosage. For the second phase of the double exponential model, k_{DE2} values were higher in the magnetic stirrer mixing conditions than those for the rapid mixing conditions. This can be interpreted as the reaction rate being influenced by the

greater second phase mixing speed provided by magnetic stirring, whereas the second phase mixing speed was reduced to 30 rpm under the varied speed mixing conditions.

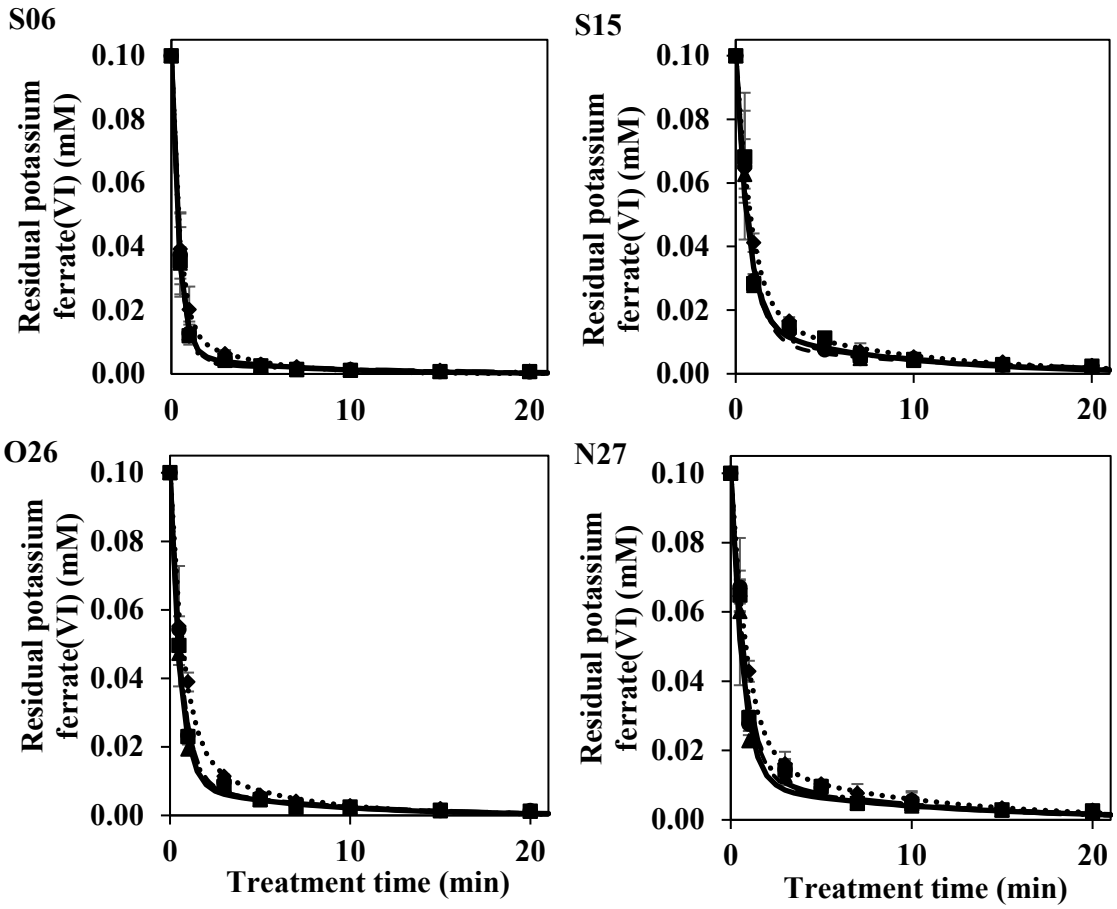

Figure 3.3 Observed residual potassium ferrate(VI) using 0.1 mM of potassium ferrate(VI) in bypass wastewater samples from different wet weather events at different mixing speeds. Mixing speeds: ● for 500 rpm; ■ for 750 rpm; ▲ for 1000 rpm; and ◆ for magnetic stirrer mixing; and double exponential model fits for different events at different mixing speeds represented by ----- for 500 rpm; – · – for 750 rpm; —— for 1000 rpm; and ..... for magnetic stirrer mixing.

Overall, the double exponential model rate constants of the phase 1 reactions, k_{DE1}, were not found to increase significantly (p-value > 0.05) with the increase of rapid

mixing speeds. This indicates that the reactions involved could be considered to be kinetically controlled because the increase in mixing speed did not affect the reaction rates. Consequently, potassium ferrate(VI) could be accommodated within existing coagulation facilities at mixing speeds as low as 500 rpm, which correspond to a velocity gradient of 1100 s^{-1}. While no speciation of the reaction products after mixing was conducted in this study, the lower limit of mixing intensity to maintain kinetically controlled conditions should be investigated in any future studies that address the kinetics of potassium ferrate(VI). On one hand, the concept of kinetically controlled reaction will justify the selection of appropriate lower mixing speeds than those currently used in coagulation practice, and on the other hand, rapid mixing facilities can be designed and operated based on lower energy consumption.

3.3.3 Modeling potassium ferrate(VI) disinfection

Modeling *E. Coli* inactivation in bypass wastewater matrix or a "high oxidant demand" water matrix has not been investigated as per the surveyed literature to date. The log-linear Chick–Watson model has been recommended for the application of potassium ferrate(VI) to secondary effluents or model *E. Coli* strains in pure water, filtered river water or phosphate buffer as depicted in Table 3.1. The Hom model has been applied to represent the disinfection data from potassium ferrate(VI) treatment of *E. Coli* in simulated ship ballast water (Jessen et al., 2008) and of Qβ bacteriophages in buffered water (Kazama, 1995).

The fitting parameter results of Chick-Watson and Hom models representing potassium ferrate(VI) disinfection data for different mixing speeds, events, and initial dosages are listed in Table A3 in Appendix A. *E. Coli* log removals for different initial potassium ferrate(VI) concentrations and mixing speeds in each bypass wastewater sample together with the Chick Watson and Hom fitted curves are plotted in Figures 3.4 and 3.5, respectively. Both the Chick-Watson and Hom models were able to fit the inactivation results with at least R^2 = 95% with the Chick-Watson model demonstrating the higher R^2 values for all conditions except the 0.075 mM potassium ferrate(VI) dosing of sample S06 at the 500 rpm mixing speed. The RMSE associated with the Chick-Watson and Hom model fits were generally low with little difference from one model to the other.

Regarding the role of mixing in disinfection and considering the Chick-Watson model, the k_{CW} values were found to be higher for varied speed mixing than for magnetic stirrer mixing-based experiments under all conditions. However, k_{CW} did not increase with increasing rapid mixing speeds in the varied speed mixing experiments. Therefore, the increase of rapid mixing speeds from 500 to 1000 rpm was not shown to improve disinfection performance. Under the conditions tested in this study, the lower mixing speed of 500 rpm (1100 s^{-1} velocity gradient) resulted in lower energy input for potassium ferrate(VI) disinfection purposes.

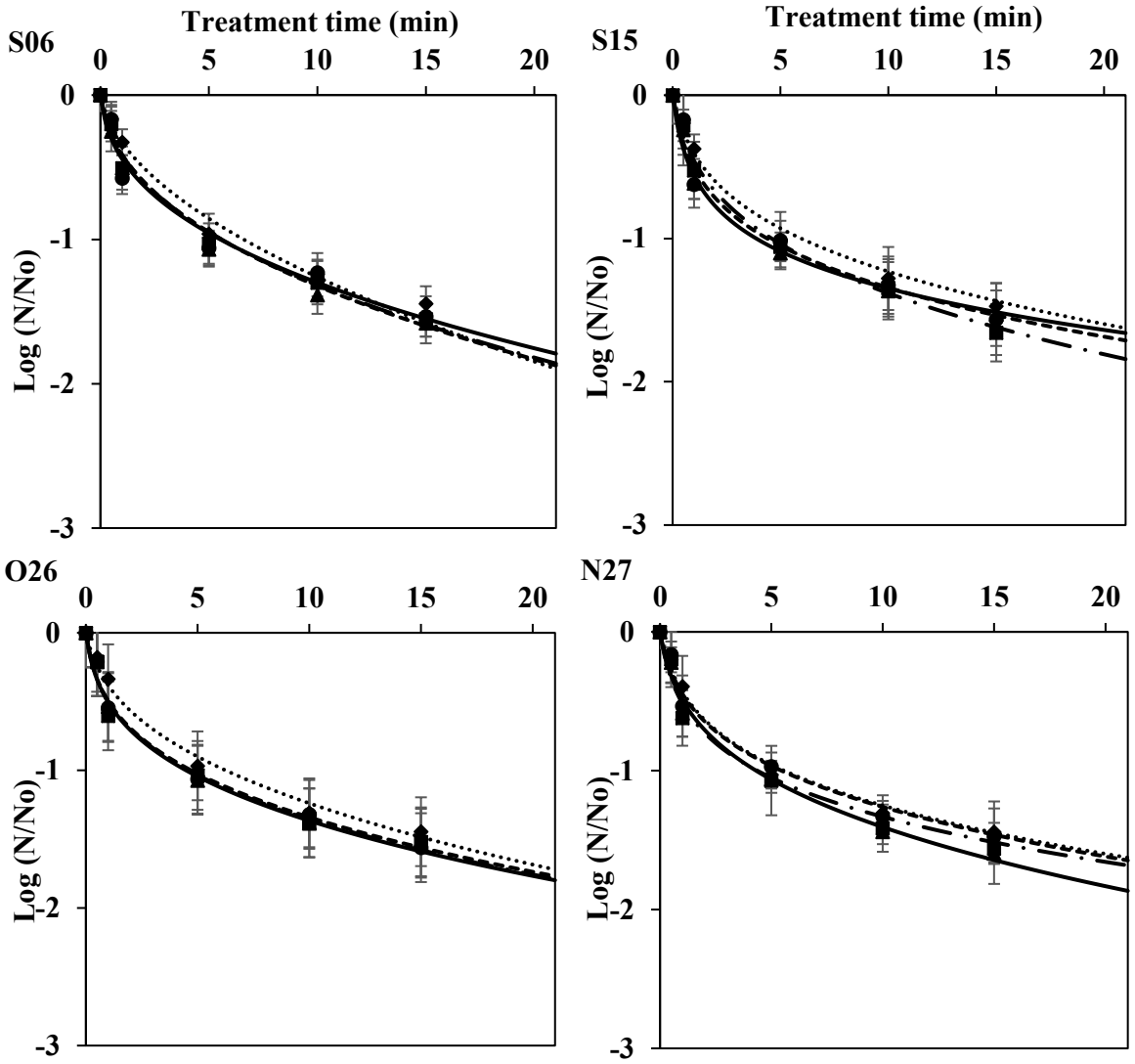

Figure 3.4 Actual disinfection data for different bypass wastewater samples from different wet weather events at different mixing speeds. Mixing speeds: ● for 500 rpm; ■ for 750 rpm;▲for 1000 rpm; and ◆for magnetic stirrer mixing and Chick–Watson model fits for different sampling events at different mixing speeds represented by ----- for 500 rpm; – · – for 750 rpm; —— for 1000 rpm; and ..... for magnetic stirrer mixing

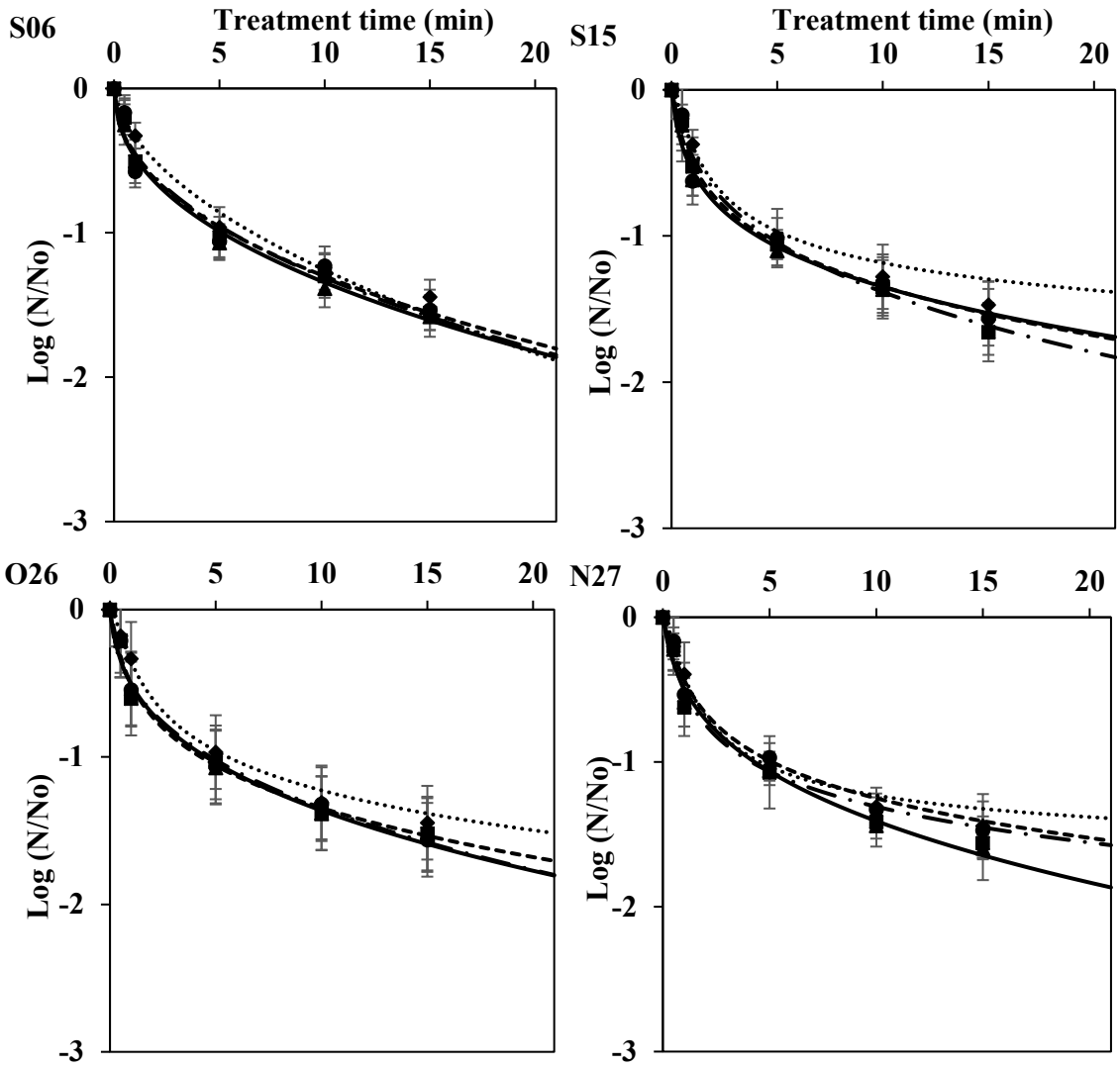

Figure 3.5 Actual disinfection data for different events at different mixing speeds. Mixing speeds: ● for 500 rpm; ■ for 750 rpm; ▲ for 1000 rpm; and ◆ for magnetic stirrer mixing and Hom model fits for bypass wastewater samples from different wet weather events at different mixing speeds represented by ----- for 500 rpm; – . – for 750 rpm; —— for 1000 rpm; and ..... for magnetic stirrer mixing

3.3.4 Effect of sedimentation stage

The samples taken in the first 21 minutes of the disinfection trials yield information about *E. Coli* chemical inactivation by potassium ferrate(VI). Beyond 21 minutes, mixing was stopped in disinfection tests that employed varied speed mixing, while mixing was continued in the tests that used magnetic stirrer mixing to duplicate the potassium ferrate(VI) disinfection conditions typically reported in the literature. As potassium ferrate(VI) had been nearly consumed during the first 21 minutes (see Figure 3.2), the only removal mechanism beyond this time in the varied speed mixing tests would be the sedimentation of *E. Coli*. Figure 3.6 shows the contribution of chemical inactivation and the sedimentation mechanisms to the overall *E. Coli* removal after 81 minutes. In addition, the *E. Coli* removal after the 81 minutes treatment time under continuous magnetic stirrer mixing is shown in Figure 3.6.

It can be seen from Figure 3.6 that there is an approximately equal contribution from the chemical inactivation by potassium ferrate(VI) and sedimentation of *E. Coli* to the overall log removal. To further weigh the relative importance of chemical inactivation and sedimentation in potassium ferrate(VI) treatment, samples tested during experiments of the N27 event at 0.1 mM potassium ferrate(VI) dosage and 1000 rpm mixing speed were allowed to settle for one day after being quenched with $Na_2S_2O_3$ to neutralize the disinfectant residual. A maximum difference of 7% percent was found in the *E. Coli* enumeration after 1-day settling (Data not shown). This proved that the

sedimentation stage was enhanced by the capability of potassium ferrate(VI) to produce flocs in the coagulation-flocculation mixing schemes.

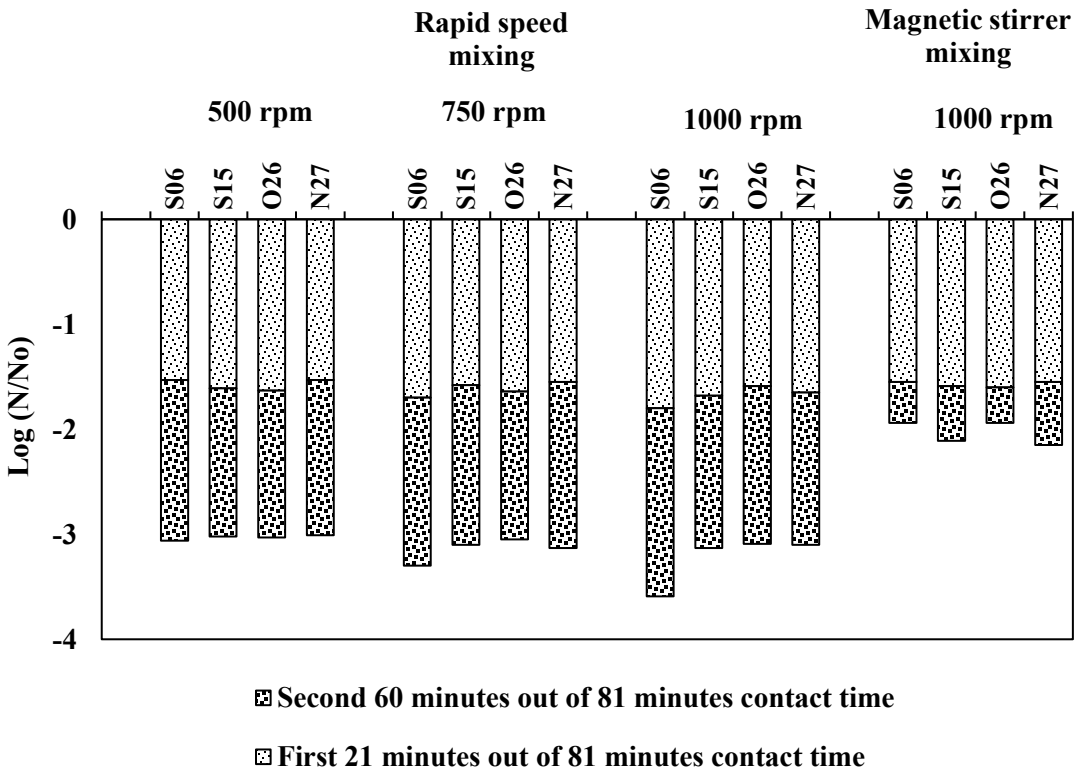

Figure 3.6 The impact of mixing and sedimentation on potassium ferrate(VI) disinfection performance after 81 minutes. Initial potassium ferrate(VI) = 0.1 mM. Test designations include sampling and mixing information. For the rapid mixing conditions, the first 21 minutes represent coagulation – flocculation stages and the second 81 minutes represent sedimentation stage. For the magnetic stirrer mixing, all 81 minutes represent continuous mixing regime.

3.3.5 Overall potassium ferrate(VI) disinfection efficiency

The potassium ferrate(VI) disinfection was consistent and nearly independent of the bypass wastewater matrix strength over all tested conditions as shown in Figure 3.6. This revealed that wastewater strength, and thus the fluctuations in the *E. Coli* indicator organism numbers over a wet weather flow event had little to do with potassium ferrate(VI) disinfection efficacy. An average 3.2 log removal was found after combined varied speed mixing and sedimentation stages while an average 2.0 log removal was observed for continuous magnetic stirrer mixing. As per the surveyed literature, only one study (Jiang et al., 2006) reported potassium ferrate(VI) efficacy on the disinfection of "high oxidant demand" wastewater such as the one reported in this study. A high potassium ferrate(VI) dosage of 0.27 mM was used by (Jiang et al., 2006) who reported more than 4 log removal of both total and fecal coliforms from raw wastewater influent. The final pH resulting from such a high dosage was not reported.

Few studies have investigated disinfection technologies for bypass wastewaters or "high oxidant demand" wastewaters such as the ones tested in this study. A 30 to 50 mg / L ozone concentration was required to achieve 2 log removal of fecal coliforms in effluent from enhanced primary treatment (Gehr et al., 2003). A dosage range from 4.5 to 6.0 mg/L of 12% PAA with a constant contact time of 60 minutes yielded 2.2 to 4.1 log reduction for fecal coliform in the same effluent (Gehr et al., 2003). Peracetic acid (PAA) at 2.5 mg / L achieved 4 log removal of *E. Coli* from combined sewer

overflows over a total treatment time of 360 min (Chhetri et al., 2014). The log removal of *E. Coli* using Performic acid was found to be above 3 using 2 to 4 mg / L with a 20 minutes contact time (Chhetri et al., 2014). The potassium ferrate(VI) treatment using varied speed mixing treatment scheme followed by sedimentation reported in this study achieved comparable log removals, which suggests the process may be appropriate to disinfect bypass flows, yet the economics of using potassium ferrate(VI) remain to be fully investigated.

3.4 Conclusions

The role of mixing on the rates of both potassium ferrate(VI) decay and microorganism inactivation was investigated in four different bypass wastewater samples. The double exponential model was found be superior to both the first-order and the second-order models in fitting experimental ferrate(VI) decay data. It represents the trend of potassium ferrate decay very well over the entire reaction period, unlike the first-order or second-order models, which fit the data well only for the rapid or slow reaction phases, respectively. The rate of potassium ferrate decay was found to be independent of mixing intensity above a mixer velocity gradient of 1100 s^{-1}. This was also the case for the rate of *E. Coli* inactivation. This suggests that relatively low mixing energy input would be required if potassium ferrate(VI) were used in existing enhanced primary treatment processes. Potassium ferrate removed *E. Coli* by chemical inactivation and by floc-assisted sedimentation. Physical removal by sedimentation represented approximately 50% of the overall *E. Coli* removal.

CHAPTER 4. ENHANCED PRIMARY TREATMENT OF MUNICIPAL WASTEWATER USING IRON ELECTROCOAGULATION: PRESPECTIVES ON SOLUBLE CHEMICAL OXYGEN DEMAND REMOVAL[3]

4.1 Introduction

A nation's ability to treat its wastewater is closely related to its level of economic and institutional development. Global trends suggest that countries in the high, middle, lower middle, and lower per-capita gross domestic product (purchasing power parity or PPP) categories treat about 70%, 38%, 28% and 8% of their municipal and industrial wastewater, respectively (UNESCO, 2017). The lower PPP category or developing countries are particularly challenged in achieving the wastewater treatment goals stated in the "2030 Agenda for Sustainable Development" due to absent or undersized infrastructure, as well as a lack of technical and institutional capacity, and funding (UN, 2015; UNESCO, 2017). It is estimated that 74% of existing urban and 66% of existing rural wastewater services are not effective in preventing human contact with untreated or partially treated wastewater (UNESCO, 2017). Therefore, a multi-faceted solution is required, with its technical aspects including (1) the construction of new facilities to increase the proportion of generated wastewater that is treated; and (2) the

[3] A version of this chapter will be submitted as "Elnakar, H. and Buchanan, I.: Enhanced primary treatment of municipal wastewater using iron electrocoagulation: Perspectives on soluble chemical oxygen demand removal".

retrofitting of existing facilities to improve their effectiveness in protecting public health. Both of these initiatives would entail securing adequate infrastructure capable of adapting to the challenges of climate change, growing population, and demographic trends (IPCC, 2007; OECD, 2011). Consequently, there is an immediate need for wastewater technological development to leverage the existing treatment systems or to provide more effective options to the new plants.

Physically and/or chemically enhanced primary sedimentation can be placed as one of the first processes in a typical wastewater treatment train (Metcalf & Eddy, 2004); can be used as a stand-alone auxiliary treatment for wastewater flows that exceed treatment plant capacity (City of Edmonton, 2000); or when followed by a disinfection step, can be used to treat wastewater generated by sources ranging from small rural communities to large cities (Gehr et al., 2003; Harleman and Murcott, 1999; Wang et al., 2009). The enhancement of primary sedimentation tanks can be done using physical means such as lamella plate settlers or by chemical means such as chemical coagulation. Such enhancements allow the primary sedimentation tanks to be designed or retrofitted to accommodate higher overflow rates which reduce capital cost. In addition, higher removal efficiencies can be achieved (Harleman and Murcott, 1999; Metcalf & Eddy, 2004).

Electrochemical processes such as electrolysis, electrocoagulation, and electroflotation are attractive alternative enhancement techniques to primary sedimentation process. Notably, iron electrocoagulation has been known for treating a

wide range of pollutants in industrial wastewater and groundwater; however, little attention has been given to its use in municipal wastewater treatment. The advantages of iron electrocoagulation over conventional chemical coagulation include: (1) abundance of low cost iron (about 0.5-0.8 $US/kg); (2) lower sludge quantities composed of mainly iron oxides/hydroxides that are easier to settle and dewater as compared to chemical coagulation; (3) no chemical additive requirement or production of by-products requiring post-treatment because the 'electron' is the focal element in the treatment; (4) better floc formation in comparison with chemical coagulation, as the applied electric field promotes flocculation of the smallest particles; and (5) easy to control process with minimal maintenance as it uses simple and easily automated equipment (Hakizimana et al., 2017; Mollah et al., 2001).

Organic pollutants in different wastewater matrices are sometimes removed from by means of iron electrocoagulation (Chou et al., 2010; Dubrawski and Mohseni, 2013b, 2013a; Eyvaz et al., 2014; Jaafarzadeh et al., 2016; Kabdaşli et al., 2009; Kalyani et al., 2009; Kuokkanen et al., 2015; Ma and Zhang, 2016; Mansouri et al., 2011; Moreno-Casillas et al., 2007; Orescanin et al., 2013, 2011; Singh et al., 2016; Tsai et al., 1997). There are two major processes involved in the electrocoagulation cell that contribute to organic pollutant removal. Firstly, metal species are generated through the electrochemical process forming precipitates which interact with contaminants through physio-chemical processes that may include: 1) inclusion, where a contaminant occupies a cavity in the precipitated metals species floc; 2) occlusion,

where a floc particle entirely surrounds a contaminant, trapping it in the floc structure, so it cannot return to the solution; or 3) adsorption, where contaminants adhere to the surface of a floc particle (Mollah et al., 2001).

The two primary goals of this research are (1) to test, for the first time, the use of iron electrocoagulation as an enhancement to primary sedimentation tanks for the removal of soluble chemical oxygen demand (sCOD) from municipal wastewater influents; and (2) to discuss and develop heuristic procedures to obtain data for the calibration of adsorption models for sCOD removal based on more appropriate data collection methods and science-based estimation of the adsorbent concentrations produced in iron electrocoagulation.

4.2 Materials and methods

4.2.1 Iron electrocoagulation treatment

Wastewater samples of grit removal process effluent were collected from a wastewater treatment plant in central Alberta, Canada during wet weather and were stored in the cold room at 4ºC. The physicochemical characteristics of the samples are shown in Table 4.1. Two sets of experiments were conducted; one at room temperature which was measured to be 23.0 ºC ± 0.5 ºC and the other at 8.0 ºC ± 0.2 ºC in a temperature-controlled laboratory.

Table 4.1 Characterization of wet weather flow wastewater used for experiments

Parameter	Units	Mean ± Standard Deviation
pH	-	7.0 ± 0.1
Zeta Potential	mV	-24.2 ± 2.8
Total Chemical Oxygen Demand	mg/L	350.0 ± 4.4
Soluble Chemical Oxygen Demand	mg/L	197.6 ± 2.5
Total Suspended Solids	mg/L	212.4 ± 29.4
Volatile Suspended Solids	mg/L	174.1 ± 23.1

A 100-mL glass beaker was used as the electrochemical cell with a 5-cm long and 1.2-cm in diameter iron anode (99.99% as Fe, VWR). In order to prevent the possibility of further dissolution from the cathode, a 303 – stainless-steel cathode was used. A 50-mL sample size was used in all experiments. The effective submerged area of the electrodes immersed in the solution was 7.5 cm^2. A 1.5 cm interelectrode distance was used in all experiments. A magnetic stirrer was placed below the middle of the cell. Samples were stirred for 5 minutes without electric current to ensure homogeneity of the sample. The velocity of the stirrer in all experiments was approximately 500 rpm, which provided vigorous mixing in the cell. The electric current was supplied by a DC-regulated power source (BK Precision 1685B 1-50 V DC and 5 A). A digital multimeter (DMiOTECH-UA92015N, China) was used to measure the voltage and current. Figure B1 in Appendix B shows the reactor setup for iron electrocoagulation used for the experiments. Three current densities (i) of 8, 15 and 22 mA/cm^2 were selected in this study and were applied for various time periods ranging from 5 to 40 minutes, where each treatment time period represents an independent experiment. The

DC-regulated power source and stirring were stopped at the designated treatment time, and a 30-minute flotation period started. Samples were then collected for measurements from the clear layer under the surface froth layer. The iron electrode was cleaned after each experiment in diluted HCl solution (5% v/v).

4.2.2 Analytical methods

The bypass wastewater samples' characteristics were measured before each experiment. TSS and volatile suspended solids (VSS) were analyzed using standard methods 2540-D and 2540-E; respectively (APHA AWWA WEF, 1998). Total and soluble chemical oxygen demand (tCOD and sCOD) was measured colorimetrically using the HACH method 8000. sCOD was measured after filtering the sample through 0.45 µm GF/C Whatman filter paper. Zeta potential was measured using a Malvern Zetasizer instrument (Malvern Instruments, Worcestershire, UK). The actual iron electrode loss was measured by gravimetric analysis of the dry anode before and after treatment time. Ferrous (Fe^{2+}) was measured using the 1,10-phenanthroline method (APHA AWWA WEF, 1998). In addition, the following parameters were also measured before and after iron electrocoagulation: pH (Accumet electrode and Accumet Excel; Fisher Scientific, Ottawa, ON, Canada)), redox potential (Accumet Platinum Pin Ag/AgCl Combination electrode and Accumet Excel; Fisher Scientific, Ottawa, ON, Canada), and dissolved oxygen (Model 52, YSI, Yellow Springs, Ohio, US).

4.3 Results and discussion

4.3.1 Overall process performance

4.3.1.1 Final pH and dissolved ferrous (Fe^{2+})

The effect of applied current density and two temperatures (a) 23°C and (b) 8°C on final pH after various electrocoagulation reaction times is shown in Figure 4.1. The initial pH for all experiments was pH = 7.0 ± 0.1. pH values were observed to increase during a test run. Over the range of treatment durations, the pH stabilized somewhere in the range of 7.9 to 8.6 for 23°C and 7.3 to 8.0 for 8°C. It is evident from Figures 4.1 that the pH increase during treatment at 8°C averaged approximately 0.5 pH units less than that at 23°C. In an iron electrocoagulation batch reactor, Fe^{2+} is generated at the anode as shown in Reaction 4.1 and pH values start to increase as hydroxides (OH^-) are generated at the cathode as per Reaction 4.2.

$$\textit{Anode:}\quad Fe(s) \rightarrow Fe^{2+}_{(aq)} + 2e^- \tag{4.1}$$

$$\textit{Cathode:}\quad 2H_2O_{(l)} + 2e^- \rightarrow H_{2\,(g)}\uparrow + 2OH^-_{(aq)} \tag{4.2}$$

Confirmation that Fe^{2+} was not entirely reacted with OH^- was obtained by measurement at the end of each test run during this study. Figure 4.2 shows the effect of the applied current density on the percentage of total iron (Fe_t) remaining as ferrous (Fe^{2+}) after various electrocoagulation reaction times at 23°C and 8°C. None of the tested conditions resulted in oxidation of all the Fe^{2+} produced during electrolysis to form $Fe(OH)_3(s)$. At the lowest current density tested in this study (8 mA/cm²), Fe^{2+}

was found to be the predominant form of aqueous iron with the average Fe^{2+} to Fe_t ratios being 70% and 90% for all reaction times at 23 and 8 °C, respectively. Some of the Fe^{2+} to Fe_t ratio measurements after 5 minutes of electrocoagulation time at 8 mA/cm^2 current density and 8 °C temperature was observed to be higher than 1. In a study that used synthetic wastewater formula, it was found that some of the experiments conducted at lower currents (<0.2 A) using stainless-steel yielded current efficiencies higher than 100% (Lee and Gagnon, 2015). This was attributed to the over 100% current efficiency which may be the result of electrochemical side-reactions that can yield higher iron concentrations than theoretically calculated using faraday's law (Lee and Gagnon, 2015).

For the tests conducted at 23°C, the increase of current density beyond 8 mA/cm^2 resulted in a decrease in the ratio of Fe^{2+} to Fe_t (to an average of 32% for all electrolysis times using 15 mA/cm^2 current density), but this ratio increased again at 22 mA/cm^2 (to an average of 38% for all electrolysis times). During the experiments at 8°C, the increase of current density beyond 8 mA/cm^2 resulted in an overall decrease to the ratio of Fe^{2+} to Fe_t with average ratios of 74% and 56% being reached for all electrolysis times using 15 mA/cm^2 and 22 mA/cm^2 current densities, respectively. Increasing electrolysis time for a given applied current density had no significant impact on Fe^{2+} to Fe_t ratio at the tested temperatures ($p > 0.05$).

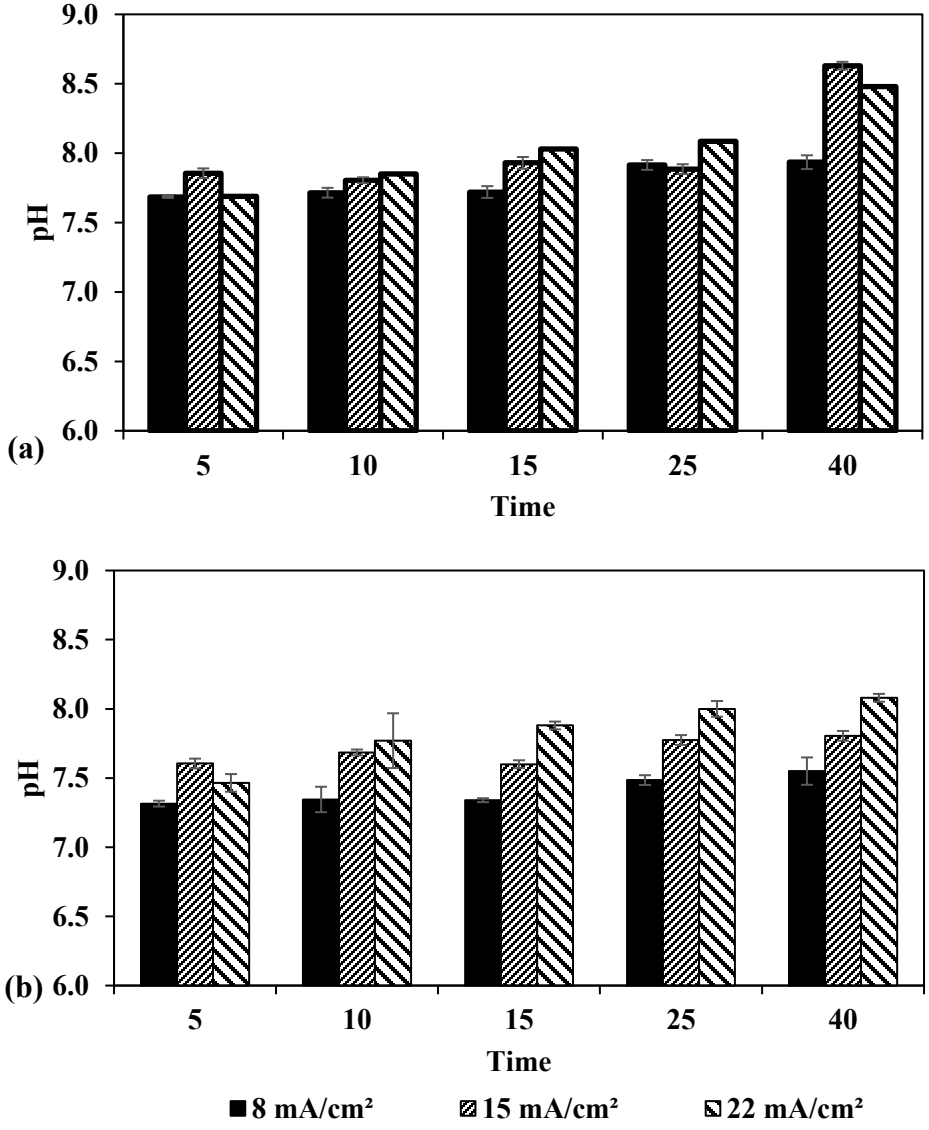

Figure 4.1 Final pH following treatment at different current densities and electrocoagulation reaction times at (a) 23°C and (b) 8°C. Initial pH for all experiments was 7.0 ± 0.1.

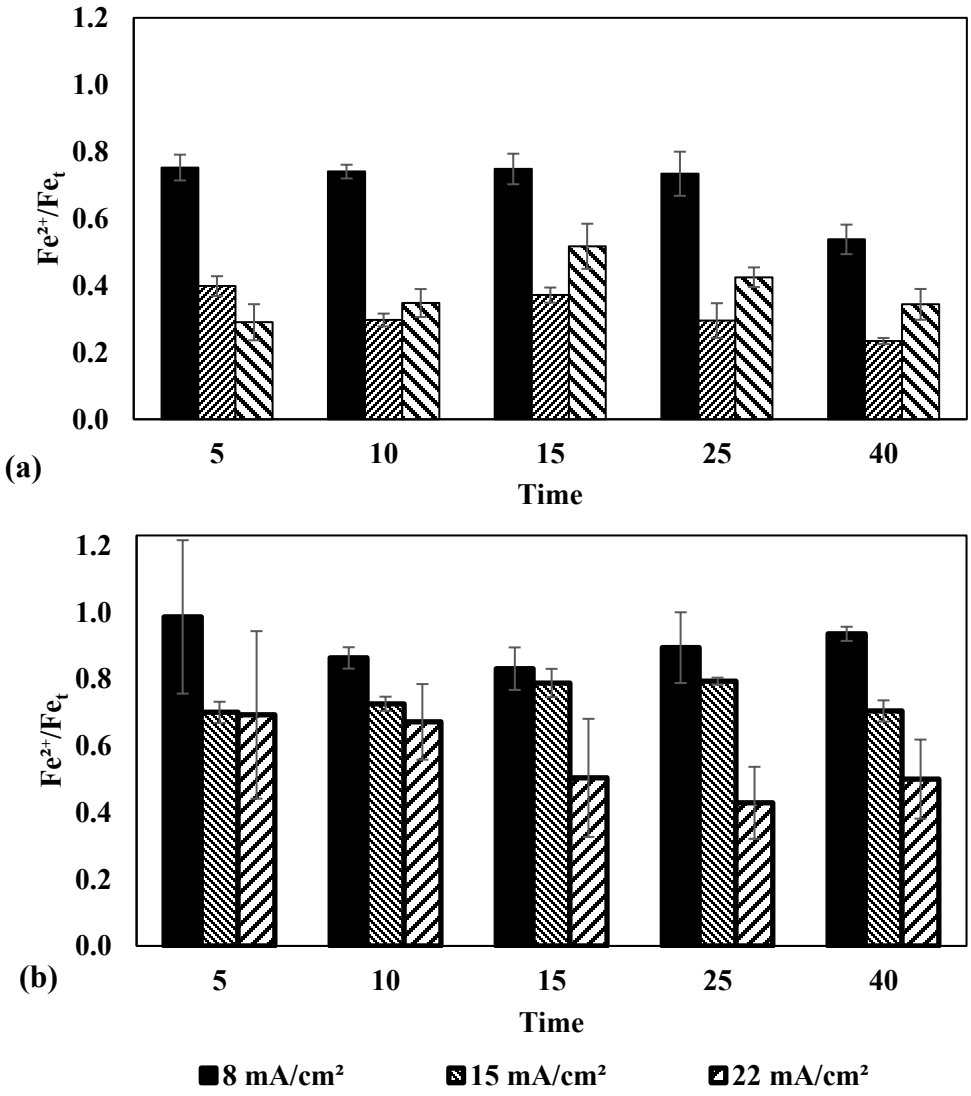

Figure 4.2 The percentage of total iron (Fe_t) remaining as ferrous (Fe^{2+}) at different current densities and after various electrocoagulation reaction times, at (a) 23°C and (b) 8°C.

The decrease of Fe^{2+} to Fe_t ratio with increasing applied current density is consistent with the increased OH^- production, according to Reaction 4.2, and subsequent increase in ferric hydroxide production, according to Reaction 4.3, that an increase in applied current would cause.

$$4[Fe^{2+}_{(aq)} + 2OH^{-}_{(aq)}] + O_2 + 2H_2O_{(l)} \rightarrow 4Fe(OH)_3(s) \quad (4.3)$$

One would expect the conversion of ferrous ion to ferric hydroxide to continue until the equilibrium conditions specified by the Pourbaix diagrams shown in Figure 4.3 was reached. In fact, the final pH had not changed when measured 30 minutes after the current had been discontinued (data not shown), suggesting that the progress of Reaction 4.3 was also limited by the availability of dissolved oxygen.

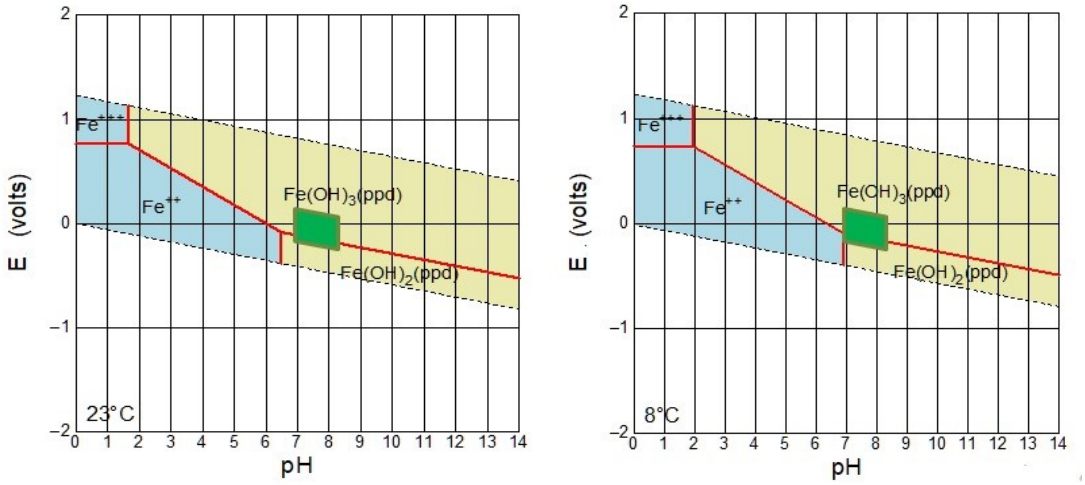

Figure 4.3 Iron Pourbaix diagram showing the area (highlighted in green) in which the iron electrocoagulation process occurs at 23°C and 8°C (after (Pourbaix, 1966)). Initial pH for all experiments was pH = 7.0 ± 0.1.

A sensitivity analysis of ferrous ion oxidation was performed with respect to the pH using the ferrous ion oxidation model of Millero et al. (Millero et al., 1987) to estimate the degree to which Fe^{2+} would be oxidized under the dissolved oxygen and salinity conditions of this study. The development of Millero et al. model is detailed in Appendix C The dissolved oxygen concentration measured in the electrocoagulation

cell at the beginning of each test was approximately 3 mg/L on average and was obvserved to change (decrease) by no more than 0.3 mg/L during any of the tests. Figure 4.4 shows the estimated proportion of Fe_t remaining as Fe^{2+} at the 3 mg/L dissolved oxygen concentration and an assumed salinity of 0.1 PSU (Hoffman and Meighan, 1984) after 40 minutes reaction time at 23°C and 8°C.

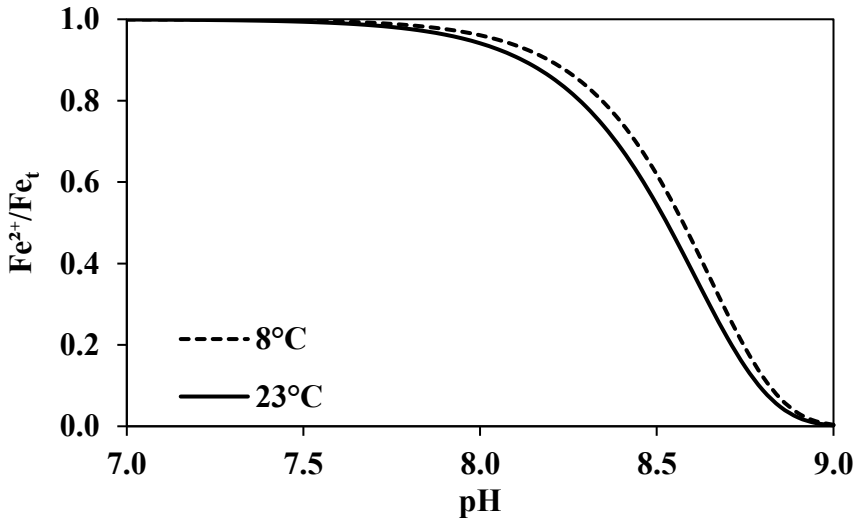

Figure 4.4 Estimated proportion of theoretically calculated total iron (Fe_t) using Faraday law remaining as ferrous (Fe^{2+}) versus pH after 40 minutes electrocoagulation reaction time at 23°C and 8°C using the ferrous oxidation model described in Millero et al. [28] (Dissolved Oxygen = 3 mg/L and Salinity = 0.1 PSU). Note: Model development for Millero et al. (1987) is detailed in Appendix C.

These calculations show that ferrous ion oxidation is not completed within a 40 minute reaction time under these conditions and that $Fe(OH)_3$ would still be forming. Thus, adsorption equilibrium could not have been established within the electrocoagulation cell during the tests that ranged from 5 to 40 minutes in duration. As was observed

experimentally, Figure 4.4 shows that an increase in temperature from 8°C to 23°C reduces the amount of Fe_t remaining as Fe^{2+}, but a considerable proportion of the total iron still remains as ferrous ion after 40 minutes within the pH range measured in the electrocoagulation cell during this study. Indeed, pH has a great effect on the rate of ferrous oxidation, with an increase of one pH unit resulting in a 100 fold increase in the ferrous ion oxidation rate. The estimated Fe^{2+} to Fe_t ratios shown in Figure 4.4 are greater than those observed in the present study and shown in Figure 4.2 for forty minute reaction times. This may be due to some aqueous Fe^{2+} forming complexes with the organic matter present in the wastewater sample. Ferrous iron bound in these complexes would not have been measured by the assay used in this study (Bagga et al., 2008; Tanneru and Chellam, 2012; Theis and Singer, 1974).

4.3.1.2 sCOD removal efficiencies

sCOD removal efficiencies increased with the electrolysis time at each of the three current densities and two temperatures tested, as shown in Figure 4.5. During the experiments conducted at 23°C as depicted in Figure 4.5-a, the percentage sCOD removal increased significantly when the current density was increased from 8 mA/cm^2 to 15 mA/cm^2; however, increasing the current density beyond 15 mA/cm^{-2} did not show any significant improvement in sCOD removal efficiency ($p > 0.05$). Data shown in Figure 4.5-b indicate that sCOD removal improved considerably with increasing current density during the treatment at 8°C.

While increasing current densities increase the amount of dissolved iron, these increases may lead to the creation of conditions favorable to the formation of other soluble species such as ferric hydroxo complexes with hydroxide ions and polymeric species that do not necessarily convert fast enough to form the insoluble $Fe(OH)_3$ and may not contribute to sCOD removal (Kalyani et al., 2009; Kobya et al., 2003). This might explain the meagre improvement in sCOD removal efficiency as the current density was increased beyond 15 mA/cm² at 23°C. The results of the experiments conducted at 8°C, contained in Figure 4.5-b, show on the other hand that the percentage sCOD removal continued to increase as the current density was increased from 8 mA/cm² to 15 mA/cm² and then to 22 mA/cm². This shows that an increase in current density at 8°C resulted in a very beneficial decrease in the proportion of Fe_t remaining as Fe^{2+}as shown in Figure 4.2, and so relatively more precipitate was available to adsorb sCOD.

Very few reports exist in the literature concerning the effect of temperature on the removal of sCOD using electrocoagulation technology (Vepsäläinen et al., 2009; Wang et al., 2010). Comparison of the sCOD removal results at each temperature shows that removal efficiencies increased considerably for a given current density when the temperature was increased from 8 to 23°C. Or for a given current density, raising the temperature from 8 to 23°C considerably reduced the treatment time required to achieve a given sCOD removal. These increases in sCOD removal efficiencies due to increased temperature can be ascribed to: (1) increased amount of

$Fe(OH)_3$ precipitate formed at 23°C to that formed at 8°C as indicated by the lesser amount of dissolved Fe^{2+} measured in solution at 23°C as compared to 8°C (Figure 4.2); and (2) faster de-passivation of the anode.

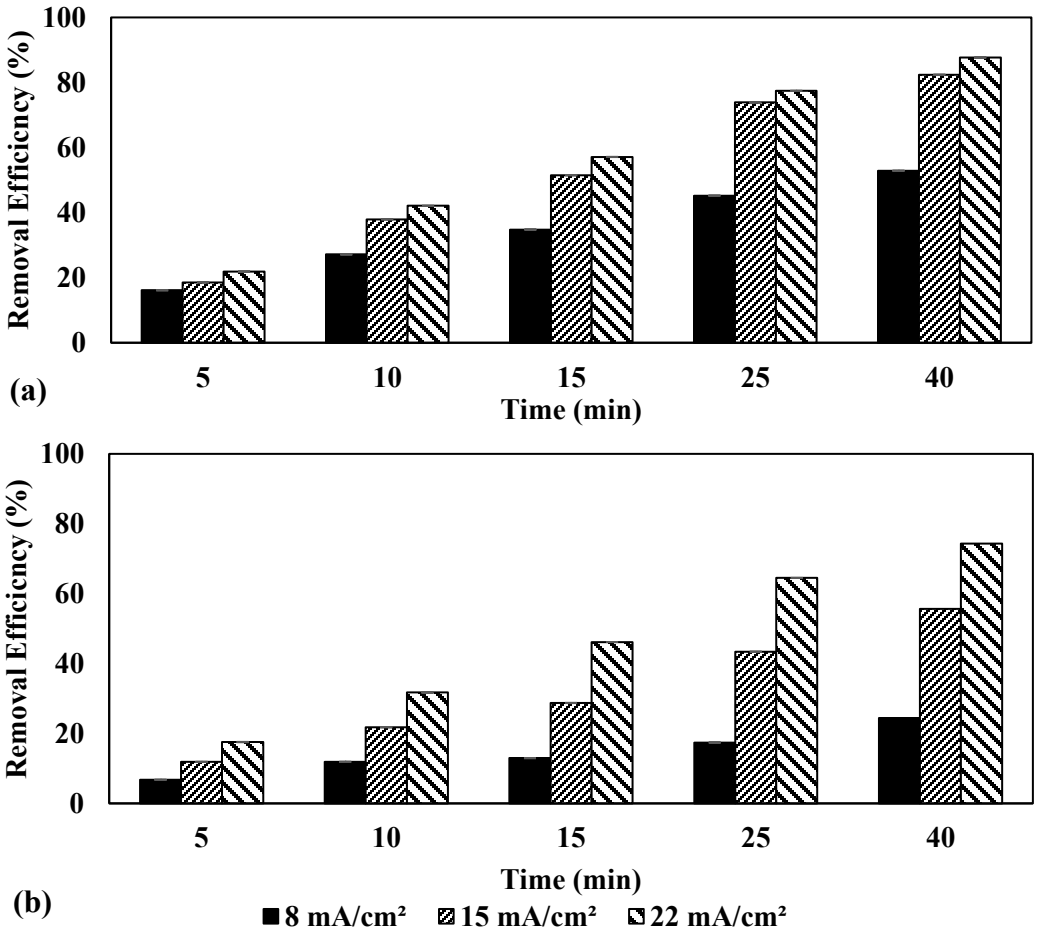

Figure 4.5 Removal efficiencies of soluble chemical oxygen demand (sCOD) at different current densities and after various electrocoagulation reaction times, at (a) 23°C and (b) 8°C temperatures.

4.3.2 Modeling the iron electrocoagulation process

The electrocoagulation process is an inherently non-equilibrium process due to the continual production of ferrous ion and its ongoing reactions to form precipitate.

Nevertheless, isotherm models have been used to describe the adsorption of material in electrocoagulation cells. While isotherm analyses may reveal valuable information regarding the interactions between adsorbent ($Fe(OH)_3$) and adsorbate (sCOD) that occur within these cells, isotherm models should not be used to model the removal process itself. Additionally, data to calibrate isotherm models must be collected in a manner that is consistent with the dynamic equilibrium underpinnings of the various models. A prudent approach would be to perform adsorption isotherm data collection in several steps similar to the approach described by Essadki et al. (Essadki et al., 2010). In this approach the adsorbent (hydroxide precipitates) are first produced from the electrocoagulation process in the absence of adsorbate. The adsorbent is then recovered, dried, and finally used in a separate set of isotherm data collection experiments. Other approaches cannot ensure that equilibrium conditions are reached. Many isotherm studies reported in the literature suffer from one or more procedural deficiencies, the most basic being a lack of well specified experimental procedure. In other studies, samples for isotherm modeling have been collected from electrocoagulation cells at designated time intervals while the DC was applied, as one would collect data during a kinetics investigation. Even if samples are collected after the DC supply is stopped, the adsorbent concentration may continue to increase if any remaining soluble Fe^{2+} concentration continues to be converted to ferric (Fe^{3+}) or iron hydroxides. Therefore, a multi-step approach that separates the production of adsorbent from its use in isotherm data collection is needed.

4.3.2.1 Modeling assumptions

For the purpose of modeling iron electrocoagulation for the removal of soluble material, clear assumptions should be stated especially with regard to defining end products and the degree to which the iron ionized from the electrode is converted to $Fe(OH)_3$. The reaction mechanisms and the likely end products surveyed in the literature are summarized in Table C1 of Appendix C. Depending on the operational conditions, the reported primary end products summarized in Table B1 varied from being predominantly $Fe(OH)_3$ to being a mixture of $Fe(OH)_2$ and $Fe(OH)_3$, or a mixture of $Fe(OH)_3$ and other polymeric hydroxy complexes similar to ferric chloride products, or a mixture of soluble Fe^{2+} and insoluble $Fe(OH)_3$/FeOOH or a mixture of $Fe(OH)_3$ and FeOOH. It can be seen that there is a conflict between these reports and the assumption that iron electrocoagulation end products are entirely $Fe(OH)_3$. This latter assumption has been generally employed in the studies that applied adsorption isotherms for iron electrocoagulation by assuming all dissolved iron, calculated using Faraday's law, is immediately converted to $Fe(OH)_3$ precipitate capable of adsorbing the organic molecules (Balasubramanian et al., 2009; Kalyani et al., 2009; Nariyan et al., 2017; Şengil and özacar, 2006; Yoosefian et al., 2017). Changing operating parameters such as pH, dissolved oxygen, actual iron released, redox potential and treatment time can lead to a significant impact on the ionic iron reactions (Lakshmanan et al., 2009); thus potentially yielding lower concentrations of precipitates than the theoretically calculated values.

Other researchers sought to provide insights into the predominant species resulting from iron electrocoagulation under the conditions tested in their studies by Pourbaix diagram (Moreno-Casillas et al., 2007). Figure 4.3 shows the regions of the current study experimental conditions superimposed upon an iron Pourbaix diagram. The superimposed highlighted regions show the area in which the reactions occur starting with the initial neutral pH measured in this study. At 23°C, the process begins and under favourable conditions would proceed to form the desirable insoluble $Fe(OH)_3$. At 8°C, the initial equilibrium position lies at the boundary between Fe^{2+} and $Fe(OH)_3$ and as the pH increases during the treatment, the equilibrium position shifts further into the precipitate region is anticipated to proceed towards forming $Fe(OH)_3$. It is postulated that the successful iron electrocoagulation process may not relate entirely to the redox potential and initial pH, but the rate of oxidation of Fe^{2+} should be equally considered. Iron Pourbaix diagrams only describe equilibrium information, and only reaction directions from thermodynamics, not any kinetic information, can be deduced. This means it is hard to determine when the hydrated Fe^{2+} ions formed by the external DC will be oxidized into the solid precipitate of ferric hydroxide, $Fe(OH)_3$ as per Reaction 4.3. In addition, theoretical estimate shown in Figure 4.4 demonstrated that the oxidation of Fe^{2+} to Fe^{3+} had not reached equilibrium (the point expected according to the Pourbaix diagram) within the reaction times allowed in the batch tests mainly because of oxygen and hydroxide limitations.

Since the attainment of equilibrium conditions during iron electrocoagulation of environmental samples, better modeling approach to the electrocoagulation system should consider the system kinetics. The development of adsorption kinetics theory for iron electrocoagulation is slow despite its importance to practical applications. Variable-order-kinetic (VOK) models have been developed for aluminum electrocoagulation systems [36,42]. These VOK models are based on either the Langmuir (Hu et al., 2007) or the Langmuir-Freundlich (Essadki et al., 2010) expressions and formulated to describe the adsorption rate. VOK models are able, with minimal complexity, to identify the effects of operating conditions such as time and current, and to predict electrocoagulation performance in removing a target contaminant.

4.3.3 Kinetic adsorption modeling

For the purpose of modeling adsorbate-coagulant interactions, four assumptions are made in this study. These are: (1) adsorption takes place on the precipitate species generated from the iron electrocoagulation process; (2) precipitate species are considered to be $Fe(OH)_3$ after deducting the Fe^{2+} concentration measured in the effluent from the theoretically supplied iron then considering the remaining iron concentration to be theoretically converted to $Fe(OH)_3$; (3) once the precipitate species are formed ($Fe(OH)_3$ in this study), their surface area is large enough to allow immediate adsorption of sCOD; and (4) sCOD removal by flotation is negligible.

In this study, a de facto estimation of the amount of dissolved iron that accounts for the presence of Fe^{2+} in the reaction mixture will be used to calculate the mass of $Fe(OH)_3$ precipitate. Furthermore, the present study treats the iron electrocoagulation batch reactor results in a manner analogous to that found extremely suitable in aluminum-based electrocoagulation (Essadki et al., 2010; Hu et al., 2007), but with some modifications. The VOK form of a Langmuir adsorption model equation before attaining equilibrium may then be represented by Equation 4.1 (Hu et al., 2007).

$$\frac{dC_t}{dt} = -\phi.\frac{I}{ZFV}.q_{Lmax}.\frac{k_L C_t}{1 + k_L C_t} \tag{4.1}$$

$$\phi = (1 - \frac{[Fe^{2+}]}{[Fe_t]}) \tag{4.2}$$

where: ϕ accounts for the efficiency of the process in forming $Fe(OH)_3$ and is calculated by Equation 4.2 that represents the percent conversion of total iron [Fe_t] to $Fe(OH)_3$ after accounting for the [Fe^{2+}]. F is Faraday's constant (96485 C(mol e^-)$^{-1}$). The charge transfer number (z) in Eq. (1), has been previously investigated and conclusively shown that z = 2 for iron (Ben Sasson et al., 2009; Lakshmanan et al., 2009). q_{Lmax} in mg/g is a constant reflecting the maximum adsorption capacity per unit mass of adsorbent; K_L in min^{-1} is a constant representing the adsorption intensity; V is the batch reactor volume (L); and C_t in mg/L is the aqueous adsorbate concentration achieved after time t of iron electrocoagulation.

Unfortunately, the integrated form of Equation 4.1 is an implicit function of aqueous adsorbate concentration, and so the mathematical expression for the treatment time

required to achieve a specific aqueous adsorbate concentration using Langmuir VOK model is represented by Equation 4.3.

$$t = \frac{ZFV}{\phi . I . q_{Lmax}} \left[(C_o - C_t) + \frac{1}{k_L} \ln \left(\frac{C_o}{C_t} \right) \right] \tag{4.3}$$

As a sorbable component is assumed to exist at two locations: in a sorbed phase on $Fe(OH)_3$ precipitates and in the bulk fluid outside precipitates, the "conservation equation" expressed in Equation 4.4 can be used and Equation 4.5 can be introduced.

$$C_o . V = C_t . V + q_t . W_t \tag{4.4}$$

$$t = \frac{ZFV}{\phi . I . q_{Lmax}} \left[\frac{q_t . W_t}{V} + \frac{1}{k_L} \ln \left(\frac{1}{1 - \frac{q_t . W_t}{V . C_o}} \right) \right] \tag{4.5}$$

where C_o in mg / L is the initial concentration of the sCOD, V is the volume of solution, W_t in g is the mass of the $Fe(OH)_3$ precipitate at time t; and q_t in mg/g is the amount of sCOD adsorbed per gram of the $Fe(OH)_3$ precipitate at time t.

The other model tested in the current study is the VOK form of a Langmuir-Freundlich adsorption model represented by Equation 4.6 (Essadki et al., 2010).

$$\frac{dC_t}{dt} = -\phi . \frac{I}{ZFV} . q_{Lmax} . \frac{k_{LF} {C_t}^n}{1 + k_{LF} {C_t}^n} \tag{4.6}$$

The mathematical expression for the treatment time required to achieve specific treatment efficiency of sCOD using the Langmuir-Freundlich VOK model is represented by Equation 4.7, and utilizing Equation 4.4, Equation 4.8 can also be deduced to represent the same model.

$$t = \frac{ZFV}{\phi\, I\, q_{LFmax}}\left[C_o - C + \frac{C_o^{(1-n)} - C^{(1-n)}}{k_{LF}(1-n)}\right] \quad (4.7)$$

$$t = \frac{ZFV}{\phi.\, I.\, q_{LFmax}}\left[\frac{q_t.\, W_t}{V} + \frac{C_o{}^{(1-n)} + \left(\frac{q_t.\, W_t}{V} - C_o\right)^{(1-n)}}{k_{LF}(1-n)}\right] \quad (4.8)$$

In the current study, calibration of the models was conducted using all the data at a given temperature based on the assumption that current density would not affect the precipitate characteristics in terms of its adsorption kinetics. This assumption is supported by the results of the mathematical models of the studies that investigated the use of Langmuir and Langmuir-Freundlich VOK models which found that the adsorption capacity and intensity did not vary when changing the the initial current or current density (Essadki et al., 2010; Hu et al., 2007). The estimates of the isotherm model parameter values and fitting statistics of the two tested models are shown in Table 4.2. Figures 4.6 and 4.7 show the simulation results of sCOD by Langmuir and Langmuir-Freundlich VOK models, respectively, at different current densities. The second order Akaike Information Criterion (AIC_c) was used in this study to evaluate the models (Sugiura, 1978). As it can be seen from Table 4.2, the Langmuir VOK model has a better fit with lower AIC_c in comparison with Langmuir-Freundlich VOK model for all current densities and at both 8 and 23°C temperatures. This indicates that Langmuir VOK provides a better description of the process under these conditions.

As shown in Table 4.2, increasing temperature from 8 to 23°C drastically increased the adsorption capacity of the insoluble $Fe(OH)_3$ for removing sCOD from domestic wastewater. This observation might give insights on the adsorption category i.e.

physisorption or chemisorption. Although the adsorption process is exothermic in nature as the residual forces on the surface of the adsorbent decrease with the increase of the adsorbate occupying the adsorption sites according to Le-Chatelier's principle, physisorption or chemisorption respond differently.

Table 4.2 Estimates of the batch adsorption kinetic model parameter values and fitting statistics

Model	Parameters and Statistics	23°C Current Density (mA/cm²)			8°C Current Density (mA/ cm²)		
		8	15	22	8	15	22
Langmuir Variable Order Kinetic Model							
	q_{Lmax}		54.47			1.18	
	k_L		1.03E-05			6.90E-04	
	Standard Error	5.38	4.22	4.14	8.29	1.62	3.02
	R^2	0.89	0.93	0.93	0.73	0.98	0.96
	AIC_c	24.28	21.85	21.66	28.60	14.82	18.49
Langmuir-Freundlich Variable Order Kinetic Model							
	q_{LFmax}		16.21			0.12	
	k_{LF}		1.24E-06			1.02E-07	
	N		1.88			3.70	
	Standard Error	4.96	5.77	6.61	8.14	4.41	2.91
	R^2	0.94	0.91	0.89	0.83	0.95	0.98
	AIC_c	41.43	42.94	44.30	46.38	40.26	36.12

On one hand, a physisorption decreases with increasing temperature due to the weak forces between the adsorbate and adsorbent. On the other hand, chemisorption initially increases with the increase in temperature as activation energy is required for chemical reactions to take place then decreases reflecting the desorption effect. The results in this study reveals that the first phase of chemisorption prevails as the adsorption capacity of the insoluble $Fe(OH)_3$ for removing sCOD from domestic wastewater

increased with increasing temperature from 8 to 23°C. Similar conculsions regarding the chemosorption nature of the iron electrocoagulation were drawn in a previous study using second order kinetics representing the removal of ciprofloxacin from hospital wastewater (Yoosefian et al., 2017).

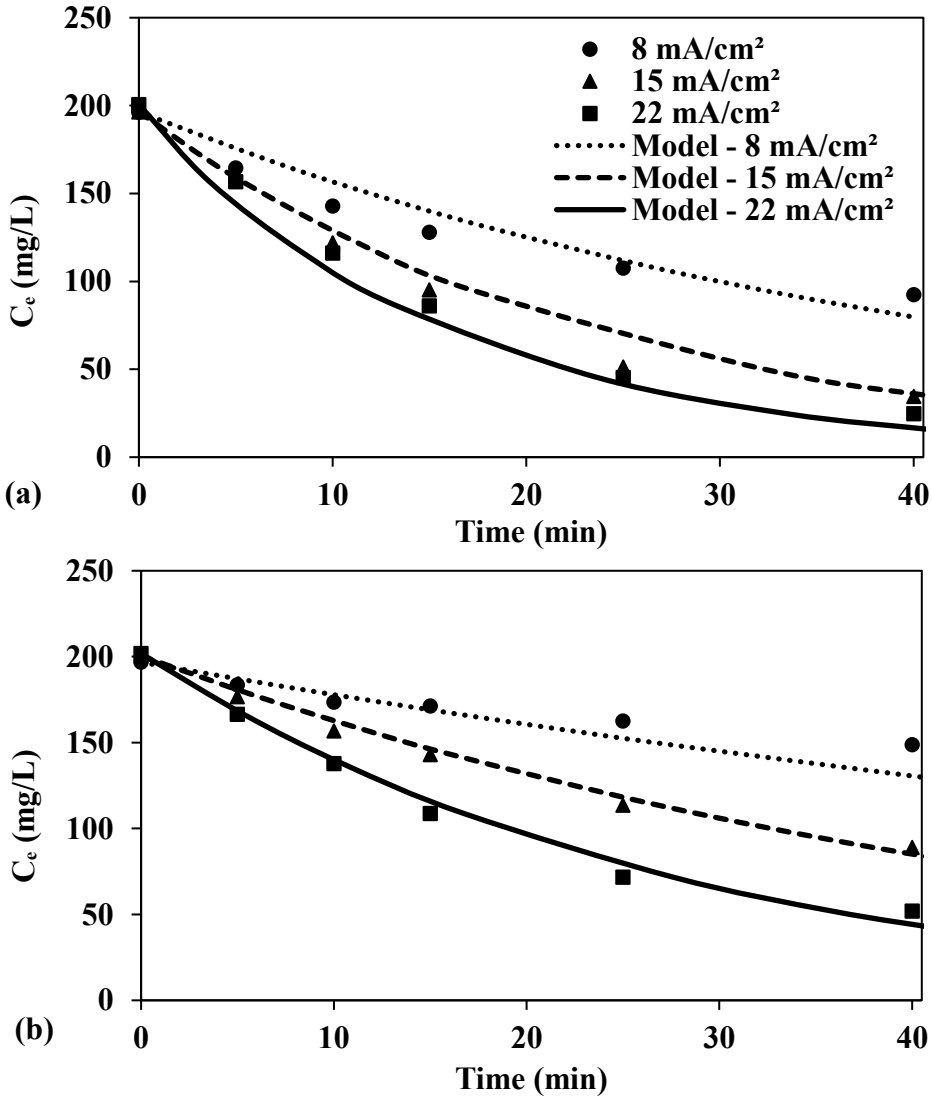

Figure 4.6 Simulation results of soluble chemical oxygen demand (sCOD) by Langmuir VOK model at different current densities and at (a) 23°C and (b) 8°C temperatures.

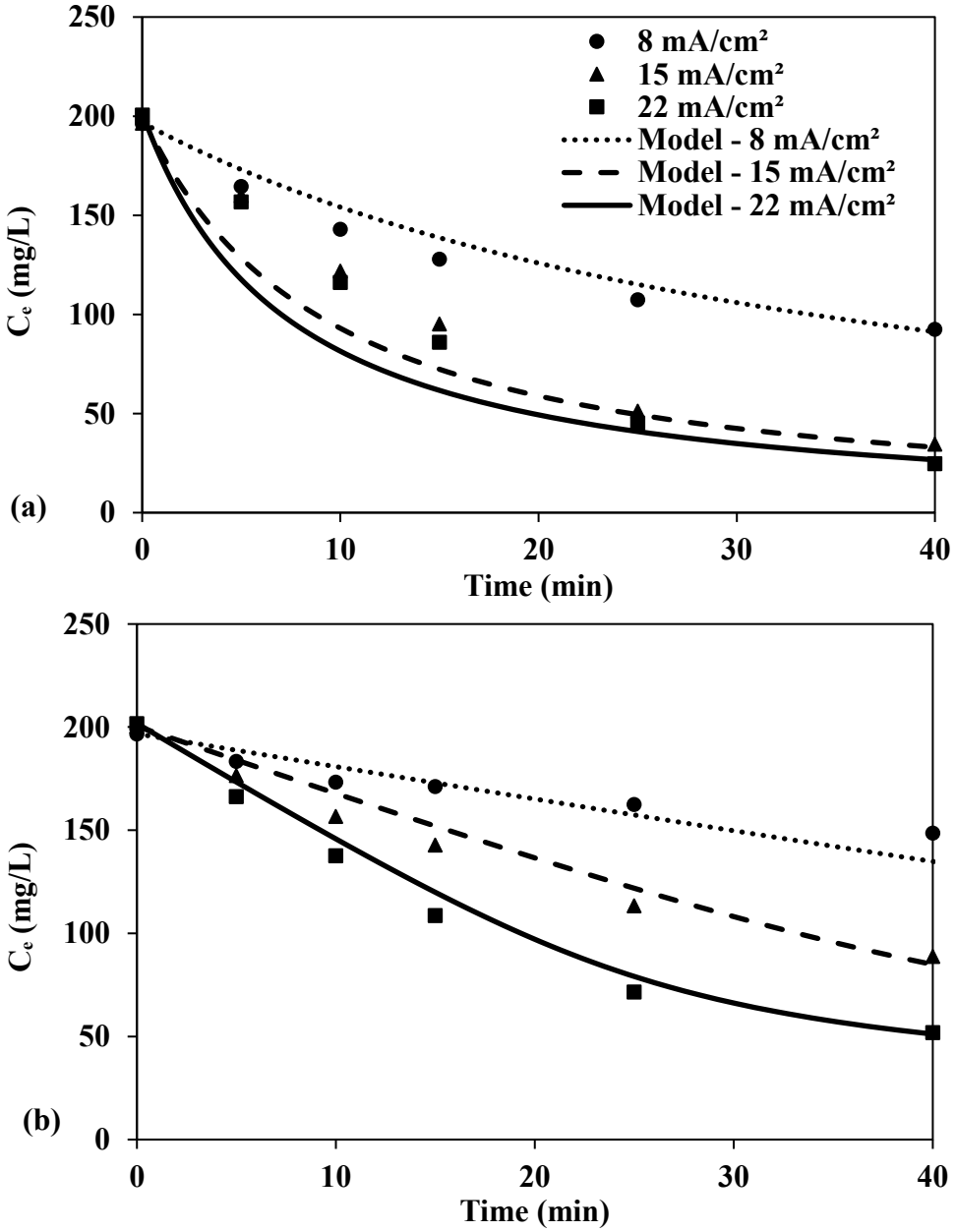

Figure 4.7 Simulation results of soluble chemical oxygen demand (sCOD) by Langmuir-Freundlich VOK model at different current densities and at (a) 23°C and (b) 8°C temperatures.

4.4 Conclusions

Iron electrocoagulation was tested in this as an enhancement option to the primary sedimentation tank treating domestic sewage. Assessment of the removal of sCOD at near neutral pH conditions by changing electrolysis time, current density, and temperature was conducted. sCOD removal efficiencies increased with the increase of electrolysis time, current density, and temperature. Particularly, the temperature effect was proven in this study for the first time for the treatment of domestic wastewater using iron electrocoagulation. It was found that at 23°C, it took 15 minutes to reach an average 52% sCOD removal efficiency while it took around 40 minutes to achieve comparable removal efficiency at 8°C; both tested at 15 mA/cm² current density. Perspectives on the using adsorption isotherms to model iron electrocoagulation process that looked at experimental protocols and modeling assumptions were included in this study. Under the operational conditions tested in this study, equilibrium could not have been established. This underscores the need researchers to be careful when applying adsorption isotherms to iron electrocoagulation systems. Alternatively, kinetic based models such as Langmuir and Langmuir-Freundlich VOK models would be more approporiate in modeling adsorption results from iron electrocoagulation. The latter models were examined in this study with suitable assumptions and consideration of the de-facto estimation of $Fe(OH)_3$ (adsorbent) that accounts for the contribution of Fe^{2+} to treatment end products. The Langmuir VOK model was found to be the better model to describe sCOD removal in the

electrocoagulation cell under all test conditions with chemisorption being considered the dominant sCOD removal mechanism.

CHAPTER 5. NOVEL INTEGRATED POTASSIUM FERRATE(VI) AND IRON ELECTROCOAGULATION FOR THE TREATMENT OF BYPASS WASTEWATER[4]

5.1 Introduction

Unplanned bypass wastewaters can be defined as the wastewater flows in excess of the capacity of an existed collection system or treatment plant that have not been accounted for during the planning and design phases. Climatic and population data are primary inputs in designing wastewater infrastructure; consequently, any significant change in climate or population density can have a dramatic effect on sewerage system components design and/or operation. Bypass wastewaters can lead to unplanned water reuse, in that water withdrawn by downstream users will contain a significant fraction of untreated or undertreated wastewater (National Research Council, 2012; Rice et al., 2016; Wiener et al., 2016). Nevertheless, such bypass wastewaters are supposed to be released in compliance with local regulations that usually include providing some sort of treatment. Every community is encouraged to investigate locally feasible remedial alternatives to address contaminants of particular concern, resulting in the development of remedial action objectives (RAO). The RAO for any community

[4] A version of this chapter will be submitted as "Elnakar, H. and Buchanan, I.: Novel integrated potassium Ferrate(VI) and electrocoagulation for the treatment of bypass wastewater".

generating wastewater should be to prevent direct contact with pollutants that may cause an intolerable risk.

Physically or chemically enhanced primary treatment is either placed as one of the first processes in a typical wastewater treatment train (Metcalf & Eddy, 2004), used as a stand-alone auxiliary treatment to the wastewater flows in excess of the wastewater treatment plant capacity (City of Edmonton, 2000) or used as the sole process treating wastewater generated from small rural communities to even large cities (Gehr et al., 2003; Harleman and Murcott, 1999; Wang et al., 2009). The enhancement of primary treatment can be done using physical means such as lamella plate settlers or chemical means such as chemical coagulation using iron or aluminum salts. Such enhancement allows the primary treatment to be designed according to much higher overflow rates which means cheaper construction, or in the case of existing primary treatment tanks, it can be retrofitted to handle higher flows with no additional tankage. In addition, higher removal efficiencies can be achieved (Harleman and Murcott, 1999; Metcalf & Eddy, 2004).

Several alternative enhancement techniques to primary wastewater treatment utilize the adsorptive and reductive properties of iron and its mineral and oxide products to remove a wide range of microorganisms, inorganic and organic contaminants. Various purities of elemental iron can be used as electrode materials in electrochemical-based treatment technologies (Mollah et al., 2001, 2004). Iron electrocoagulation has been known for treating industrial wastewater and groundwater. Although iron

electrocoagulation has several advantages as listed everywhere (Hakizimana et al., 2017; Mollah et al., 2001), little attention has been given to its use in municipal wastewater treatment. In addition, the high proportions of total iron remaining as soluble ferrous (Fe^{2+}) under acidic to neutral pH conditions represent a challenge (Lakshmanan et al., 2009). Lakshmanan et al., 2009 suggested some alternatives for the efficient operation of iron electrocoagulation process to reduce Fe^{2+} concertation in the effluent (Lakshmanan et al., 2009). These suggestions and related potential drawbacks include: (a) increasing the dissolved oxygen concentration of the influent through aeration that might add to the energy costs; (b) increasing the initial pH values beyond 7.5 which might require downstream pH adjustment facilities; (c) lengthening the treatment time to allow complete Fe^{2+} oxidation which might not be feasible for some applications that needs fast treatment such as the treatment of peak flows and as also Fe^{2+} complexation with organic matter can cause any treatment time increase unmeaningful (Bagga et al., 2008) and (d) adding oxidant which requires further investigation on the suitable oxidants that can be added to the electrochemical cell without producing harmful by-products;

The integration of iron electrocoagulation with oxidation technologies has emerged to benefit from the synergetic effect of the coupled processes by accelerating the dissolution of the iron anode and enhancing the removal of the pollutants through chemical oxidation (Garcia-Segura et al., 2017). Some of the tested oxidation techniques coupled with electrocoagulation were sonication (Kovatcheva and

Parlapanski, 1999; Maha Lakshmi and Sivashanmugam, 2013; Raschitor et al., 2014), ultraviolet irradiation (Cotillas et al., 2013; Farhadi et al., 2012; Jaafarzadeh et al., 2016), and hydrogen peroxide (Brillas et al., 2003, 1998, 1997; Farhadi et al., 2012; Yazdanbakhsh et al., 2015). Several configurations of micro- or ultrafiltration technologies have been coupled as well with iron electrocoagulation to mitigate colloidal natural organic matter membrane fouling (Bagga et al., 2008; Ben-Sasson et al., 2013; Harif et al., 2006; Timmes et al., 2009). None of these techniques addressed the residual Fe^{2+} arising from iron electrocoagulation treatment of raw domestic wastewater.

This study investigates for the first time one of the iron salts in its +6-oxidation state known as potassium ferrate(VI) as an alternative to enhance the iron electrocoagulation process. Potassium ferrate(VI) is also considered one of the promising multi-purpose chemical enhancement alternatives for primary wastewater treatment and is regarded as "green cleaner" in wastewater treatment (Murmann and Robinson, 1974; Sharma, 2002). Although potassium ferrate(VI) development and applications started a long time ago, there are still several gaps in knowledge regarding its applications in domestic wastewater treatment, and its full-scale application has not yet been achieved. There are mixed reports on potassium ferrate(VI) coagulation capability in further removing organic matter and particles. It is found that potassium ferrate(VI) oxidation had a significant effect on enhancing the coagulation of surface waters, especially when the waters had high organic content (Lv et al., 2018; Ma and Liu, 2002). Another

study showed that there was much better floc formation in terms of floc index with potassium ferrate(VI) than with ferric chloride at a neutral pH (Graham et al., 2010). On the other hand, particles resulting from potassium ferrate(VI) as compared with ferric chloride have been shown to comprise significantly more nano-size particles with negative charges which contribute to the colloidal suspension stability (Goodwill et al., 2015). Therefore, it was recommended that potassium ferrate(VI) might not eventually assist the dual-function of oxidant and coagulant in a way that entirely disregards the usage for a coagulation process succeeding peroxidation process (Goodwill et al., 2015; Jiang et al., 2015). However, potassium ferrate(VI) resultant particles shown smooth and granular characteristics with evidence to the existence of iron(III) oxide (Fe_2O_3) particles known to be used as adsorbents (Goodwill et al., 2015).

This study focuses on investigating the enhancement of primary wastewater treatment by hybrid potassium ferrate(VI) – iron electrocoagulation system. Through using the response surface methodology Box Behnken design response surface methodology, the specific goals are to: (1) study the feasibility of utilizing the oxidation capability of potassium ferrate(VI) to remove soluble chemical oxygen demand (sCOD) and of its resultant nanoparticles to improve the coagulation capabilities of iron electrocoagulation to remove the particulate matter; and (2) to evaluate the applicability of using potassium ferrate(VI) as one of the options to reduce the high

concentrations of Fe^{2+} found as one of the reaction products of iron based electrocoagulation treatment process at near neutral pH conditions.

5.2 Materials and methods

5.2.1 Hybrid potassium ferrate(VI) – iron electrocoagulation treatment

Wastewater samples of aerated grit removal process effluent were collected from a wastewater treatment plant in central Alberta, Canada during wet weather and were stored at 4°C in a cold room. The sample was allowed to warm to room temperature before being used in subsequent tests. The physicochemical characteristics of the samples are shown in Table 5.1. A 100-mL glass beaker was used as the electrochemical cell with a 5-cm long and 1.2-cm in diameter iron anode (99.99% as Fe, VWR). In order to prevent the possibility of further dissolution from the cathode, a 303 – stainless-steel cathode was used. Figure B1 in Appendix B shows the reactor setup for iron electrocoagulation used for the experiments. A 50-mL sample size was used in all experiments. The effective submerged area of the electrodes immersed in the solution was 7.5 cm^2. Three interelectrode distances (7, 15 and 23 mm) were tested in this study as per Table 5.2. A magnetic stirrer was placed below the middle of the cell. Samples were stirred for 5 minutes without electric current to ensure homogeneity of the sample. The speed of the stirrer in all experiments was approximately 500 rpm, which provided vigorous mixing in the cell. The electric current was supplied by a DC-regulated power source (BK Precision 1685B 1-50 V DC and 5 A). A digital

multimeter (DMiOTECH-UA92015N, China) was used to measure the voltage and current.

Three current densities (i) of 8, 15 and 22 mA/cm² were tested in this study and were applied for various time periods (30, 45, and 60 min) as per Table 5.2. Current densities were normalized based on the anode surface area. Each treatment time period represents an independent experiment. The DC-regulated power source and stirring were stopped at the designated treatment time, and a 60-minute flotation period started. Samples were then collected for measurements from the clear layer under the surface froth layer. The iron electrode was cleaned after each experiment in diluted HCl solution (5% v/v).

Table 5.1 Characterization of wet weather flow wastewater used for experiments

Parameter	Units	Mean ± Standard Deviation
pH	-	7.0 ± 0.1
Total Chemical Oxygen Demand	mg/L	353.0 ± 3.9
Soluble Chemical Oxygen Demand	mg/L	196.5 ± 3.3
Total Suspended Solids	mg/L	199.3 ± 27.2
Volatile Suspended Solids	mg/L	151.4 ± 20.3

Table 5.2 Levels of the factors tested in the Box−Behnken Experimental Design

Independent Factors	Units	Symbol	Coded and absolute levels		
			-1	0	1
Current Density	mA/cm²	X_1	8	15	22
Potassium ferrate(VI) Dosage	mM	X_2	0.050	0.075	0.100
Interelectrode distance	mm	X_3	7	15	23
Time	min	X_4	30	45	60

A preliminary set of experiments was conducted to determine the best order in which to apply the individual treatment steps (potassium ferrate(VI) treatment and iron electrocoagulation) as a hybrid treatment system. This sequence of treatment steps was applied in all subsequent tests.

5.2.2 Analytical methods

The bypass wastewater samples' characteristics were measured before each experiment. TSS and volatile suspended solids (VSS) were analyzed using standard methods 2540-D and 2540-E; respectively (APHA AWWA WEF, 1998). Total and soluble chemical oxygen demand (tCOD and sCOD) was measured colorimetrically using the HACH method 8000. sCOD was measured after filtering the sample through 0.45 μm GF/C Whatman filter paper. Zeta potential was measured using a Malvern Zetasizer instrument (Malvern Instruments, Worcestershire, UK). The actual iron electrode loss was measured by gravimetric analysis of the dry anode before and after treatment time. Ferrous (Fe^{2+}) was measured using the 1,10-phenanthroline method (APHA AWWA WEF, 1998). pH was also measured before and after treatment (Accumet electrode and Accumet Excel; Fisher Scientific, Ottawa, ON, Canada).

The purity of potassium ferrate(VI) was measured at the day of each set of experiments by both the 2,2'-azino-bis(3-ethylbenzothiazoline-6-sulphonic acid) or ABTS method at 415 nm and the spectrophotometric method at 510 nm and was found to be higher than 87%. (Cataldo et al., 2017; Lee et al., 2005). For experiments that required measuring the residual potassium ferrate(VI), samples containing residual potassium

ferrate(VI) were quenched by ABTS as soon as they were withdrawn from the test beaker. This assay was utilized because ABTS can immediately quench the residual potassium ferrate(VI) in a sample and allows a time lag between quenching and absorbance measurement (Cataldo et al., 2017). Stock solutions of potassium ferrate(VI) were freshly prepared just before conducting the experiments involving potassium ferrate(VI) by dissolving its solid form in ultrapure water. Potassium ferrate(VI) and reagent-grade ABTS and other reagents were purchased from Sigma-Aldrich. All aqueous solutions were prepared with ultrapure water produced by a Milli-Q system (Millipore, Sigma, USA). Zeta potential was measured offline using a Malvern Zetasizer instrument (Malvern Instruments, Worcestershire, UK).

5.2.3 Experimental Design

A response surface method (RSM) was applied using Box-Behnken Design (BBD). BBD features independent and quadratic rotatability and requires fewer treatment combinations than central composite design when there are more than two factors (Montgomery, 2001). In this study, the effects of four main factors; namely: current density (X_1), potassium ferrate(VI) dosage (X_2), interelectrode distance (X_3), and time (X_4) were evaluated based on sCOD removal efficiency and percentage of total iron remaining as ferrous as responses. Table 5.2 summarizes the experimental conditions of the four variables (X_1, X_2, X_3, and X_4), each at three levels, coded as −1, 0, and +1, for low, middle, and high values, respectively.

Current density, defined as the ratio of current over electrode surface, is an essential operational parameter as it controls the coagulant's dosing rate, hydrogen gas release rate, and the size of both gas bubbles and flocs (Song et al., 2017). The higher the hydrogen gas bubble formation rate is, the better is the flocculation performance due to enhanced turbulence (Song et al., 2017). Potassium ferrate(VI) addition was evaluated in some experimental runs using two dosages selected based on the authors' judgment from previous work in addition to the literature. The third tested operational parameter is the interelectrode distance. The lower the distance is between electrodes, the more gas bubbles are generated which increases hydrodynamic turbulence leading to a better mass transfer as well as to a high chance that contaminants get adsorbed to the generated coagulant species (Hakizimana et al., 2017). In addition, the lower distance between electrodes leads to decreased resistance which results in reduced energy consumption (Hakizimana et al., 2017). The electrocoagulation time factor was evaluated to check its impact on getting ferrous converted to ferric and consequently achieving higher sCOD removal. The effects of the independent variables on the two responses, sCOD removal efficiency and the final percentage of Fe^{2+} to Fe_t , were examined using 27 experiments performed in triplicates as per the statistical matrices developed by the RSM. The response variables were fitted by a second-order - nonlinear regression model in the form of a quadratic polynomial equation represented by Equation 5.1.

$$\eta = \beta_0 + \sum_{i=1}^{k} \beta_i x_i + \sum_{i=1}^{k} \beta_{ii} x_i^2 + \sum_{i,j=1} \sum_{i<j} \beta_{ij} x_i x_j \quad (5.1)$$

where β_0 is a constant, β_i are the k first-order coefficients, $\beta_{ii}$are the k quadratic coefficients, and β_{ij} are the $k(k-1)/2$ cross-product or interaction coefficients for the model written in terms of the factors, x_i and x_j.

The parameters and responses used in the experiments were evaluated using Minitab 18 Statistical Software (Minitab Inc., State College, PA, USA). Analysis of variance (ANOVA) was employed to perform diagnostic tests on the adequacy of the developed model. The statistical significance of the proposed model and parameters tested in the model were examined using F-value and P-value at 95% confidence level. The fitness of the multi-regression model was expressed by the adjusted coefficient of determination (Adj R^2), and standard error of the estimate.

5.3 Results and discussion

5.3.1 Investigation of the hybrid system arrangement and its advantage

Enhancing the iron electrocoagulation system using potassium ferrate(VI) is investigated to provide a versatile treatment combination capable of increasing the sCOD removal efficiency and reducing the percentage of electrochemically supplied Fe_t that remains as Fe^{2+}. The preliminary investigation involved determining the effects of the order in which the treatment steps were applied in sequence. Potassium ferrate(VI) can contribute to achieving higher treatment efficiency in the hybrid system used in this study through three pathways: oxidation, by assisting in coagulation, and

by elevating the pH. The relative contributions of each of these pathways was also investigated. Figure 5.1 contains the results of three hybrid treatment sequences (a, c, and e) and two additional tests (b and d) conducted to serve as control experiments.

The first pathway is through oxidation. As indicated in Figure 5.1-a, potassium ferrate(VI) treatment initially oxidized 11.3% of the sCOD and increased the pH from 7.0 to 8.3. The product of potassium ferrate(VI) treatment was then transferred to iron electrocoagulation cell in which a further 41.8% of the initial sCOD was removed (overall sCOD removal for the two processes in sequence was 53.1%). The experiment, shown in Figure 5.1-b, was then conducted in order to differentiate the possible effects of the iron nanoparticles formed during potassium ferrate(VI) treatment from those of the increased pH on the outcome of iron electrocoagulation (shown in Figure 5.1-a). Comparing the results shown in Figures 5.1-a and 5.1-b reveals that when the initial pH was adjusted to 8.3 iron electrocoagulation achieved 44.9% sCOD removal, which is very similar to the electrocoagulation contribution to sCOD removal in the sequential treatment shown in Figure 5.1-a (41.8%). This suggests that the nanoparticles formed during potassium ferrate(VI) treatment had an insignificant effect on sCOD removal in the subsequent electrocoagulation treatment.

Reversing the order in which the treatment was applied (Figure 5.1-c) resulted in 36.9% sCOD removal in the initial electrocoagulation step and an increase in pH from 7.0 to 8.1. Subsequent potassium ferrate(VI) treatment increased overall sCOD removal by 12.1% to 46.0% and further increased pH to 9.1. Figure 5.1d contains the

results of a subsequent test conducted to assess the effect on the potassium ferrate treatment of the pH increase to 8.1. The 15.1% sCOD removal achieved by potassium ferrate(VI) treatment under this condition is somewhat greater than the 12.1% achieved under the sequential treatment arrangement shown in Figure 5.1-c. Research showed that providing an iron source through dosing ferric chloride prior to the addition of potassium ferrate(VI) catalyzed the decomposition of potassium ferrate(VI) which reduces its contact time with the target contaminant thereby reducing its oxidative ability (Jiang et al., 2015). Overall, the low range of sCOD removal efficiency using potassium ferrate(VI) as a sole treatment has been reported elsewhere (Jiang et al., 2007; Li et al., 2016; Wang et al., 2018).Figure 5.1-e contains the results of the concurrent application of the two treatment methods. The 52.4% sCOD removal is similar to that achieved by either of the other two application sequences (Figures 5.1-a and 5.1-c), as is the final pH of 8.6.

With respect to the three proposed treatment pathways, these results indicate that the benefit to sCOD removal provided by potassium ferrate(VI) included its oxidative ability and the resultant increase in pH. As may be expected, its effect on coagulation had no impact on sCOD removal. It is postulated that increasing the initial pH values beyond 7.5 can increase the rate of Fe^{2+} conversion to desirable ferric hydroxide ($Fe(OH)_3$) precipitates; thus, achieving higher sCOD removal efficiency (Lakshmanan et al., 2009).

a) Potassium ferrate(VI) treatment followed by electrocoagulation

	Treatment	Results	Treatment	Cumulative Results
Initial pH=7.0	Potassium ferrate(VI)	pH=8.3 % sCOD Removal=11.3 Negligible Fe^{2+}	Iron Electrocoagulation	pH=8.9 % sCOD Removal=53.1 % $Fe^{2+}$to Fe_t=9.8

b) pH adjusted to 8.3 before electrocoagulation treatment

	Treatment	Results
Initial pH=8.3	Iron Electrocoagulation	pH=8.8 % sCOD Removal=44.9 % $Fe^{2+}$to Fe_t=10.9

c) Electrocoagulation followed by potassium ferrate treatment

	Treatment	Results	Treatment	Cumulative Results
Initial pH=7.0	Iron Electrocoagulation	pH=8.1 % sCOD Removal=36.9 % $Fe^{2+}$to Fe_t=38.2	Potassium ferrate(VI)	pH=9.1 % sCOD Removal=49.0 % $Fe^{2+}$to Fe_t=11.2

d) pH adjusted to 8.1 before potassium ferrate(VI) treatment

	Treatment	Results	
Initial pH=8.1	Potassium ferrate(VI)	pH=9.3 % sCOD Removal=15.1	Negligible Fe^{2+}

e) Potassium ferrate(VI) applied at the start of electrocoagulation

		Results
Initial pH=7.0	Potassium ferrate(VI) and Iron Electrocoagulation	pH=8.6 %sCOD Removal=52.4 %Fe^{2+} to Fe_t = 8.6

Figure 5.1 Dosing options of potassium ferrate(VI): (a) before, (b) at the start of, or (c) after iron electrocoagulation and its implications on sCOD removal efficiency and percentage of the electrochemically supplied Fe_t that remains as Fe^{2+}. Other experimental conditions are: Iron Electrocoagulation (Current density=15 mA/cm²; Interelectrode distance: 7 mm; Flotation Time 60 minutes), Potassium ferrate(VI) (Dose= 0.1 mM; Mixing Time=20 minutes). Hybrid System (Current density=15 mA/cm²; Interelectrode distance: 7 mm; Flotation Time 60 minutes; Potassium ferrate(VI) Dose= 0.1 mM).

In addition, although the oxidation potential of potassium ferrate(VI) decreases with increasing pH, its stability increases as does the deprotonation of organic compounds. De-protonated compounds have been found to be more readily oxidized (Li et al., 2005) so overall potassium ferrate(VI) benefits from the pH increase during iron electrocoagulation process (Li et al., 2005). Comparing the overall sCOD removal achieved by potassium ferrate(VI) followed by iron electrocoagulation or vice versa (Figure 5.1-a and Figure 5.1-c) with a hybrid system in which both processes occur concurrently in the same cell (Figure 5.1-e) shows that the concurrent process achieved comparable overall removal efficiency within shorter time, which in practice would mean a smaller treatment process footprint and lower capital cost. Further development, improvement and optimization of the concurrent hybrid process are conducted using RSM-BBD experimental design.

5.3.2 Experimental design analysis

BBD for statistical analysis using the RSM was employed to investigate the effects of the four independent variables (X_1, X_2, X_3, and X_4) shown in Table 5.2 on the response function and to determine the optimal conditions maximizing sCOD removal efficiency and minimizing the final percentage of Fe^{2+} with respect to the electrochemically supplied Fe_t. The results for the sCOD removal efficiency and the final Fe^{2+} to Fe_t percent ratio are listed in Table 5.3. Regression coefficients, standard deviations, t-values and probability values are summarized in Table 5.4. The response function coefficients were determined using the regression of the experimental data. Table 5.5 represents the ANOVA analysis for all responses. The ANOVA test was

conducted to estimate the fitness of the response functions and the significance of the effects of the independent variables.

5.3.2.1 sCOD removal efficiency response factor

As shown in Table 5.4, the linear coefficients (β_1, β_2, and β_4), the second-degree coefficients (β_{11} and β_{44}), and the interaction coefficient (β_{12}, β_{13}, β_{14}, and β_{23}) demonstrate significant influences. The coefficient values show that the effects of all parameters represented by the linear coefficients and their interactions on sCOD removal efficiency are positive whereas that of the second-degree coefficient β_{44} representing time (X_4) is negative. The response function for sCOD removal efficiency (%) is shown in Equation 5.2 in terms of the coded levels of the factors. Equation 5.2 only describes the significant independent and the interaction terms which have probability values (p-values) less than 0.05.

$$\% \text{ sCOD removal} = 44.72 + 5.17X_1 + 9.37X_2 + 0.46X_4 + 1.86X_1^2 - 1.77X_4^2 + 2.09X_1X_2 + 1.51X_1X_3 + 0.56X_1X_4 + 1.70X_2X_3 \quad (5.2)$$

Table 5.5 shows the results of the statistical testing of the model with F-test for ANOVA. The value of F-statistic calculated for the sCOD removal efficiency (the response) is found to be 613.70 which is much higher than the tabulated value of $F_{0.05,14,66}$ (1.845). This shows that most of the variability in the response can be explained by the regression equation. The high value of the coefficient of determination (Adj R^2= 99.08%) shows good agreement between measured and modeled values of this response. In addition, the p-value probability is less than <0.05 as shown in Table 5.5 which reflects no evidence of lack of fit for the model.

Table 5.3 The Box-Behnken experimental design matrix of four variables along with the related experimental and calculated response

X_1: Current Density (mA/cm^2)	X_2: Potassium Ferrate(VI) (mM)	X_3: Interelectrode distance (mm)	X_4: Time (min)	% sCOD Removal Efficiency (Measured)	% sCOD Removal Efficiency (Modeled)	% Fe^{2+} to Fe_t (Measured)	% Fe^{2+} to Fe_t (Modeled)
15	0.00	22	45	33.05±1.39	47.03	34.91±1.86	34.66
8	0.05	15	60	39.73±0.88	47.56	52.85±1.93	49.91
8	0.05	15	30	39.14±0.55	48.45	50.88±1.08	51.28
22	0.05	22	45	52.73±0.71	66.32	17.38±1.05	16.85
15	0.10	7	45	52.16±0.33	55.23	8.33±0.27	7.12
22	0.05	15	30	48.79±1.01	57.86	17.81±1.52	18.73
22	0.05	15	60	51.63±1.33	59.21	17.37±0.43	14.97
15	0.00	7	45	37.60±0.19	40.54	36.00±0.08	34.66
15	0.05	7	60	42.68±0.40	46.25	20.37±0.49	17.94
15	0.05	7	30	42.22±0.54	46.02	19.90±0.96	20.50
15	0.10	15	60	52.70±0.09	60.68	7.55±1.28	5.84
15	0.10	15	30	51.94±0.16	60.45	7.81±0.40	8.40
8	0.10	15	45	49.22±0.35	56.83	38.44±1.19	38.49
15	0.05	22	30	42.50±0.75	55.91	20.69±0.48	20.50
15	0.05	22	60	43.27±1.13	56.14	20.38±0.06	17.94
15	0.00	15	60	33.29±0.40	42.36	36.37±0.78	33.37
15	0.00	15	30	33.20±0.29	42.13	36.58±1.18	35.94
22	0.05	7	45	49.98±0.32	53.40	17.27±0.29	16.85
22	0.10	15	45	63.57±0.48	71.53	4.63±0.53	4.74
8	0.05	22	45	39.25±0.23	52.96	52.31±1.11	50.59
22	0.00	15	45	39.71±0.42	49.05	34.02±0.91	32.28
8	0.05	7	45	42.57±0.15	46.10	52.34±0.88	50.59
8	0.00	15	45	33.70±0.36	42.69	66.62±0.49	66.03
15	0.10	22	45	54.30±0.06	68.52	8.00±0.87	7.12
15	0.05	15	45	45.45±0.34	53.16	19.36±0.62	19.22
15	0.05	15	45	44.54±0.09	53.16	15.27±10.18	19.22
15	0.05	15	45	44.13±0.34	53.16	20.03±0.99	19.22

Table 5.4 Estimated regression coefficients for different responses using coded levels (-1,0,1)

Response	sCOD				% Fe^{2+}/Fe_t			
Coefficient	Value	Standard Error	T-value	P-Value	Value	Standard Error	T-value	P-Value
β_o	44.72	0.24	185.16	0.000	19.92	0.33	60.41	0.000
β_1	5.17	0.12	42.78	0.000	-17.08	0.17	-103.61	0.000
β_2	9.37	0.12	77.58	0.000	-14.15	0.17	-85.82	0.000
β_3	-0.18	0.12	-1.45	0.151	-0.05	0.16	-0.27	0.784
β_4	0.46	0.12	3.77	0.000	0.11	0.17	0.67	0.504
β_{11}	1.86	0.18	10.31	0.000	14.50	0.25	58.79	0.000
β_{22}	-0.09	0.18	-0.47	0.637	1.66	0.25	6.75	0.000
β_{33}	-0.37	0.18	-2.01	0.050	0.24	0.25	0.97	0.333
β_{44}	-1.77	0.18	-9.72	0.000	0.33	0.25	1.32	0.191
β_{12}	2.09	0.21	10.00	0.000	-0.30	0.29	-1.07	0.290
β_{13}	1.51	0.21	7.27	0.000	0.06	0.28	0.22	0.829
β_{14}	0.56	0.21	2.70	0.009	-0.60	0.29	-2.12	0.038
β_{23}	1.70	0.21	8.16	0.000	0.16	0.28	0.55	0.583
β_{24}	0.17	0.21	0.79	0.429	-0.01	0.29	-0.04	0.967
β_{34}	0.09	0.21	0.43	0.670	-0.19	0.28	-0.67	0.505

Table 5.5 Analysis of Variance (ANOVA) Results

Response		Degree of freedom	Sum of square	Mean square	F-statistic	P-value
sCOD	Model	14	4485.0	320.4	613.70	0.000
Adj R^2 = *99.08%*	Error	66	34.5	0.5		
	Total	80	4519.5			
$\%Fe^{2+}/Fe_t$	Model	14	21705.6	1550.4	1593.5	0.000
Adj R^2= 99.64%	Error	66	64.2	1.0		
	Total	80	21769.8			

The assumption that the residuals are normally distributed was checked by the normal probability plot shown in Figure 5.2-a. Figure 5.2-a illustrates that most of the residuals are distributed near the 45 degree line indicating that residuals are normally distributed. The two-dimensional (2D) contour plot representing the effect of the interaction between the current density and potassium ferrate(VI) concentration on the sCOD removal efficiency is shown in Figure 5.3-a. The values of interelectrode distance (X_3) and time (X_4) were held at 15 mm and 45 min; respectively. Contours in Figure 5.3-a indicate that there is no point of maximum or minimum response and is considered as a saddle point. The sCOD removal efficiency is found to increase with the increase of both the current density and potassium ferrate(VI) dosage.

5.3.2.2 Percentage Fe^{2+} to the electrochemically supplied Fe_t

The response function in terms of the coded levels of the factors for the percent of Fe^{2+} to electrochemically supplied Fe_t in the treated wastewater is shown in Equation 5.3 based on the significant independent factors and their interaction terms with p-values less than 0.05. The F-value of the model was 1593.5 for the percentage Fe^{2+}in the treated wastewater with respect to the electrochemically supplied Fe_t. This F-Value is even greater than the one reported for the sCOD removal efficiency and shows that most of the variables in the response can adequately be described by the regression equation.

$$\% Fe^{2+}/Fe_t = 19.92 - 17.08X_1 - 14.15X_2 + 14.50X_1^2 + 1.66X_2^2 - 0.60X_1X_4 \qquad (5.3)$$

Linear coefficients (β_1 and β_2) were found to be the only linear variables with statistical significance (Table 5.4). The second-degree variables (β_{11} and β_{22}) are also significant. For interaction variables, all variables were insignificant except for the interaction between current density and time (β_{14}). The Adj R^2 statistic indicates that the model representing percentage of Fe^{2+} to electrochemically supplied Fe_t response factor can describe 99.64% of the variability which is a little bit higher than that estimated for sCOD removal efficiency response factor (99.08%). The residuals were found to be normally distributed as shown in Figure 5.2-b.

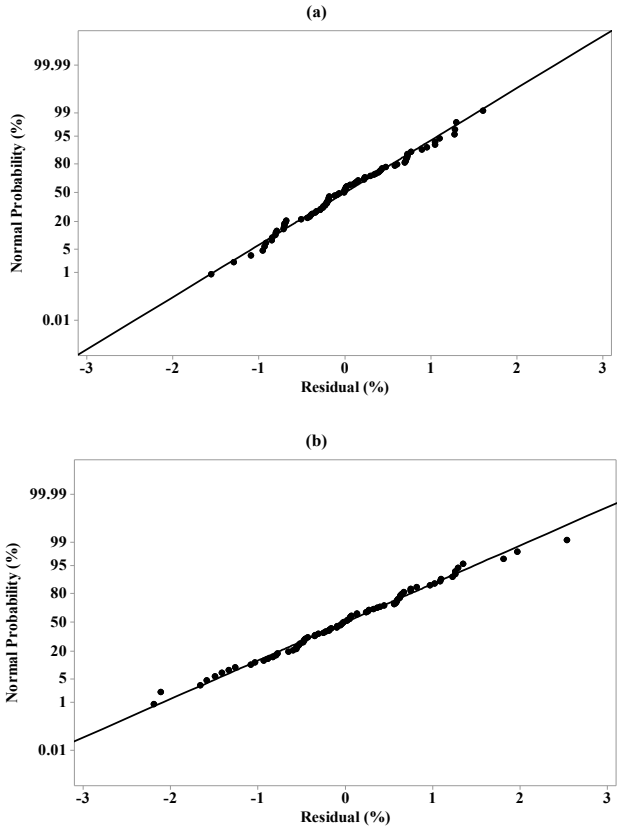

Figure 5.2 Residuals Normal Probability Plot of (a) sCOD removal efficiency and (b) percent ratio of the Fe^{2+} to the electrochemically supplied Fe_t.

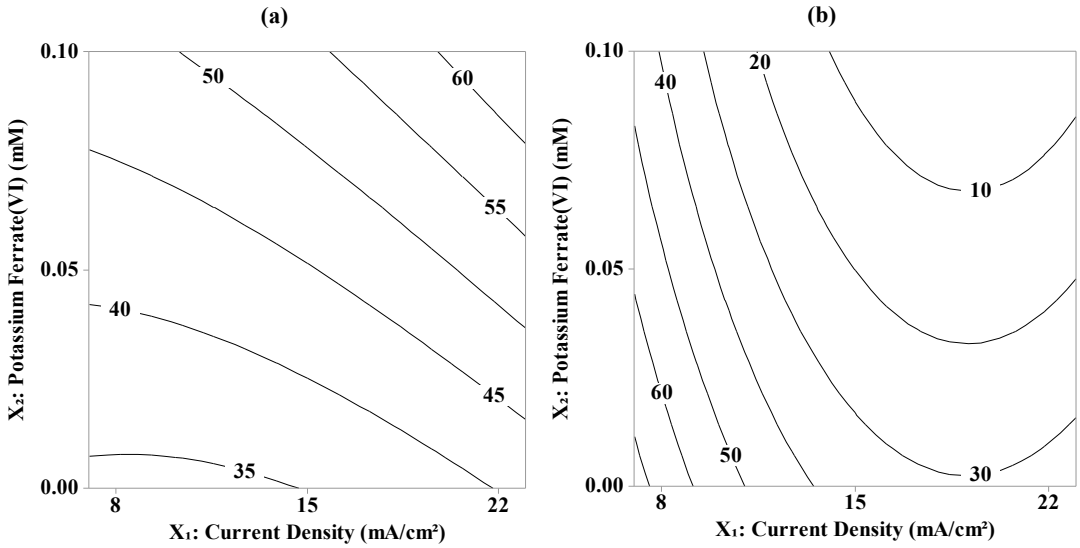

Figure 5.3 Contour plot of the effect of the interaction between current density and potassium ferrate(VI) concentration on (a) sCOD removal efficiency and (b) percentage of the electrochemically supplied Fe_t that remains as Fe^{2+}. (Constant Values: Interelectrode distance (X_3) = 15 mm; Time (X_4)= 45 min)

Figure 5.3-b shows the two-dimensional (2D) contour plot of the effect of the interaction between the current density and potassium ferrate(VI) concentration on the percent of Fe^{2+} to electrochemically supplied Fe_t. Similar to Figure 5.3-a, it should be noted that Figure 5.3-b was developed while holding the values of interelectrode distance (X_3) at 15 mm and time (X_4) at 45 min. Unlike sCOD removal efficiency response factor, contours in Figure 5.3-b exhibited optimal response with respect to current density. The percentile of Fe^{2+} to electrochemically supplied Fe_t is found to decrease with the increase of both the current density and potassium ferrate(VI) dosage until an optimum current density is obtained at about 19 mA/cm². As the current density increases beyond the optimum level, maintaining lower percentiles of Fe^{2+} to

electrochemically supplied Fe_t requires higher potassium ferrate(VI) concentrations. This means that beyond 19 mA/cm², the generated Fe^{2+} are produced more quickly than they can be oxidized to ferric at the prevailing pH produced through electrocoagulation and assistance in this regard is required from providing higher potassium ferrate(VI) dosage.

5.3.3 Zeta potential change during hybrid potassium ferrate(VI) – iron electrocoagulation treatment

Figures 5.4-a and 5.4-b show zeta potential and sCOD removal, respectively, during the course of each of these treatments. It can be seen that zeta potential increased quite slowly during potassium ferrate(VI) treatment. The isoelectric point (where the zeta potential value reaches zero) was not achieved when potassium ferrate(VI) was employed alone. In the experiments that tested iron electrocoagulation alone using the optimum current density of 19 mA/cm² deduced from the RSM-BBD experiments, zeta potential increased sharply and reached the isoelectric point after 47 minutes of electrolysis. The hybrid process though had relatively lower rate of zeta potential increase than the iron electrocoagulation alone and brought the system very close to the isoelectric point after 60 minutes. This might be due to the negatively charged nanoparticles resulting from potassium ferrate(VI) decay (Goodwill et al., 2015).

The sCOD removal efficiencies were poor using potassium ferrate(VI) alone as shown in Figure 5.4-b. Iron electrocoagulation alone archived triple the removal efficiency of potassium ferrate(VI). The hybrid system resulted in the highest sCOD removal

efficiencies of sCOD regardless of the retarding effect in bringing the system to the isoelectric point caused by the negatively charged nanoparticles resulted from potassium ferrate(VI) oxidation.

A closer look at Figures 5.4 shows that there is no significant sCOD removal beyond 30 minutes (corresponds to -11 mV zeta potential) in the hybrid system treatment and beyond 40 minutes in the iron electrocoagulation treatment (corresponds to -14 mV zeta potential). This suggests that lengthening the process beyond those times might not be useful for sCOD reduction. These results also draw the attention towards the definition of near neutral conditions has been found to vary based on the application. For instance, an operational zeta potential window between -10 to +2 mV was claimed to be effective in attaining optimum removal of both algal cells and extracellular organic matter and could be achieved by a combination of coagulant dose and/or pH adjustment (Henderson et al., 2008a). When algae was the major pollutant at pH 7, the zeta potential operating window was found to be extended to -15 mV (Henderson et al., 2008b). Another study reported a range between -10 to +5 mv of zeta potential to achieve optimum dissolved organic carbon removal (Sharp et al., 2005). This is similar to the results shown in Figures 5.4 in which sCOD removal reaches a plateau at zeta potentials between approximately -11 and +5 mV. There is no comprehensive study to date on the range of zeta potentials that can be considered neutral in municipal wastewater treatment applications, and such study is warranted.

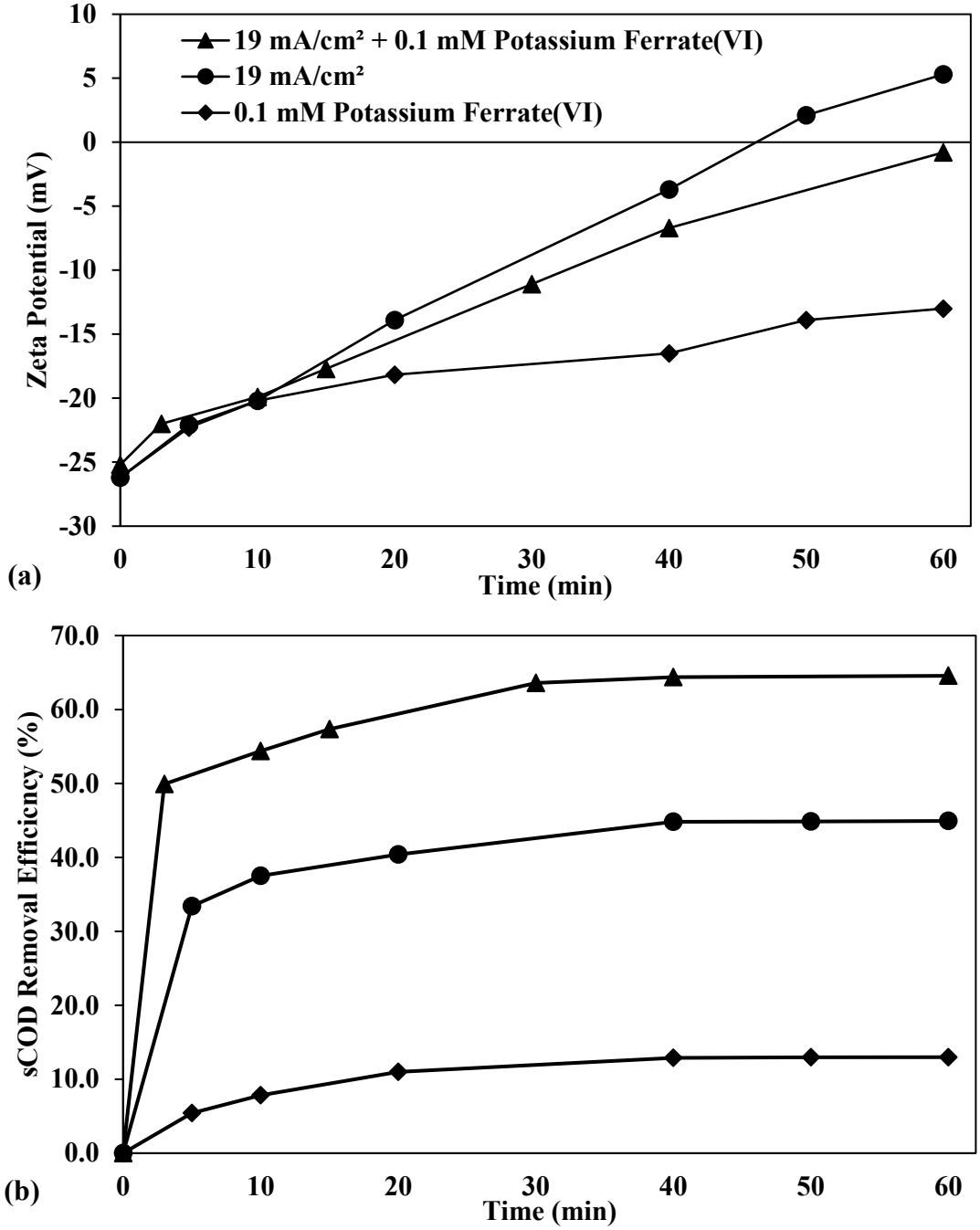

Figure 5.4 Performance of iron electrocoagulation system, potassium ferrate(VI), and a hybrid system of with time as assessed by (a) zeta potential; and (b) sCOD.

It is not possible to draw a mathematical correlation between the zeta potential and the reduction of sCOD under the conditions tested in this study. This is likely due to charge neutralization not being the sole mechanism responsible for sCOD removal in these systems. In addition to the oxidation that occurs in the systems that involved the addition of potassium ferrate(VI), two mechanisms have been postulated as being likely for the removal of dissolved organics by hydrolyzing iron species (Duan and Gregory, 2003). The first removal mechanism involves the binding of positively charged iron species to negatively charged substances leading to charge neutralization and reduced solubility which for large molecules can lead to precipitation, flocculation and subsequent removal by sedimentation or in an electrocoagulation cell, also by flotation. The second removal mechanism is the adsorption of the soluble substances on the iron hydroxide precipitates which causes a lesser amount of charge neutralization relative to the former mechanism. This later mechanism is likely the predominant removal mechanism based on the results shown in Figures 5.4 which show that sCOD removal efficiencies have achieved a plateau beyond -14 mV for iron electrocoagulation treatment and -11 mV zeta potential in the hybrid system treatment, but that the extent of sCOD removal is not related directly to zeta potential.

5.4 Conclusions

The current study introduced a novel enhancement technique of primary wastewater treatment by hybrid potassium ferrate(VI) – iron electrocoagulation system. Out of the three pathways through which potassium ferrate(VI) can be beneficial in enhancing

iron electrocoagulation, oxidation contribution and pH increase were found to be the most significant factors. Oxidation can help increase the sCOD removal by about 10% while pH increase promoted favorable conditions to quickly oxidize Fe^{2+} to form $Fe(OH)_3$ precipitates. By using response surface methodology – Box Behnken design, current density and potassium ferrate(VI) and their interaction were shown to be significant in achieving higher sCOD removal and faster Fe^{2+}oxidation. Interelectrode distance and time were found to cause minimal effect; thus, the hybrid technology can use fewer iron electrodes per tank and provide rapid treatment. While an isoelectric point was achieved for both iron the electrocoagulation and hybrid potassium ferrate(VI) and iron electrocoagulation systems, it was not possible to correlate zeta potential measurements to sCOD reduction. This indicates that the sCOD removal mechanisms were not entirely related to charge neutralization.

CHAPTER 6. GENERAL CONCLUSIONS AND RECOMMENDATIONS

6.1 Thesis overview

Bypass wastewaters need an appropriate auxiliary treatment capable of attenuating the contamination magnitude prior to their discharge into water bodies. Two iron-based treatment technologies; namely potassium ferrate(VI) and iron electrocoagulation in addition to a hybrid process of both processes were tested in this Ph.D. research for the enhancement of primary wastewater treatment as a standalone or auxiliary treatment.

The first phase of the current work included a study on enhanced primary treatment using potassium ferrate(VI). This aimed at testing its efficacy in enhancing the disinfection and coagulation capabilities of the primary treatment of bypass wastewater for the removal of *Escherichia coli* (*E. Coli*), Fecal Coliform (FC), Total Suspended Solids (TSS), and Orthophosphates (PO_4^{3-}). In this regard, the focus was given to studying the effect of rapid mixing speeds used in existing wastewater treatment plants' coagulation facilities on the removal of each of the five responses monitored (i.e., *E. Coli*, FC, TSS, and PO_4^{3-}). In addition, potassium ferrate(VI) consumption and inactivation characteristic were modeled at different rapid mixing speeds in high oxidant demand bypass wastewaters. Furthermore, the contribution of

the coagulation capability of potassium ferrate(VI) in further enhancing the overall *E. Coli* removal was examined.

The second phase of this Ph.D. research focused on examining iron electrocoagulation process in removing soluble chemical oxygen demand (sCOD) from bypass wastewater at neutral pH, two different temperatures (8°C and 23°C), and different current densities. A critical discussion was included on the limitations of applying adsorption isotherm models in iron electrocoagulation system. Alternative variable order kinetic models (VOK) were proposed and were based on a realistic estimation of the adsorbent mass.

The third part of this study aimed at enhancing primary wastewater treatment by novel hybrid potassium ferrate(VI) – iron electrocoagulation system. This included a study on the feasibility of the three pathways potassium ferrate(VI) can contribute within enhancing iron electrocoagulation process. The three pathways are: 1) utilizing the oxidation capability of potassium ferrate(VI) to remove sCOD; (2) employing its resultant nanoparticles to improve the coagulation capabilities of iron electrocoagulation; and (3) increasing the pH of the system thus promoting favourable conditions for ferrous (Fe^{2+}) oxidation, a problematic product of iron electrocoagulation at near neutral pH prevailing in environmental wastewater samples. Moreover, the relationship between the coagulant dosage generated during hybrid potassium ferrate(VI) - iron electrocoagulation process and the increased zeta potential of wastewater samples was investigated over time at optimum treatment conditions.

6.2 Conclusions

Based on the experimental results and analyses obtained from all three phases of this research, the following conclusions were drawn.

6.2.1 Potassium ferrate(VI)

- Each bypass wastewater out of each sampling event is unique in its characteristics, and the challenge with such type of wastewaters is to find a treatment receptive to such large changes. Potassium ferrate(VI) can be a viable treatment alternative given its dual capacity as a disinfectant/oxidant and coagulant.
- Controlling both mixing speed and potassium ferrate(VI) dosages was found to be of paramount importance to maximize the potassium ferrate(VI) treatment efficiency in tackling *E. Coli*, FC, TSS, and PO_4^{3-}. Under the conditions tested in this study, *E. Coli* and FC removals were found to increase with the increase of both the mixing intensity and potassium ferrate(VI) dosages.
- Potassium ferrate(VI) could very effectively remove PO_4^{3-} with at least 88.7% removal and meet the 1 mg/L limit for safe discharge to surface water guidelines in all cases tested.
- Optimum operating parameters for potassium ferrate(VI) treatment to maximize TSS removal were found to be achieved by setting the mixing speed at 806 rpm and applying a dosage of 0.09 mM. Increasing mixing intensity

from the low to optimum level was beneficial for TSS removal but increasing it above the center level was detrimental. This suggests that sweep floc formation was a dominant TSS removal mechanism.

- The double exponential model was able to represent the potassium ferrate(VI) decay in all conditions with a high coefficient of determination and low mean square error. In addition, the dissociation of potassium ferrate(VI) and rate of disinfection in bypass wastewater were higher using varied speed mixing conditions than for magnetic stirrer mixing for the same initial dosage and sampling event.
- There was no significant increase in the potassium ferrate(VI) dissociation rates with the increase of the rapid mixing speeds, and a similar conclusion could be drawn for the rates of disinfection. This revealed that the reactions were kinetically controlled.
- The contribution of physical removal by sedimentation to the overall *E. Coli* removal and was enhanced by the potassium ferrate(VI)'s floc-forming capability.
- Potassium ferrate(VI) can be used in the current primary sedimentation tanks enhanced by coagulation and flocculation mixing facilities, yet lower energy inputs from lower rapid mixing speeds may be used.

6.2.2 Iron electrocoagulation

- For iron electrocoagulation enhancement option, sCOD removal efficiencies increased with the increase of electrolysis time, current density, and temperature.
- The temperature effect was proven such that at 23°C, it took 15 minutes to reach an average 52% sCOD removal efficiency while it took around 40 minutes to achieve comparable removal efficiency at 8°C; both tested at 15 mA/cm^2 current density.
- Equilibrium could not have been established under the operational conditions tested in this study which emphasises the need researchers to be careful when applying adsorption isotherms to iron electrocoagulation systems.
- Alternatively, kinetic based models such as Langmuir and Langmuir-Freundlich VOK models would be more appropriate in modeling adsorption results from iron electrocoagulation. The latter models were examined in this study with suitable assumptions and consideration of the de-facto estimation of ferric hydroxide ($Fe(OH)_3$) (adsorbent) that accounts for the contribution of ferrous (Fe^{2+}) to treatment end products. The Langmuir VOK model was found to be the better model to describe sCOD removal in the electrocoagulation cell under all test conditions with chemisorption being considered the dominant sCOD removal mechanism.

6.2.3 Hybrid potassium ferrate(VI) and iron electrocoagulation system

- A novel enhancement technique of primary wastewater treatment by hybrid potassium ferrate(VI) – iron electrocoagulation system was found very effective in sCOD removal.
- Out of the three pathways through which potassium ferrate(VI) can be beneficial in enhancing iron electrocoagulation, oxidation contribution and pH increase were found to be the most significant factors.
- By using response surface methodology – Box Behnken design, current density and potassium ferrate(VI) and their interaction were found significant in achieving higher sCOD removal and faster Fe^{2+}oxidation.
- Interelectrode distance and time were found to cause minimal effect; thus, the hybrid technology can use fewer iron electrodes per tank and provide rapid treatment.
- An isoelectric point was achieved for both iron the electrocoagulation and hybrid potassium ferrate(VI) and iron electrocoagulation systems; but this did not result in a correlation between zeta potential measurements to sCOD reduction. This shows that the sCOD removal mechanisms were not completely associated with charge neutralization.

6.3 Future Research and Recommendations

- Bypass wastewater might pose a significant toxic effect on the receiving environment. Consequently, it is advisable to work on exploring the potential

toxic contaminants in bypass wastewater and their environmental impact. Monitoring bypass particle size distribution and the level of contamination associated with each size range can also help in understanding the fate and transport of certain contaminants in the environment. This will help in establishing better standards that reflect on the receiving environment characteristics, intended water uses, and reuse alternatives.

- Fractionation of the primary wastewater particles prior to the addition of potassium ferrate(VI) may be of interest to identify the particles that might be of inhibitory effect to potassium ferrate(VI).
- A comprehensive study that aims at providing suggestions on minimum mixing conditions for different initial pH and oxidant demand wastewaters is recommended using the concept of kinetically controlled reaction hypothesis for potassium ferrate(VI) employed in this study which means an increase in mixing speed should have no effect on the reaction rate.
- Researchers are advised to report the mixing scheme of their oxidation experiments and verify that the rate constants they derive were collected at kinetically controlled conditions.
- Combination of the potassium ferrate(VI) and iron electrocoagulation processes may offer unique synergetic advantages which should be investigated such as providing disinfection.

- Zeta potential operating window that can be considered neutral in municipal wastewater treatment applications should be investigated.
- Although destabilization and aggregation of particles are the core of any coagulation process by definition, there is a gap of knowledge in the characterization and the implications of the resultants particles out of iron-based electrocoagulation process; thus, a research study is recommended.

REFERENCES

Alberta Government, 2013. Wastewater systems standards for performance and design, in: Standards and Guidelines for Municipal Waterworks, Wastewater and Storm Drainage Systems. Alberta Queen's Printer, p. 42.

Alsheyab, M., Jiang, J.-Q., Stanford, C., 2009. On-line production of ferrate with an electrochemical method and its potential application for wastewater treatment - A review. J. Environ. Manage. 90, 1350–1356. doi:10.1016/j.jenvman.2008.10.001

Amirtharajah, A., Mills, K.M., 1982. Rapid-mix design for mechanisms of alum coagulation. J. Am. Water Works Assoc. 74, 210–216.

APHA AWWA WEF, 1998. Standard methods for the examination of water and wastewater, 20th ed. APHA-AWWA-WEF, Washington, D.C.

Bagga, A., Chellam, S., Clifford, D.A., 2008. Evaluation of iron chemical coagulation and electrocoagulation pretreatment for surface water microfiltration. J. Memb. Sci. 309, 82–93. doi:10.1016/j.memsci.2007.10.009

Balasubramanian, N., Kojima, T., Srinivasakannan, C., 2009. Arsenic removal through electrocoagulation: Kinetic and statistical modeling. Chem. Eng. J. 155, 76–82. doi:10.1016/j.cej.2009.06.038

Bandala, E.R., Miranda, J., Beltran, M., Vaca, M., López, R., Torres, L.G., 2009. Wastewater disinfection and organic matter removal using ferrate (VI) oxidation.

J. Water Health 7, 507–513. doi:10.2166/wh.2009.003

Barlsçl, S., Dimoglo, A., 2016. Review on the Stability of Ferrate (VI) Species in Aqueous Medium and Oxidation of Pharmaceuticals and Personal Care Products (PPCPs) by Ferrate (VI): Identification of Transformation By-Products, in: ACS Symposium Series. pp. 287–335.

Basu, A., Williams, K.R., Modak, M.J., 1987. Ferrate Oxidation of Escherichia coli DNA Polymerase-I. J. Biol. Chem. 262, 9601–9607.

Ben-Sasson, M., Zidon, Y., Calvo, R., Adin, A., 2013. Enhanced removal of natural organic matter by hybrid process of electrocoagulation and dead-end microfiltration. Chem. Eng. J. 232, 3380–345. doi:10.1016/j.cej.2013.07.101

Ben Sasson, M., Calmano, W., Adin, A., 2009. Iron-oxidation processes in an electroflocculation (electrocoagulation) cell. J. Hazard. Mater. 171, 704–709. doi:10.1016/j.jhazmat.2009.06.057

Brillas, E., Boye, B., Ángel Baños, M., Calpe, J.C., Garrido, J.A., 2003. Electrochemical degradation of chlorophenoxy and chlorobenzoic herbicides in acidic aqueous medium by the peroxi-coagulation method. Chemosphere 51, 227–235. doi:10.1016/S0045-6535(02)00836-6

Brillas, E., Sauleda, R., Juan, C., 1998. Degradation of 4-Chlorophenol by Anodic Oxidation, Electro-Fenton, Photoelectro-Fenton, and Peroxi-Coagulation Processes. J. Electrochem. Soc. 145, 759–765.

Brillas, E., Sauleda, R., Juan, C., 1997. Peroxi-coagulation of Aniline in Acidic Medium Using an Oxygen Diffusion Cathode. J. Electrochem. Soc. 144, 2374. doi:10.1149/1.1837821

Cataldo, M.A.H., May, A., Bonakdapour, A., Mohseni, M., Wilkinson, D.P., 2017. Analytical quantification of electrochemical ferrates for drinking water treatments. Can. J. Chem. 95, 105–112.

CCME, 2014. Canada-wide strategy for the management of municipal wastewater effluent. Winnipeg, Manitoba.

Chhetri, R.K., Bonnerup, A., Andersen, H.R., 2016. Combined Sewer Overflow pretreatment with chemical coagulation and a particle settler for improved peracetic acid disinfection. J. Ind. Eng. Chem. 37, 372–379. doi:10.1016/j.jiec.2016.03.049

Chhetri, R.K., Thornberg, D., Berner, J., Gramstad, R., Öjstedt, U., Sharma, A.K., Andersen, H.R., 2014. Chemical disinfection of combined sewer overflow waters using performic acid or peracetic acids. Sci. Total Environ. 490, 1065–1072. doi:10.1016/j.scitotenv.2014.05.079

Cho, M., Lee, Y., Choi, W., Chung, H., Yoon, J., 2006a. Study on Fe(VI) species as a disinfectant: Quantitative evaluation and modeling for inactivating Escherichia coli. Water Res. 40, 3580–3586. doi:10.1016/j.watres.2006.05.043

Cho, M., Lee, Y., Choi, W., Chung, H., Yoon, J., 2006b. Study on Fe(VI) species as a

disinfectant: Quantitative evaluation and modeling for inactivating Escherichia coli. Water Res. 40, 3580–3586. doi:10.1016/j.watres.2006.05.043

Chou, W.L., Wang, C.T., Hsu, C.W., Huang, K.Y., Liu, T.C., 2010. Removal of total organic carbon from aqueous solution containing polyvinyl alcohol by electrocoagulation technology. Desalination 259, 103–110. doi:10.1016/j.desal.2010.04.025

City of Edmonton, 2000. The City of Edmonton Combined Sewer Overflow (CSO) Control Strategy Implementation Plan Prepared for : Alberta Environment June 2000 Prepared by : City of Edmonton Asset Management and Public Works Drainage Services. Edmonton.

Cornwell, D.A., Bishop, M.M., 1983. Determining velocity gradients in laboratory and full-scale systems. J. Am. Water Work. Assoc. 75, 470–475. doi:10.1017/CBO9781107415324.004

Cotillas, S., Llanos, J., Cañizares, P., Mateo, S., Rodrigo, M.A., 2013. Optimization of an integrated electrodisinfection/electrocoagulation process with Al bipolar electrodes for urban wastewater reclamation. Water Res. 47, 1741–1750. doi:10.1016/j.watres.2012.12.029

Crittenden, J.C., Trussell, R.R., Hand, D.W., Howe, K.J., Tchobanoglous, G., 2012. MWH's water treatment : principles and design. John Wiley and Sons.

Duan, J., Gregory, J., 2003. Coagulation by hydrolysing metal salts. Adv. Colloid

Interface Sci. 100–102, 475–502. doi:10.1016/S0001-8686(02)00067-2

Dubrawski, K.L., Mohseni, M., 2013b. In-situ identification of iron electrocoagulation speciation and application for natural organic matter (NOM) removal. Water Res. 47, 5371–5380. doi:10.1016/j.watres.2013.06.021

Dubrawski, K.L., Mohseni, M., 2013a. Standardizing electrocoagulation reactor design: Iron electrodes for NOM removal. Chemosphere 91, 55–60. doi:10.1016/j.chemosphere.2012.11.075

Dubrawski, K.L., Van Genuchten, C.M., Delaire, C., Amrose, S.E., Gadgil, A.J., Mohseni, M., 2015. Production and transformation of mixed-valent nanoparticles generated by Fe(0) electrocoagulation. Environ. Sci. Technol. 49, 2171–2179. doi:10.1021/es505059d

Environment and Climate Change Canada, 2017. Report on the Comprehensive Review of the Events Leading to the Discharge of Untreated City of Montreal in November 2015.

Essadki, A.H., Gourich, B., Azzi, M., Vial, C., Delmas, H., 2010. Kinetic study of defluoridation of drinking water by electrocoagulation/electroflotation in a stirred tank reactor and in an external-loop airlift reactor. Chem. Eng. J. 164, 106–114. doi:10.1016/j.cej.2010.08.037

Eyvaz, M., Gürbulak, E., Kara, S., 2014. Preventing of Cathode Passivation / Deposition in Electrochemical Treatment Methods – A Case Study on Winery

Wastewater with Electrocoagulation. Mod. Electrochem. Methods Nano, Surf. Corros. Sci. 201–238. doi:10.5772/57202

Farhadi, S., Aminzadeh, B., Torabian, A., Khatibikamal, V., Alizadeh Fard, M., 2012. Comparison of COD removal from pharmaceutical wastewater by electrocoagulation, photoelectrocoagulation, peroxi-electrocoagulation and peroxi-photoelectrocoagulation processes. J. Hazard. Mater. 219–220, 35–42. doi:10.1016/j.jhazmat.2012.03.013

Feng, C., Li, M., Guo, X., Zhao, C., Zhang, Z., Sugiura, N., 2012. Electrochemical Technology Applied in Treatment of Wastewater and Ground Water.

Field, R., 1973. Combined sewer overflow seminar papers. Washington, D.C.

Fono, L.J., Sedlak, D.L., 2005. Use of the chiral pharmaceutical propranolol to identify sewage discharges into surface waters. Environ. Sci. Technol. 39, 9244–9252. doi:10.1021/es047965t

Gandhi, R., Ray, A.K., Sharma, V.K., Nakhla, G., 2014. Treatment of Combined Sewer Overflows Using Ferrate (VI). Water Environ. Res. 86, 2202–2211. doi:10.2175/106143014X14062131178475

Garcia-Segura, S., Eiband, M.M.S.G., de Melo, J.V., Martínez-Huitle, C.A., 2017. Electrocoagulation and advanced electrocoagulation processes: A general review about the fundamentals, emerging applications and its association with other technologies. J. Electroanal. Chem. 801, 267–299.

doi:10.1016/j.jelechem.2017.07.047

Gehr, R., Wagner, M., Veerasubramanian, P., Payment, P., 2003. Disinfection efficiency of peracetic acid, UV and ozone after enhanced primary treatment of municipal wastewater. Water Res. 37, 4573–4586. doi:10.1016/S0043-1354(03)00394-4

Ghernaout, D., Naceur, M.W., 2011. Ferrate(VI): In situ generation and water treatment – A review. Desalin. Water Treat. 30, 319–332. doi:10.5004/dwt.2011.2217

Gilbert, M.B., Waite, T.D., Hare, C., 1976. An Investigation of the Applicability of Ferrate Ion for Disinfection. J. / Am. Water Work. Assoc. 68, 495–497.

Goodwill, J.E., Jiang, Y., Reckhow, D.A., Gikonyo, J., Tobiason, J.E., 2015. Characterization of particles from ferrate preoxidation. Environ. Sci. Technol. 49, 4955–4962. doi:10.1021/acs.est.5b00225

Government of Canada, 2017. Wastewater regulations overview [WWW Document]. URL https://www.canada.ca/en/environment-climate-change/services/wastewater/regulations.html (accessed 4.29.18).

Government of Canada, 1985. Fisheries Act [WWW Document]. URL http://laws-lois.justice.gc.ca/eng/acts/f-14/ (accessed 7.20.18).

Graham, N.J.D., Khoi, T.T., Jiang, J.-Q., 2010. Oxidation and coagulation of humic substances by potassium ferrate. Water Sci. Technol. 62, 929–936.

doi:10.2166/wst.2010.369

Haas, C.N., Karra, S.B., 1984a. Kinetics of microbial inactivation by chlorine-II Kinetics in the presence of chlorine demand. Water Res. 18, 1451–1454. doi:10.1016/0043-1354(84)90016-2

Haas, C.N., Karra, S.B., 1984b. Kinetics of microbial inactivation by chlorine - I. Review of results in demand-free systems. Water Res. 18, 1443–1449. doi:10.1016/0043-1354(84)90015-0

Hakizimana, J.N., Gourich, B., Chafi, M., Stiriba, Y., Vial, C., Drogui, P., Naja, J., 2017. Electrocoagulation process in water treatment: A review of electrocoagulation modeling approaches. Desalination 404, 1–21. doi:10.1016/j.desal.2016.10.011

Halász, G., Gyüre, B., Jánosi, I.M., Szabó, K.G., Tél, T., 2007. Vortex flow generated by a magnetic stirrer. Am. J. Phys. 75, 1092. doi:10.1119/1.2772287

Harif, T., Hai, M., Adin, A., 2006. Electroflocculation as potential pretreatment in colloid ultrafiltration. Water Sci. Technol. Water Supply 6, 69–78. doi:10.2166/ws.2006.008

Harleman, D.R.F., Murcott, S., 1999. The role of physicalchemical wastewater treatment in the mega-cities of the developing world. Water Sci. Technol. 40, 75–80.

Henderson, R., Parsons, S.A., Jefferson, B., 2008a. The impact of algal properties and

pre-oxidation on solid-liquid separation of algae. Water Res. 42, 1827–1845. doi:10.1016/j.watres.2007.11.039

Henderson, R., Parsons, S.A., Jefferson, B., 2008b. Successful removal of algae through the control of zeta potential. Sep. Sci. Technol. 43, 1653–1666. doi:10.1080/01496390801973771

Henze, M., Comeau, Y., 2008. Wastewater characterization, in: Henze, M., Loosdrecht, M.C.M. van, Ekama, G.A., Brdjanovic, D. (Eds.), Biological Wastewater Treatment: Principles Modelling and Design. IWA Publishing, London, UK, p. 21.

Hoffman, R.W., Meighan, R.B., 1984. The Impact of Combined Sewer Overflows from San Francisco on the Western Shore ofCentral San Francisco Bay. J. (Water Pollut. Control Fed. 56, 1277–1285. doi:10.1016/S0262-1762(99)80122-9

Hu, C.Y., Lo, S.L., Kuan, W.H., 2007. Simulation the kinetics of fluoride removal by electrocoagulation (EC) process using aluminum electrodes. J. Hazard. Mater. 145, 180–185. doi:10.1016/j.jhazmat.2006.11.010

Hu, L., Page, M.A., Sigstam, T., Kohn, T., Mariñas, B.J., Strathmann, T.J., 2012. Inactivation of bacteriophage MS2 with potassium ferrate(VI). Environ. Sci. Technol. 46, 12079–12087. doi:10.1021/es3031962

Imam, E.H., Elnakar, H.Y., 2014. Design flow factors for sewerage systems in small arid communities. J. Adv. Res. 5. doi:10.1016/j.jare.2013.06.011

IPCC, 2007. Mitigation of climate change: Contribution of working group III to the fourth assessment report of the Intergovernmental Panel on Climate Change, Intergovernmental Panel on Climate Change. doi:http://www.ipcc.ch/publications_and_data/.htm

Jaafarzadeh, N., Omidinasab, M., Ghanbari, F., 2016. Combined electrocoagulation and UV-based sulfate radical oxidation processes for treatment of pulp and paper wastewater. Process Saf. Environ. Prot. 102, 462–472. doi:10.1016/j.psep.2016.04.019

Jessen, A., Randall, A., Reinhart, D., Daly, L., 2008. Effectiveness and kinetics of ferrate as a disinfectant for ballast water. Water Environ. Res. 80, 561–569. doi:10.2175/193864708X267423

Jiang, J.-Q., 2007. Research progress in the use of ferrate(VI) for the environmental remediation. J. Hazard. Mater. 146, 617–623. doi:10.1016/j.jhazmat.2007.04.075

Jiang, J.-Q., Lloyd, B., 2002. Progress in the development and use of ferrate(VI) salt as an oxidant and coagulant for water and wastewater treatment. Water Res. 36, 1397–1408. doi:10.1016/S0043-1354(01)00358-X

Jiang, J.-Q., Lloyd, B., Grigore, L., 2001. Preparation and evaluation of potassium ferrate as an oxidant and coagulant for potable water treatment. Environ. Eng. Sci. 18, 323–328. doi:10.1089/10928750152726041

Jiang, J.-Q., Wang, S., Panagoulopoulos, A., 2007. The role of potassium ferrate(VI)

in the inactivation of Escherichia coli and in the reduction of COD for water remediation. Desalination 210, 266–273. doi:10.1016/j.desal.2006.05.051

Jiang, J.-Q., Wang, S., Panagoulopoulos, A., 2006. The exploration of potassium ferrate(VI) as a disinfectant/coagulant in water and wastewater treatment. Chemosphere 63, 212–219. doi:10.1016/j.chemosphere.2005.08.020

Jiang, Y., Goodwill, J.E., Tobiason, J.E., Reckhow, D.A., 2015. Effect of different solutes, natural organic matter, and particulate Fe(III) on ferrate(VI) decomposition in aqueous solutions. Environ. Sci. Technol. 49, 2841–2848. doi:10.1021/es505516w

Jolis, D., Ahmad, M., 2004. Evaluation of High-rate Clarification for Wet-Weather-Only Treatment Facilities. Water Environ. Res. 76, 474–480. doi:10.2175/106143004X151563

Kabdaşli, I., Keleş, A., Ölmez-Hanci, T., Tünay, O., Arslan-Alaton, I., 2009. Treatment of phthalic acid esters by electrocoagulation with stainless steel electrodes using dimethyl phthalate as a model compound. J. Hazard. Mater. 171, 932–940. doi:10.1016/j.jhazmat.2009.06.093

Kalyani, K.S.P., Balasubramanian, N., Srinivasakannan, C., 2009. Decolorization and COD reduction of paper industrial effluent using electro-coagulation. Chem. Eng. J. 151, 97–104. doi:10.1016/j.cej.2009.01.050

Kazama, F., 1995. Viral inactivation by potassium ferrate. Water Sci. Technol.

doi:10.1016/0273-1223(95)00259-P

Kobya, M., Can, O.T., Bayramoglu, M., 2003. Treatment of textile wastewaters by electrocoagulation using iron and aluminum electrodes. J. Hazard. Mater. 100, 163–178. doi:10.1016/S0304-3894(03)00102-X

Kovatcheva, V.K., Parlapanski, M.D., 1999. Sono-electrocoagulation of iron hydroxides. Colloids Surfaces A Physicochem. Eng. Asp. 149, 603–608. doi:10.1016/S0927-7757(98)00414-2

Kralchevska, R.P., Prucek, R., Kolařík, J., Tuček, J., Machala, L., Filip, J., Sharma, V.K., Zbořil, R., 2016. Remarkable efficiency of phosphate removal: Ferrate(VI)-induced in situ sorption on core-shell nanoparticles. Water Res. 103, 83–91. doi:10.1016/j.watres.2016.07.021

Kuokkanen, V., Kuokkanen, T., Rämö, J., Lassi, U., 2015. Electrocoagulation treatment of peat bog drainage water containing humic substances. Water Res. 79, 79–87. doi:10.1016/j.watres.2015.04.029

Kwon, J.H., Kim, I.K., Park, K.Y., Kim, Y. Do, Cho, Y.H., 2014. Removal of phosphorus and coliforms from secondary effluent using ferrate(VI). KSCE J. Civ. Eng. 18, 81–85. doi:10.1007/s12205-013-0024-7

Lakshmanan, D., Clifford, D.A., Samanta, G., 2009. Ferrous and ferric ion generation during iron electrocoagulation. Environ. Sci. Technol. 43, 3853–3859. doi:10.1021/es8036669

Lee, S.Y., Gagnon, G.A., 2015. The rate and efficiency of iron generation in an electrocoagulation system. Environ. Technol. (United Kingdom) 36, 2419–2427. doi:10.1080/09593330.2015.1032367

Lee, Y., Cho, M., Kim, J.Y., Yoon, J., 2004. Chemistry of ferrate (Fe (VI)) in aqueous solution and its applications as a green chemical. J. Ind. Eng. Chem. 10, 161–171.

Lee, Y., Kissner, R., Von Gunten, U., 2014. Reaction of ferrate(VI) with ABTS and self-decay of ferrate(VI): Kinetics and mechanisms. Environ. Sci. Technol. 48, 5154–5162. doi:10.1021/es500804g

Lee, Y., Yoon, J., Von Gunten, U., 2005. Spectrophotometric determination of ferrate (Fe(VI)) in water by ABTS. Water Res. 39, 1946–1953. doi:10.1016/j.watres.2005.03.005

Lee, Y., Zimmermann, S.G., Kieu, A.T., Gunten, U. von, 2009. Ferrate (Fe (VI)) application for municipal wastewater treatment: A novel process for simultaneous micropollutant oxidation and phosphate removal. Environ. Sci. Technol. 43, 3831–3838. doi:10.1021/es803588k

Li, C., Li, X.Z., Graham, N., 2005. A study of the preparation and reactivity of potassium ferrate. Chemosphere 61, 537–543. doi:10.1016/j.chemosphere.2005.02.027

Li, N., Deng, Y., Sarkar, D., 2016. Ferrate(VI) Reaction with Effluent Organic Matter (EfOM) in Secondary Effluent for Water Reuse. ACS Symp. Ser. 1238, 411–420.

doi:10.1021/bk-2016-1238.ch015

Lv, D., Zheng, L., Zhang, H., Deng, Y., 2018. Coagulation of colloidal particles with ferrate(vi). Environ. Sci. Water Res. Technol. 4, 701–710. doi:10.1039/c8ew00048d

Ma, J., Liu, W., 2002. Effectiveness of ferrate (VI) preoxidation in enhancing the coagulation of surface waters. Water Res. 36, 4959–4962. doi:10.1016/S0043-1354(02)00224-5

Ma, S.S., Zhang, Y.G., 2016. Electrolytic removal of alizarin red S by Fe/Al composite hydrogel electrode for electrocoagulation toward a new wastewater treatment. Environ. Sci. Pollut. Res. 23, 22771–22782. doi:10.1007/s11356-016-7483-6

Maha Lakshmi, P., Sivashanmugam, P., 2013. Treatment of oil tanning effluent by electrocoagulation: Influence of ultrasound and hybrid electrode on COD removal. Sep. Purif. Technol. 116, 378–384. doi:10.1016/j.seppur.2013.05.026

Manoli, K., Nakhla, G., Ray, A.K., Sharma, V.K., 2017. Enhanced oxidative transformation of organic contaminants by activation of ferrate(VI): Possible involvement of FeV/FeIV species. Chem. Eng. J. 307, 513–517. doi:10.1016/j.cej.2016.08.109

Mansouri, K., Elsaid, K., Bedoui, A., Bensalah, N., Abdel-Wahab, A., 2011. Application of electrochemically dissolved iron in the removal of tannic acid from water. Chem. Eng. J. 172, 970–976. doi:10.1016/j.cej.2011.07.009

Marsalek, J., Rochfort, Q., 2004. Urban Wet-Weather Flows: Sources of Fecal Contamination Impacting on Recreational Waters and Threatening Drinking-Water Sources. J. Toxicol. Environ. Heal. Part A 67, 1765–1777. doi:10.1080/15287390490492430

Masi, F., Rizzo, A., Bresciani, R., Conte, G., 2017. Constructed wetlands for combined sewer overflow treatment: Ecosystem services at Gorla Maggiore, Italy. Ecol. Eng. 98, 427–438. doi:10.1016/j.ecoleng.2016.03.043

Metcalf & Eddy, 2004. Wastewater engineering: treatment and reuse, 4th ed. McGraw-Hill.

Millero, F.J., Sotolongo, S., Izaguirre, M., 1987. The oxidation kinetics of Fe(II) in seawater. Geochim. Cosmochim. Acta 51, 793–801. doi:10.1016/0016-7037(87)90093-7

Mollah, M.Y., Schennach, R., Parga, J.R., Cocke, D.L., 2001. Electrocoagulation (EC)-Science and Applications. J. Hazard. Mater. 84, 29–41. doi:10.1016/S0304-3894(01)00176-5

Mollah, M.Y.A., Morkovsky, P., Gomes, J.A.G., Kesmez, M., Parga, J., Cocke, D.L., 2004. Fundamentals, present and future perspectives of electrocoagulation. J. Hazard. Mater. 114, 199–210. doi:10.1016/j.jhazmat.2004.08.009

Montgomery, D.C., 2001. Design and analysis of experiments, 5th ed. John Wiley & Sons.

Moreno-Casillas, H.A., Cocke, D.L., Gomes, J.A.G., Morkovsky, P., Parga, J.R., Peterson, E., 2007. Electrocoagulation mechanism for COD removal. Sep. Purif. Technol. 56, 204–211. doi:10.1016/j.seppur.2007.01.031

Morrissey, S.P., Harleman, D.R.F., 1992. Retrofitting Conventional Primary Treatment Plants for Chemically Enhanced Primary Treatment in the USA, in: Klute, R., Hahn, H.H. (Eds.), Water and Wastewater Treatment II. p. 493.

Murmann, R.K., Robinson, P.R., 1974. Experiments utilizing FeO42− for purifying water. Water Res. 8, 543–547. doi:10.1016/0043-1354(74)90062-1

Nariyan, E., Sillanpää, M., Wolkersdorfer, C., 2017. Electrocoagulation treatment of mine water from the deepest working European metal mine – Performance, isotherm and kinetic studies. Sep. Purif. Technol. 177, 363–373. doi:10.1016/j.seppur.2016.12.042

National Research Council, 2012. Water Reuse: Potential for Expanding the Nation's Water Supply Through Reuse of Municipal Wastewater. doi:10.17226/13303

NSF, US EPA, 2002. Performance of induction mixers for disinfection of wet weather flows. Bradley, IL.

OECD, 2011. Project on Strategic Transport Infrastructure To 2030 - Pension Funds Investment in Infrastructure: a Survey.

Olson, J.H., Stout, L.E., 1967. Mixing and cemical reactions, in: Uhl, V.W., Gray, J.B. (Eds.), Mixing: Theory and Practice. London, UK, p. 340.

Ontario Government, 2016. F-5-5: Determination of treatment requirements for municipal and private combined [WWW Document]. Guidel. F-5 Levels Treat. Munic. Priv. Sew. Treat. Work. Discharging to Surf. Waters. URL https://www.ontario.ca/page/f-5-5-determination-treatment-requirements-municipal-and-private-combined#section-5 (accessed 3.7.17).

Orescanin, V., Kollar, R., Mikelic, I.L., Nad, K., 2013. Electroplating wastewater treatment by the combined electrochemical and ozonation methods. J. Environ. Sci. Heal. - Part A Toxic/Hazardous Subst. Environ. Eng. 48, 1450–1455. doi:10.1080/10934529.2013.781904

Orescanin, V., Kollar, R., Nad, K., 2011. The application of the ozonation/electrocoagulation treatment process of the boat pressure washing wastewater. J. Environ. Sci. Heal. - Part A Toxic/Hazardous Subst. Environ. Eng. 46, 1338–1345. doi:10.1080/10934529.2011.606423

Passerat, J., Ouattara, N.K., Mouchel, J.M., Vincent Rocher, Servais, P., 2011. Impact of an intense combined sewer overflow event on the microbiological water quality of the Seine River. Water Res. 45, 893–903. doi:10.1016/j.watres.2010.09.024

Patterson, J.A., Thompson, J.A., Entenmann, C., 2001. Ferrate-based water disinfectant and method. US 6,267,896 B1.

Plum, V., Dahl, C.P., Bentsen, L., Petersen, C.R., Napstjert, L., Thomsen, N.B., 1998. The Actiflo method. Water Sci. Technol. 37, 269–275. doi:10.1016/S0273-

1223(97)00778-6

Pourbaix, M., 1966. Atlas of Electrochemical Equilibria in Aqueous Solutions, First. ed. Pergamon.

Raschitor, A., Fernandez, C.M., Cretescu, I., Rodrigo, M.A., Cañizares, P., 2014. Sono-electrocoagulation of wastewater polluted with Rhodamine 6G. Sep. Purif. Technol. 135, 110–116. doi:10.1016/j.seppur.2014.08.003

Rice, J., Wutich, A., White, D.D., Westerhoff, P., 2016. Comparing actual de facto wastewater reuse and its public acceptability: A three city case study. Sustain. Cities Soc. 27, 467–474. doi:10.1016/j.scs.2016.06.007

Rush, J.D.J., Zhao, Z., Bielski, B.H.J.B., 1996. Reaction of Ferrate(VI)/Ferrate(V) with Hydrogen Peroxide and Superoxide Anion - A Stopped-Flow and Premix Pulse Radiolysis Study. Free Radic. Res. 24, 187–198. doi:10.3109/10715769609088016

Schink, T., Waite, T.D., 1980. Inactivation of f2 virus with ferrate (VI). Water Res. 14, 1705–1717. doi:10.1016/0043-1354(80)90106-2

Şengil, I.A., özacar, M., 2006. Treatment of dairy wastewaters by electrocoagulation using mild steel electrodes. J. Hazard. Mater. 137, 1197–1205. doi:10.1016/j.jhazmat.2006.04.009

Shah, S.I.A., Kostiuk, L.W., Kresta, S.M., 2012. The effects of mixing, reaction rates, and stoichiometry on yield for mixing sensitive reactions - Part I: Model

development. Int. J. Chem. Eng. 2012. doi:10.1155/2012/750162

Sharma, V.K., 2002. Potassium ferrate(VI): An environmentally friendly oxidant. Adv. Environ. Res. 6, 143–156. doi:10.1016/S1093-0191(01)00119-8

Sharma, V.K., Kazama, F., Hu, J., Ray, A.K., 2005. Ferrates (iron(VI) and iron(V)): Environmentally friendly oxidants and disinfectants. J. Water Health 3, 45–58.

Sharp, E.L., Banks, J., Billica, J.A., Gertig, K.R., Henderson, R., Parsons, S.A., Wilson, D., Jefferson, B., 2005. Application of zeta potential measurements for coagulation control: Pilot-plant experiences from UK and US waters with elevated organics. Water Sci. Technol. Water Supply 5, 49–56.

Shin, J., Lee, Y., 2016. Elimination of Organic Contaminants during Oxidative Water Treatment with Ferrate(VI): Reaction Kinetics and Transformation Products, in: Ferrites and Ferrates: Chemistry and Applications in Sustainable Energy and Environmental Remediation. ACS Symposium Series, pp. 255–273. doi:10.1021/bk-2016-1238.ch010

Singh, S., Singh, S., Lo, S.L., Kumar, N., 2016. Electrochemical treatment of Ayurveda pharmaceuticals wastewater: Optimization and characterization of sludge residue. J. Taiwan Inst. Chem. Eng. 67, 385–396. doi:10.1016/j.jtice.2016.08.028

Song, P., Yang, Z., Zeng, G., Yang, X., Xu, H., Wang, L., Xu, R., Xiong, W., Ahmad, K., 2017. Electrocoagulation treatment of arsenic in wastewaters: A

comprehensive review. Chem. Eng. J. 317, 707–725. doi:10.1016/j.cej.2017.02.086

Stevenson, C., Davies, R.J., 1995. Potassium ferrate as a DNA chemical sequencing reagent and probe of secondary structure. Biochem. Soc. Trans. 23, 387S.

Struck, S.D., Rowney, A.C., Pechacek, L.D., 2009. Innovative Approaches for Urban Watershed Wet-Weather Flow Management and Control. Cincinnati, OH.

Sugiura, N., 1978. Further analysts of the data by akaike' s information criterion and the finite corrections. Commun. Stat. - Theory Methods 7, 13–26. doi:10.1080/03610927808827599

Talaiekhozani, A., Talaei, M.R., Rezania, S., 2017. An overview on production and application of ferrate (VI) for chemical oxidation, coagulation and disinfection of water and wastewater. J. Environ. Chem. Eng. 5, 1828–1842. doi:10.1016/j.jece.2017.03.025

Tanneru, C.T., Chellam, S., 2012. Mechanisms of virus control during iron electrocoagulation - Microfiltration of surface water. Water Res. 46, 2111–2120. doi:10.1016/j.watres.2012.01.032

Theis, T.L., Singer, P.C., 1974. Complexation of Iron(II) by Organic Matter and Its Effect on Iron(II) Oxygenation. Environ. Sci. Technol. 8, 569–573. doi:10.1021/es60091a008

Thompson, G., Ockerman, L., Schreyer, J., 1951. Preparation and purification of

potassium ferrate. VI. J. Am. Chem. Soc. 425, 67–69. doi:10.1021/ja01147a536

Tien, K.T., Graham, N., Jiang, J.-Q., 2008. Evaluating the coagulation performance of ferrate: A preliminary study, in: Sharma, V.K. (Ed.), Ferrates. ACS Symposium Series, pp. 292–305. doi:10.1021/bk-2008-0985.ch017

Timmes, T.C., Kim, H., Dempsey, B.A., 2009. Electrocoagulation pretreatment of seawater prior to ultra filtration : Bench-scale applications for military water puri fi cation systems. Desalination 249, 895–901. doi:10.1016/j.desal.2009.07.002

Tiwari, D., Kim, H.-U., Choi, B.-J., Lee, S.-M., Kwon, O.-H., Choi, K.-M., Yang, J.-K., 2007. Ferrate(VI): a green chemical for the oxidation of cyanide in aqueous/waste solutions. J. Environ. Sci. Health. A. Tox. Hazard. Subst. Environ. Eng. 42, 803–10. doi:10.1080/10934520701304674

Tsai, C.T., Lin, S.T., Shue, Y.C., Su, P.L., 1997. Electrolysis of soluble organic matter in leachate from landfills. Water Res. 31, 3073–3081. doi:10.1016/S0043-1354(96)00297-7

U.S. EPA, 2013. Emerging Technologies for Wastewater Treatment and In-Plant Wet Weather Management. Virginia.

U.S. EPA, 2008. A Screening Assessment of the Potential Impacts of Climate Change on Combined Sewer Overflow (CSO) Mitigation in the Great Lakes and New England Regions. Washington, DC.

U.S. EPA, 1999a. Combined Sewer Overflow Technology Fact Sheet: Sewer

Separation, United States Environmental Protection Agency (U.S. EPA). Washington, D.C. doi:EPA 832-F-99-041

U.S. EPA, 1999b. Combined Sewer Overflow Technology Fact Sheet: Alternative Disinfection Methods. Washington, D.C. doi:EPA 832-F-99-041

UN, 2015. Transforming our world: The 2030 agenda for sustainable development. doi:10.1007/s13398-014-0173-7.2

UNEP, 2013. City-level decoupling: Urban resource flows and the governance of infrastructure transitions. . Summary for Policy Makers.

UNESCO, 2017. The United Nations World Water Development Report 2017: Wastewater - The Untapped Resource. UNESCO on behalf of UN-Water, France.

Vadasarukkai, Y.S., Gagnon, G.A., 2015. Application of low-mixing energy input for the coagulation process. Water Res. 84, 333–341. doi:10.1016/j.watres.2015.07.049

Vepsäläinen, M., Ghiasvand, M., Selin, J., Pienimaa, J., Repo, E., Pulliainen, M., Sillanpää, M., 2009. Investigations of the effects of temperature and initial sample pH on natural organic matter (NOM) removal with electrocoagulation using response surface method (RSM). Sep. Purif. Technol. 69, 255–261. doi:10.1016/j.seppur.2009.08.001

Vik, E.A., Carlson, D.A., Eikum, A.S., Gjessing, E.T., 1984. Electrocoagulation of Potable Water. Water Res. 18, 1355–1360.

Waite, T.D., 1979. Feasibility of wastewater treatment with ferrate. J. Environ. Eng. Div. 105, 1023–1034.

Wang, C.T., Chou, W.L., Huang, K.Y., 2010. Treatment of polyvinyl alcohol from aqueous solution via electrocoagulation. Sep. Sci. Technol. 45, 212–220. doi:10.1080/01496390903423808

Wang, H., Li, F., Keller, A.A., Xu, R., 2009. Chemically enhanced primary treatment (CEPT) for removal of carbon and nutrients from municipal wastewater treatment plants: A case study of Shanghai. Water Sci. Technol. 60, 1803–1809. doi:10.2166/wst.2009.547

Wang, H., Li, H., Ding, N., Li, M., Wang, N., 2018. Using potassium ferrate as advanced treatment for municipal wastewater. Desalin. Water Treat. 106, 90–97. doi:10.5004/dwt.2018.22064

WHO, 2006. WHO Guidelines for the safe use of wastewater, excerta, and greywater. WHO Press, World Health Organization, Geneva.

Wiener, M.J., Jafvert, C.T., Nies, L.F., 2016. The assessment of water use and reuse through reported data: A US case study. Sci. Total Environ. 539, 70–77. doi:10.1016/j.scitotenv.2015.08.114

Xie, P., Chen, Y., Ma, J., Zhang, X., Zou, J., Wang, Z., 2016. A mini review of preoxidation to improve coagulation. Chemosphere 155, 550–563. doi:10.1016/j.chemosphere.2016.04.003

Yang, B., Ying, G.G., Zhao, J.L., Liu, S., Zhou, L.J., Chen, F., 2012. Removal of selected endocrine disrupting chemicals (EDCs) and pharmaceuticals and personal care products (PPCPs) during ferrate(VI) treatment of secondary wastewater effluents. Water Res. 46, 2194–2204. doi:10.1016/j.watres.2012.01.047

Yazdanbakhsh, A.R., Massoudinegad, M.R., Eliasi, S., Mohammadi, A.S., 2015. The influence of operational parameters on reduce of azithromyin COD from wastewater using the peroxi-electrocoagulation process. J. Water Process Eng. 6, 51–57. doi:10.1016/j.jwpe.2015.03.005

Yoosefian, M., Ahmadzadeh, S., Aghasi, M., Dolatabadi, M., 2017. Optimization of electrocoagulation process for efficient removal of ciprofloxacin antibiotic using iron electrode; kinetic and isotherm studies of adsorption. J. Mol. Liq. 225, 544–553. doi:10.1016/j.molliq.2016.11.093

Zgheib, S., Moilleron, R., Chebbo, G., 2012. Priority pollutants in urban stormwater: Part 1 – Case of separate storm sewers. Water Res. 46, 6683–6692. doi:10.1016/J.WATRES.2011.12.012

Zheng, L., Deng, Y., 2016. Settleability and characteristics of ferrate(VI)-induced particles in advanced wastewater treatment. Water Res. 93, 172–178. doi:10.1016/j.watres.2016.02.015

APPENDIX A: Supplementary Information for Chapter 3

Table A1 Sampling times used during the study

Experiments	Sampling times (minutes)
E. Coli Inactivation / Sedimentation tests	0, 0.5, 1, 5, 10, 15, 21, 25, 40, 50, 81
Potassium ferrate consumption tests	0, 1, 3, 5, 7, 10, 15, 20, 25, 30, 40, 50, 60, 80

Table A2 Fitting parameters results of the first-order, second-order and double exponential models representing the potassium ferrate(VI) consumption of 0.1 mM dosage for different mixing speeds and bypass wastewater events

Mixing Regime	Rapid Speed Mixing												Magnetic Stirrer Mixing			
rpm / s^{-1}	500 / 1100				750 / 1950				1000 / 2890				1000 / 1200			
Sample ID	S06	S15	O26	N27	S06	S15	O26	N27	S06	S15	O26	N27	S06	S15	O26	N27
First-Order Model																
k_1	1.986	0.997	1.303	0.991	2.078	0.958	1.403	0.983	2.082	1.029	1.540	1.200	1.723	0.731	0.942	0.713
R^2 (%)	99.54	96.97	98.45	95.63	99.63	95.28	98.88	96.43	99.51	95.93	98.72	96.26	99.11	97.12	98.44	97.27
RMSE	0.002	0.006	0.004	0.007	0.002	0.007	0.003	0.006	0.002	0.007	0.004	0.006	0.003	0.006	0.004	0.006
Second-Order Model																
k_2	42.98	17.21	23.67	16.73	46.27	16.15	26.34	16.94	46.15	17.74	29.29	20.44	35.31	13.87	18.05	13.60
R^2 (%)	98.92	97.47	98.30	96.80	99.02	96.72	98.92	97.74	99.26	97.90	98.76	97.29	99.63	99.39	99.13	99.41
RMSE	0.003	0.005	0.004	0.006	0.003	0.006	0.003	0.005	0.003	0.005	0.004	0.006	0.002	0.003	0.003	0.003
Double Exponential Model																
X	0.96	0.90	0.91	0.89	0.96	0.88	0.91	0.88	0.94	0.85	0.91	0.90	0.86	0.82	0.82	0.83
k_{DE1}	2.197	1.258	1.571	1.296	2.277	1.294	1.681	1.317	2.386	1.445	1.847	1.510	2.148	1.135	1.314	1.089
k_{DE2}	0.112	0.088	0.128	0.088	0.105	0.099	0.133	0.105	0.154	0.124	0.139	0.092	0.252	0.133	0.184	0.106
R^2 (%)	99.86	98.39	99.35	97.37	99.91	97.20	99.80	98.36	99.92	98.23	99.58	97.93	99.95	99.90	99.66	99.98
RMSE	0.001	0.004	0.003	0.006	0.001	0.006	0.001	0.004	0.001	0.004	0.002	0.005	0.001	0.001	0.002	0.001

Mixing Speed (rpm) / Velocity Gradient (s^{-1}); RMSE: Root mean square error; R^2: Adjusted R-square

Table A3 Fitting parameters results of Chick–Watson and Hom models representing potassium ferrate(VI) disinfection data for different mixing speeds, events, and initial dosages

Mixing Regime	Rpm / s^{-1}	Potassium ferrate(VI) (mM)	Sample ID	Chick–Watson				Hom				
				a_{CW}	k_{CW}	R^2 (%)	RMSE	a_H	b_H	k_H	R^2 (%)	RMSE
Rapid Speed Mixing	500 / 1100	0.075	S06	0.54	9.2	95.0	0.32	0.15	0.58	1.97	95.1	0.31
		0.100	S15	0.70	12.0	97.1	0.25	0.74	1.04	13.75	96.1	0.28
		0.125	O26	0.64	10.0	98.5	0.18	1.18	1.47	65.45	98.2	0.20
		0.100	N27	0.67	9.2	98.4	0.18	1.27	1.50	63.09	98.3	0.18
	750 / 1950	0.075	S06	0.54	9.8	96.4	0.27	0.03	0.50	1.21	97.8	0.21
		0.100	S15	0.64	8.5	99.1	0.15	0.72	1.07	11.16	98.8	0.17
		0.125	O26	0.64	10.0	97.2	0.24	0.39	0.77	4.41	96.5	0.27
		0.100	N27	0.71	12.0	98.1	0.20	1.19	1.39	58.26	97.9	0.22
	1000 / 2890	0.075	S06	0.58	12.0	97.7	0.23	0.17	0.60	2.28	98.7	0.17
		0.100	S15	0.75	16.0	97.6	0.22	0.59	0.87	8.99	96.8	0.26
		0.125	O26	0.64	11.0	97.8	0.22	0.58	0.95	8.48	97.0	0.25
		0.100	N27	0.64	10.0	98.8	0.16	0.65	1.01	10.47	98.4	0.19
Magnetic Stirrer Mixing	1000 / 1200	0.075	S06	0.46	5.2	99.3	0.12	0.41	0.95	4.37	99.1	0.13
		0.100	S15	0.66	7.5	99.3	0.12	1.75	1.87	224.6	99.9	0.04
		0.125	O26	0.58	5.6	98.9	0.15	2.15	2.36	777.2	99.9	0.05
		0.100	N27	0.68	8.5	98.8	0.15	1.97	2.04	469.6	99.6	0.09

Mixing Speed (rpm) / Velocity Gradient (s^{-1}); RMSE: Root mean square error; R^2: Adjusted R-square

APPENDIX B: Iron Electrocoagulation Experimental Setup

Experimental Setup

Figure B1 shows the reactor setup for iron electrocoagulation used for the experiments detailed in chapters 4 and 5. It comprises a 100 mL beaker (A) containing one iron rod anode (B) and stainless-steel rod cathode (C) attached to a digital multimeter (D) and a DC power supply (E). The beaker is continuously stirred during electrolysis by a magnetic stir plate (F). The system is open to the atmosphere.

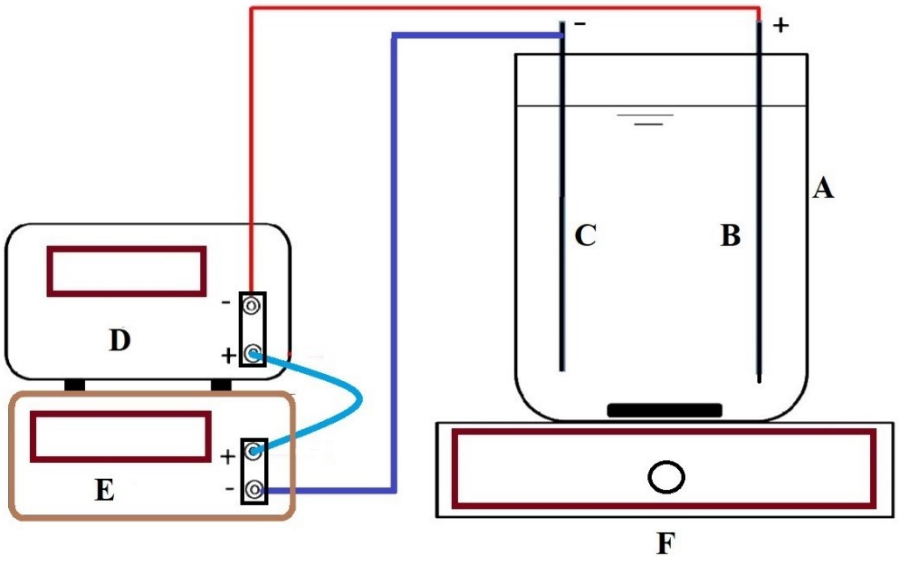

Figure B1. A schematic diagram of the iron electrocoagulation setup

APPENDIX C: Supplementary Information for Chapter 4

Table B1: Reaction mechanisms and the likely end products of iron electrocoagulation.

Reaction mechanisms	Water matrix	pH range	Current (mA / cm^2)	Primary end products	Ref.
• Fe^{2+} is released from the Fe anode at all pH values and current densities • Fe^{2+} was either hydrolyzed to produce insoluble $Fe(OH)_2(s)$ or oxidized to Fe^{3+} leading to $Fe(OH)_3$ formation	Presented for any water matrix	Not Specified	Not Specified	$Fe(OH)_2(s)$ / $Fe(OH)_3$	[1]
• Fe^{3+} is released from the Fe anode at all pH values and current densities, then through hydrolysis, $Fe(OH)_3(s)$ is produced	Presented for any water matrix	Not Specified	Not Specified	$Fe(OH)_3$ and other polymeric hydroxy complexes similar to Ferric Chloride Products	[2,3]
• Theoretical explanation that suggests that Fe^{2+} ions are the common ions generated the dissolution of iron anode and OH^- ions are produced at the cathode. Mixing the solution will produce hydroxide species leading to the removal of dyes and cations by adsorption and coprecipitation	Dairy wastewater	3.5 – 10.0	0.3 – 1.8	Dominant species of $Fe(OH)_3$ at pH range from 6 to 10 according to predominance-zone diagrams for Fe(III) chemical species in aqueous solution	[4]
• Fe^{2+} is released from the Fe anode at all pH values and current densities	Synthetic tap water	5.0 – 9.0	0.86 - 6.9	No clear identification	[5]

Reaction mechanisms	Water matrix	pH range	Current (mA / cm^2)	Primary end products	Ref.
• At pH equal to or lower than 7, high rate dissolution to iron anode (Fe^{2+}) has been noticed in the absence of an electric current. • At higher pH, other side reactions can cause the iron dissolution rate to be significantly lower than the values derived by Faraday's law. • The oxygen saturation level in the solution remains steady or decreases during the electrocoagulation process. • The electrochemical oxidation rate of Fe^{2+} to Fe^{3+} was nearly similar to the chemical oxidation.					
• Fe^{2+} is released from the Fe anode at all pH values and current densities • The rate of oxidation of Fe^{2+} to Fe^{+3} increased with increasing pH and DO concentration, and complete oxidation was achieved at pH 8.5	Synthetic groundwater	6.5 –8.5	1.32 to 21.1 mA/cm^2 under atmospheric conditions	• pH 8.5: $Fe(OH)_3(s)$/ FeOOH(s) • pH 6.5 and 7.5: mixture of soluble Fe^{2+} and insoluble $Fe(OH)_3(s)$/FeOOH(s)	[6]

Reaction mechanisms	Water matrix	pH range	Current (mA / cm^2)	Primary end products	Ref.
• Fe^{2+} is released from the Fe anode at all pH values and current densities by dissolved oxygen (DO) existing in the aerobic cell or through hydrolysis of water in the anaerobic cell. • Mixed-valent Fe phases (Magnetite) may only be formed when DO was absent or very low in all conditions.	• Anaerobic cell: ultrapure water with different concentrations of Na_2SO_4 and/or NaCl • Aerobic cell: unbuffered and buffered solutions to represent synthetic groundwaters in addition to real groundwater	7.0 – 9.5	5.0 to 125.0 mA/cm^2 under anaerobic conditions and 5.0 to 20.0 mA/cm^2 under aerobic conditions	• DO present: Lepidocrocite (γ-FeOOH) • DO absent: Mainly Green Rust when CO_3^{2-}, SO_4^{2}, and PO_4^{3-} are present and within minutes of the reaction	[7]

Theoretical Ferrous Calculations

The end-product(s) of iron electrocoagulation depends upon environmental conditions chief among which are pH, temperature, solution composition and oxidation rate. The following equations for the estimation of Fe^{2+} concentration and rate constant are adapted from Millero et al. (1987) [8].

The oxidation of Fe^{2+} follows the pseudo first order reaction shown in Equation B.1.

$$\frac{-d[Fe^{2+}]}{dt} = k_1[Fe^{2+}] \tag{B.1}$$

where k_1 is the pseudo first order reaction (min^{-1}) and is calculated as per Equation B.2.

$$k_1 = k[OH^-]^2[O_2] \tag{B.2}$$

where k is the overall rate constant (mol^{-3} kg $L^3 min^{-1}$) calculated as per Equation B.3 and $[O_2]$ is the dissolved oxygen (mole/L).

$$\log k = \log k_o - 3.291.I^{\frac{1}{2}} + 1.52.I \tag{B.3}$$

where k_o is a rate constant depends on temperature (T) in kelvin as per Equation B.4 and I is the ionic strength which depends on salinity (S) and is calculated as per Equation B.5

$$\log k_o = 21.56 - \frac{1545}{T} \quad \text{(B.4)}$$

$$I = 19.9201 * S/(10^3 - 1.00488 * S) \quad \text{(B.5)}$$

While the model of Millero et al. (1987) was developed for the oxidation kinetics of Fe^{2+} in seawater, the model applicability was reported to be for salinities in the range from 0 to 35 PSU which could accommodate the salinities range normally reported elsewhere in wastewater samples as shown (Hoffman and Meighan, 1984; Metcalf & Eddy, 2004) [9,10]. Specifically, Hoffman and Meighan (1984) reported that salinities of the wastewater overflows were usually less than 1 PSU and could reach 18 to 25 PSU at places where there was a possibility for seawater intrusion [9]. By performing sensitivity analysis using the model of Millero et al. (1987) with respect to the salinity over salinities from 0 to 1.5 PSU, it was found that the rate constants of the oxidation of Fe^{2+} generally decrease with the increase of salinity values, but without a significant statistical difference. In this study, a salinity value of 0.1 PSU was assumed to give more conservative and eventually higher values to the Fe^{2+} conversion rate constants which means less Fe^{2+} concentrations in the effluent.

References

[1] M.Y. Mollah, R. Schennach, J.R. Parga, D.L. Cocke, Electrocoagulation (EC)-Science and Applications., J. Hazard. Mater. 84 (2001) 29–41. doi:10.1016/S0304-3894(01)00176-5.

[2] M.Y.A. Mollah, P. Morkovsky, J.A.G. Gomes, M. Kesmez, J. Parga, D.L. Cocke, Fundamentals, present and future perspectives of electrocoagulation, J. Hazard. Mater. 114 (2004) 199–210. doi:10.1016/j.jhazmat.2004.08.009.

[3] K.S.P. Kalyani, N. Balasubramanian, C. Srinivasakannan, Decolorization and COD reduction of paper industrial effluent using electro-coagulation, Chem. Eng. J. 151 (2009) 97–104. doi:10.1016/j.cej.2009.01.050.

[4] I.A. Şengil, M. özacar, Treatment of dairy wastewaters by electrocoagulation using mild steel electrodes, J. Hazard. Mater. 137 (2006) 1197–1205. doi:10.1016/j.jhazmat.2006.04.009.

[5] M. Ben Sasson, W. Calmano, A. Adin, Iron-oxidation processes in an electroflocculation (electrocoagulation) cell, J. Hazard. Mater. 171 (2009) 704–709. doi:10.1016/j.jhazmat.2009.06.057.

[6] D. Lakshmanan, D.A. Clifford, G. Samanta, Ferrous and ferric ion generation during iron electrocoagulation, Environ. Sci. Technol. 43 (2009) 3853–3859. doi:10.1021/es8036669.

[7] K.L. Dubrawski, C.M. Van Genuchten, C. Delaire, S.E. Amrose, A.J. Gadgil, M. Mohseni, Production and transformation of mixed-valent nanoparticles generated by Fe(0) electrocoagulation, Environ. Sci. Technol. 49 (2015) 2171–2179. doi:10.1021/es505059d.

[8] F.J. Millero, S. Sotolongo, M. Izaguirre, The oxidation kinetics of Fe(II) in seawater, Geochim. Cosmochim. Acta 51(1987) 793–801. doi:10.1016/0016-7037(87)90093-7

[9] Hoffman, R.W., Meighan, R.B., 1984. The Impact of Combined Sewer Overflows from San Francisco on the Western Shore ofCentral San Francisco Bay. J. (Water Pollut. Control Fed. 56, 1277–1285. doi:10.1016/S0262-1762(99)80122-9

[10] Metcalf & Eddy, 2004. Wastewater engineering: treatment and reuse, 4th ed. McGraw-Hill.